Stable and flexible representations in mouse mPFC across different behaviors

Dissertation for obtaining a doctorate degree in natural sciences

presented to the
Faculty of Biosciences of J.W. Goethe University
in Frankfurt am Main

by

Johannes Hahn

from Frankfurt am Main, Germany

Frankfurt am Main, 2023

(D 30)

Accepted by the Faculty of Biosciences
of Goethe University as a PhD dissertation

Dean: Prof. Dr. Sven Klimpel

Advisor: Dr. Torfi Sigurdsson

1st expert assessor: Prof. Dr. Manfred Kössl

2nd expert assessor: Prof. Dr. Jochen Roeper

Date of disputation 08.05.2024

Contents

Abstract

The prefrontal cortex (PFC) is considered the cognitive center of the mammalian brain. It is involved in a variety of cognitive functions such as decision making, working memory, goal-directed behavior, processing of emotions, flexible action selection, attention, and others (Fuster, 2015). In rodents, these functions are associated with the medial prefrontal cortex (mPFC). Experiments in mice and rats have shown that neurons in the mPFC are necessary for successful performance of many cognitive tasks. Moreover, measurements of neural activity in the mPFC show excitation or inhibition in different cells in relation to specific aspects of the tasks to be solved. To date, however, it is largely unknown whether prefrontal neurons are stably activated during the same behaviors within a task and whether similar aspects are represented by the same neurons in different tasks. In addition, it is unclear how specifically neurons are activated, for example, whether cells that are activated in response to reward are activated in a different task without reward in a different situation or remain inactive. To address these questions, we recorded the same neurons in the mPFC of mice over the course of several weeks while the animals performed various behaviors.

To do this, we expressed GCaMP6 in pyramidal neurons in the mPFC of mice. A small lens was implanted in the same location and a miniature microscope ("miniscope") was used to record neural activity. Later the extracted neurons got aligned based on their shape and position across multiple days and sessions. The mice performed five different behavioral tests while neural activity was measured: A spatial working memory test in a T-maze, exploration of the elevated plus maze (EPM), a novel object recognition (NO) test including free open field (OF) exploration, a social interaction (SI) test and discriminatory auditory fear conditioning (FC). Each task was repeated at least twice to check for stable task encoding across sessions. Behavioral performance and neural correlates to specific task events were similar to earlier studies across all tasks. We utilized generalized linear models (GLM) to determine which behavioral variables most strongly influence neural activity in the mPFC. The position of the mouse in the environment was found to explain most of the variance in neural activity, together with movement speed they were the strongest predictors of neural activity across all tasks. Reward time points in the working memory test, the conditioned stimulus after fear conditioning, or head direction in general were also strongly encoded in the mPFC.

Many of the recorded neurons showed a stable spatial activity profile across multiple sessions of the same task. Similarly, cells that coded for position in one task tended to code for position in other tasks. Not only did the same cells code for position across multiple tasks, but cells also coded for movement speed and head direction. This indicates that at least these general

behavioral variables are each represented by the same neurons in the mPFC. Interestingly, the stability of position or speed coding did not depend on the time between two sessions, but only on whether it was within the same or across different tasks. Within the same task, stability was slightly higher than across different tasks.

To find out whether task-specific behavioral aspects were also stably encoded in the mPFC, difference scores as the difference in neural activity between two task aspects like left- and right-choice trials or exposed and enclosed locations were calculated. Many cells encoded these aspects stably across different sessions of each task. Both the left-right differences in the different phases of the working memory test, the open-closed-arm differences in the elevated plus maze, the different activity between center and corners in the open field, the social target-object differences in the social interaction test, and the differences between the two tones during fear conditioning were all stably encoded across the population of mPFC cells. Only the distinction between the novel and the familiar object during object recognition was not stably encoded, but also the preference for the novel object was not present in the second session of novel object exploration.

There was also an overlap in coding for different aspects within a task across multiple sessions. For example, cells stably encoded left-right differences in the T-maze between different sessions as a function of walking direction across different phases of working memory, an aspect that we could already show within one session (Vogel, **Hahn** et al., 2022). During fear conditioning, the same cells showed a discrimination between CS+ and CS- that also responded to the start of CS+.

Consistency in the neurons activity across different tasks was also found, but only between tasks with similar demands, the elevated plus-maze and free exploration of the open field. Cells that were more active in the open arms also showed more activity in the center of the open field and vice versa. This could be an indicator that the cells were coding for anxiety or exposure across those tasks, indicating that neurons in the mPFC also stably encode general task aspects independent of the specific environment. However, it remains unclear what exactly these neurons encode; in the case of a general fear signal, one would also expect activation during fear conditioning which could not be found.

Overall, we found that neurons in the mPFC of mice encoded multiple general behavioral variables across multiple tasks and task-specific variables were encoded stably within each of the tested tasks. However, we found little task-specific variables that were systematically encoded by the same neurons with the exception being the elevated plus-maze and open field exploration, two tasks with similar features.

Zusammenfassung

Der präfrontale Kortex (PFC) gilt als kognitives Zentrum des Säugergehirns. Er ist bei Menschen, Primaten, aber auch Nagetieren, involviert in einer Vielzahl von kognitiven Funktionen wie der Entscheidungsfindung, dem Arbeitszeitgedächtnis, zielgerichtetem Verhalten, Verarbeitung von Emotionen, flexiblem Verhalten, Aufmerksamkeitssteuerung und anderem (Fuster, 2015). Bei Nagern werden diese Funktionen im medialen präfrontalen Kortex (mPFC) verortet. Experimente in Mäusen und Ratten haben gezeigt, dass Nervenzellen im mPFC notwendig für die erfolgreiche Durchführung einiger kognitiver Aufgaben sind. Zudem zeigen Messungen von Nervenaktivität im mPFC die Aktivierung oder Inhibierung von verschiedenen Zellen im Zusammenhang mit bestimmten Teilaspekten der zu lösenden Aufgaben oder Verhaltensweisen. So werden zahlreiche Zellen unterschiedlich aktiviert in Abhängigkeit von bestimmten Positionen, in denen sich das Versuchstier befindet. Diese können unterschiedlich ausfallen in Abhängigkeit von bestimmten Zielen oder zu merkenden Positionen, sozialen Interaktionen, wie furchteinflößend oder exponiert eine aktuelle Position ist, ob Objekte unbekannt oder bekannt sind, aber auch mit der erlernten Relevanz bestimmter Signale wie Töne oder Lichter (Adhikari et al., 2011; Baeg et al., 2001; Milad & Quirk, 2002; Pezze et al., 2015, 2017; Spellman et al., 2015; Vogel, **Hahn** et al., 2022). Bisher ist es allerdings weitgehend unbekannt, ob präfrontale Neurone stabil bei den gleichen Verhaltensweisen innerhalb einer Aufgabe aktiviert werden und ob ähnliche Aspekte in verschiedenen Aufgaben von den gleichen Nervenzellen abgebildet werden. Zudem ist unklar, wie spezifisch Neurone aktiviert werden, beispielsweise ob Zellen, die bei Belohnung aktiviert werden, in einer anderen Aufgabe ohne Belohnung in einer anderen Situation aktiviert werden oder inaktiv bleiben.

Zur Klärung dieser Fragen habe ich dieselben Neurone im mPFC von Mäusen über den Zeitraum von mehreren Wochen aufgenommen, während die Tiere verschiedene Verhaltensweisen zeigten. Dazu wurden mittels eines eingebrachten Vektors Pyramidenzellen im prälimbischen Cortex des mPFC dazu gebracht, ein Protein, GCaMP6, zu exprimieren, das bei Bindung mit Kalzium fluoresziert. Eine kleine Linse wurde ebenfalls fest im mPFC implantiert und ein Halter auf dem Schädel der Maus fixiert, um während der Versuchsdurchführung ein Miniaturfluoreszenzmikroskop („Miniscope“) zu befestigen. Mittels dieses Mikroskops lässt sich anschließend indirekt die Nervenaktivität messen, da bei es Aktivierung von Neuronen zum Kalziumeinstrom in den Zellkörper kommt, der dann durch Fluoreszenz sichtbar gemacht wird. Dieses Signal wird zunächst als Video an einen Computer übertragen und im Anschluss kann die Aktivität der einzelnen Nervenzellen im Sichtfeld extrahiert werden. Die Neurone können anschließend anhand ihrer Form und relativen

Position zueinander ausgerichtet werden und somit als gleiche Zelle über verschiedene Tage und Sessions erkannt werden. Die Mäuse wurden fünf verschiedenen Verhaltenstests unterzogen, während die Nervenaktivität gemessen wurde:

- Ein Test des räumlichen Arbeitsgedächtnisses in einem T-Labyrinth. Zunächst sitzen die Mäuse in der Startbox am Fuß des T-Labyrinths. Von dort werden sie in der ersten Phase, der Musterphase, in einen der beiden Zielarme geleitet, wo sie eine kleine Belohnung in Form von gesüßter Kondensmilch erhalten, der andere Zielarm ist durch eine Tür versperrt. Anschließend kehren sie in die Startbox zurück und müssen dort für 15 s oder 60 s verweilen (Verzögerungsphase). Nach Ablauf können sie nun, in der Entscheidungsphase, frei zwischen einem der beiden Zielarme wählen, um eine Belohnung zu erhalten, müssen sie den gegenüberliegenden wählen, in den sie nicht in der Musterphase geleitet wurden.
- Ein Ängstlichkeitstest in einem erhöhten Plus-Labyrinth, bei dem jeweils zwei gegenüberliegende Arme entweder einen hohen Rand oder keinen Rand haben.
- Ein Test zur Erkennung eines neuartigen Objekts, bei dem die Tiere zunächst eine leere Arena erkunden können. Nach 10 Minuten werden zwei identische Objekte eingebracht, nach weiteren 10 Minuten wird eins der Objekte durch ein neues Objekt ausgetauscht.
- Ein Test von sozialer Interaktion, bei dem die Versuchsmaus entweder mit einem Artgenossen oder einer Plastikmaus interagieren kann.
- Ein Test zur Furchtkonditionierung, bei der ein zunächst neutraler Ton (konditionierter Stimulus, CS+) mit einem milden Elektroschock gepaart wird, um eine Furchtreaktion auszulösen. Ein weiterer Ton (Kontrollstimulus, CS-) wird ebenso abgespielt, aber nicht mit einem Elektroschock gepaart. Anschließend werden beim Extinktionstraining beide Töne ohne Elektroschock präsentiert, um einen neuen Lernprozess zu starten, so dass der CS+ keine Gefahr mehr signalisiert.

Der Arbeitsgedächtnistest wird mehrfach wiederholt, die spontanen Verhaltenstests (Plus Labyrinth, Objekterkennung, Soziale Interaktion) werden jeweils zweifach durchgeführt, die Furchtkonditionierung nur einmal, allerdings mit zwei Extinktionstrainingssessions. Somit konnte auch die Nervenaktivität im gleichen Versuchsaufbau an verschiedenen Tagen verglichen werden.

Während des Arbeitsgedächtnistests wurden, wie von uns bereits veröffentlicht (Vogel, **Hahn** et al., 2022), zahlreiche Zellen gefunden, die an verschiedenen Positionen entlang des Labyrinths konsistent in Abhängigkeit von der Laufrichtung aktiviert werden. Ebenso gibt es zahlreiche Neurone, die zwischen dem linken und rechten Zielarm unterschiedliche Aktivität

zeigen, in der Musterphase, sobald die Maus den Zielarm betreten hat und schließlich bis sie in die Startbox zurückgekehrt ist, in der Entscheidungsphase auch schon bevor die Maus sich tatsächlich im entsprechenden Arm befindet. Während der Verzögerungsphase konnte ich jedoch keine signifikanten Unterschiede in der neuronalen Aktivität zwischen den Zielarmen als Gedächtnissignal feststellen.

Während des erhöhten Plus-Labyrinth-Tests verbrachten die Mäuse erwartungsgemäß mehr Zeit in den geschlossenen Armen als in den offenen Armen. Zahlreiche Zellen codierten den Arm-typ, in dem sich die Maus gerade befand. In der leeren Arena zeigte sich ein ähnliches Bild, die Mäuse bevorzugten den Bereich nahe den Wänden und mieden das exponierte Zentrum, auch hier wurden die unterschiedlich angsteinflößenden Bereiche in den Nervenzellen codiert.

Während des Objekterkennungstests verbrachten die Mäuse gleich viel Zeit mit beiden Objekten in Phase I, in Phase II jedoch verbrachten sie mehr Zeit beim neuen Objekt und erkundeten es öfter. Die Korrelation von Besuchen der beiden Objekte mit der neuronalen Aktivität war erhöht in Phase I. In Phase zwei war sie beim bekannten Objekt wieder verringert auf Zufallsniveau, beim neuartigen Objekt jedoch stark erhöht. Während des Tests von sozialer Interaktion verbrachten die Versuchstiere zunächst mehr Zeit mit ihren Artgenossen und besuchten diese häufiger in Phase I, in Phase II konnte jedoch kein Unterschied festgestellt werden. In der zweiten Session war der Unterschied in der Interaktionszeit bereits in Phase I verringert und die Anzahl der Besuche unterschied sich nicht.

Während der Furchtkonditionierung zeigten die Mäuse Erstarrung, wenn sie den Ton hörten, der zunächst mit einem Elektroschock gepaart wurde (konditionierter Stimulus). Die Zeit, die sie bewegungslos verbrachten, nahm in der zweiten Extinktionstrainingssession gegenüber der ersten ab. Zahlreiche präfrontale Neurone zeigten Aktivität im Zusammenhang mit dem konditionierten Stimulus und differenzierten zwischen dem Ton, der mit dem milden Elektroschock gepaart wurde, und dem ungepaarten Ton.

Zur weiterführenden Analyse setzte ich generalisierte lineare Modelle (GLM) ein, um herauszufinden, welche Verhaltensvariablen die Nervenaktivität im mPFC am stärksten beeinflussen. Wir testeten sowohl wie viel Varianz einer Zelle mit einer einzelnen Variable erklärt werden kann, als auch um wie viel sich die Varianz reduziert, wenn eine Variable vom Modell entfernt wird. Dies entspricht dem einzigartigen Beitrag der Variable, der nicht durch andere Variablen im Modell erklärt werden kann. Es zeigte sich, dass die Position der Maus in der aktuellen Umgebung bei den meisten Neuronen einen großen Teil der Varianz der Aktivität erklärt. Selbst während der Furchtkonditionierung spielt die Position eine große Rolle für die Nervenaktivität, obwohl hier die Position nicht aufgabenrelevant ist. Zahlreiche Zellen sind

jedoch von mehr als einer Variablen moduliert. Die Bewegungsgeschwindigkeit, die neben der Position in allen Versuchsaufbauten gemessen wurde, moduliert ebenfalls zahlreiche Zellen. Aber auch der Belohnungszeitpunkt im Arbeitsgedächtnistest, der konditionierte Stimulus nach der Furchtkonditionierung oder generell die Blickrichtung korrelieren stark mit der Aktivität einiger Nervenzellen.

Um festzustellen, ob die Positionskodierung stabil über verschiedene Sessions desselben Verhaltens ist, habe ich die Aktivitätskarten der Neurone korreliert und festgestellt, dass ein Großteil der Zellen ein stabiles Aktivitätsprofil zeigt. Ebenso tendierten Zellen, die in einer Aufgabe für Positionen codierten, dazu, dass sie auch in anderen Aufgaben für Positionen codierten. Hierzu korrelierten wir den einzigartigen Beitrag der Zellen zur erklärten Varianz in unserem GLM zwischen zwei Sessions, in denen die Zelle aufgenommen wurde. Es zeigte sich, dass auch mit dieser Methode die Mehrheit der Zellen innerhalb einer Aufgabe, aber mehrerer Sessions, für Positionen codierte.

Mit dieser zweiten Methode konnten ich auch die Stabilität über verschiedene Verhaltensvariablen testen, sowohl innerhalb einer als auch über mehrere Aufgaben. Es stellte sich heraus, dass sowohl bei der Codierung für Positionen als auch für Geschwindigkeit über verschiedene Aufgaben eine hohe Stabilität herrschte. Dies ist ein Hinweis darauf, dass zumindest diese generellen Verhaltensvariablen stabil im mPFC abgebildet werden. Zahlreiche andere Verhaltensvariablen wurden ebenso mit großer Stabilität abgebildet. Zellen die für Positionen codierten tendierten außerdem dazu für Geschwindigkeit oder die Blickrichtung, sowohl innerhalb einer Aufgabe, aber auch zwischen mehreren Aufgaben.

Interessanterweise war die Stabilität der Positions- oder Geschwindigkeitscodierung nicht von der Zeit zwischen zwei Sessions abhängig, sondern nur davon, ob es sich um die gleichen oder unterschiedliche Aufgaben gehandelt hat. Innerhalb der gleichen Aufgabe war die Stabilität etwas höher als über verschiedene Aufgaben.

Um herauszufinden, ob auch aufgabenspezifische Verhaltensaspekte stabil im mPFC abgebildet werden, habe ich verschiedene Aspekte über die Differenz in der Nervenaktivität zwischen zwei Verhaltenssituationen korreliert. Es zeigte sich, dass die Mehrheit der Zellen diese stabil zwischen verschiedenen Sessions einer Aufgabe abbildet. Sowohl die Links-Rechts-Unterschiede in den einzelnen Phasen des Arbeitsgedächtnistests, die Offen-Geschlossen-Arm-Unterschiede im erhöhten Plus-Labyrinth, die unterschiedliche Aktivität zwischen Zentrum und Ecken in der leeren Arena, die Unterschiede zwischen Artgenossen und Objekt beim Test für soziale Interaktion, als auch die Unterschiede zwischen den beiden Tönen während der Furchtkonditionierung wurden allesamt stabil in den meisten Zellen kodiert. Lediglich für die Unterscheidung zwischen dem neuartigen und dem bekannten Objekt

konnten wir keine Stabilität feststellen, allerdings gab es von vornherein sehr wenige Neurone, die für diesen Aspekt codierten.

Auch zwischen verschiedenen Aspekten innerhalb einer Aufgabe gab es Überlappungen. So codierten Zellen Links-Rechts-Unterschiede im T-Labyrinth stabil zwischen verschiedenen Sessions in Abhängigkeit von der Laufrichtung, ein Aspekt, den wir schon innerhalb einer Session zeigen konnten (Vogel, **Hahn** et al., 2022). Während der Furchtkonditionierung zeigten die gleichen Zellen eine Unterscheidung zwischen CS+ und CS-, die auch auf den Start des CS+ reagierten.

Als Indikator dafür, dass die Zellen tatsächlich für Angst oder Exposition kodieren, gab es auch eine gerichtete Konsistenz in den Neuronen zwischen dem erhöhten Plus-Labyrinth und der freien Erkundung der leeren Arena. Zellen, die im offenen Arm aktiver waren, zeigten auch mehr Aktivität im Zentrum der Arena und umgekehrt. Dies zeigt, dass die gleichen Nervenzellen im mPFC auch allgemeine Aufgabenaspekte unabhängig von der spezifischen Umgebung über mehrere Aufgaben und Tage abbilden. Unklar bleibt allerdings, was genau diese Nervenzellen kodieren, bei einem allgemeinen Furchtsignal würde man auch eine Aktivierung während der Furchtkonditionierung erwarten.

Insgesamt konnte ich also zeigen, dass Neurone im mPFC meist mehrere allgemeine Verhaltensvariablen abbilden und dies stabil über verschiedene Aufgaben hinweg. Auch spezifische Verhaltens- oder Umgebungsvariablen werden über verschiedene Aufgaben hinweg stabil abgebildet. Es bleibt jedoch unklar, wie die Gruppierung von Zellen mit ähnlichen Aktivitätsmustern zustande kommt, so könnten beispielsweise unterschiedliche Projektionsziele oder Inputquellen dafür verantwortlich sein. Darüber hinaus ist weitere Forschung notwendig, um festzustellen, ob diese Stabilität auch über längere Zeiträume gegeben ist.

List of abbreviations

ACC	Anterior cingulate cortex
ANCOVA	Analysis of covariance
ANOVA	Analysis of variance
BLA	Basolateral amygdala
Cg	Cingulate areas / Cingulate cortex
CR	Conditioned response
CS	Conditioned stimulus
DA	Dopamine
DAQ	Data acquisition system
DLC	DeepLabCut
dlPFC	Dorsolateral prefrontal cortex
dmPFC	Dorsomedial prefrontal cortex
DNMS	Delayed non-match-to-sample
EPM	Elevated plus maze
FC	Fear conditioning
FOV	Field of view
GLM	Generalized linear model
GRIN	Gradient refractive index
HPC	Hippocampus
IL	Infralimbic cortex
IR	Infrared
L	Left arm (in the T-maze)
LED	Light emitting diode
MD	Mediodorsal nucleus of the thalamus
mPFC	Medial prefrontal cortex
NAc	Nucleus accumbens
NMDA	N-methyl-D-aspartate
NMS	Non-match-to-sample
NO	Novel object recognition
OF	Open field
OFC	Orbitofrontal cortex
PCP	Phencyclidine / phenylcyclohexyl piperidine
PI / PII	Phase I / Phase II
PFC	Prefrontal cortex
PL	Prelimbic cortex
PrCm	Medial precentral area
PTSD	Post-traumatic stress disorder
PV	Parvalbumin positive neurons
R	Right arm (in the T-maze)
RAM	Radial arm maze
SI	Social Interaction
SOM	Somatostatin positive neurons
SWM	Spatial working memory
US	Unconditioned stimulus
UV	ultraviolet
vlPFC	Ventrolateral prefrontal cortex
vmPFC	Ventromedial prefrontal cortex
WM	Working memory

Table of figures

Introduction

The prefrontal cortex

To survive in a complex and ever-changing environment, it is beneficial for animals to learn abstract rules and principles, update, use and focus on the relevant information to react quickly and appropriately in common, as well as novel situations. Humans, in comparison with other species, have an exceptional ability to do so. One reason for that seems to be the much more pronounced human prefrontal cortex (PFC) in comparison to other animals (Miller et al., 2002). The PFC is a part of the cerebral cortex and consists of the anterior part of the frontal lobe in the mammalian brain. One commonly used definition of the PFC is that it receives input from the mediodorsal nucleus of the thalamus (MD, Fuster, 2015) but a clear consensus across species is still lacking.

Previous research has shown that the PFC is linked to the processing of a variety of cognitive functions and executive processes like goal directed behavior, decision making, working memory, emotion, behavioral flexibility, attention and others in humans, primates, and rodents (Fuster, 2015). It is a highly interconnected brain structure and receives input from a variety of other brain regions. The outgoing projections from the PFC target areas across the whole brain (Euston et al., 2012; Gabbott et al., 2005; Gao et al., 2022). These dense connections might be what enables the PFC to be one of the major control hubs for all kinds of behaviors.

Already in the thirties of the last century Jacobsen found that bilateral lesions of the monkey PFC led to impairments in a delayed response task but not task solving in general (Jacobsen, 1935). This already indicated a crucial role during spatial memory processing. He already speculated that the region could play a role in either recalling memories or keeping the information through a delay by sustained activity, which was later confirmed by recordings in the PFC (Fuster & Alexander, 1971). Further studies in monkeys lesioning different parts of the PFC found other negative influences on attention (Fuster & Bauer, 1974), emotional control (Butter et al., 1970), behavioral flexibility (Iversen & Mishkin, 1970) and non-spatial memories (Fuster & Bauer, 1974). Since then, studies on prefrontal areas in other species, particularly rodents, became increasingly important as it combines the use of advanced research tools with lower housing and breeding cost and fewer ethical constraints (Bryda, 2013; Laubach et al., 2018).

The prefrontal cortex in primates

Originally, the PFC was defined by Brodmann as the presence of a granular layer IV in the cortical areas in front of the motor and premotor areas, a definition purely defined by cytoarchitectonic characteristics (Brodmann, 1909). Later a different definition using

connectivity-based characteristics was proposed and widely accepted, that the PFC is defined as the “essential cortical projection area of the mediodorsal nucleus of the thalamus (MD)” (Fuster, 2015; Preuss, 1995). Nowadays the PFC in humans and non-human primates is still mostly defined as the granular and orbital parts of the frontal cortex, although there are also agranular and dysgranular parts (Carlén, 2017). But the definition, that it is the area receiving input from MD is not sufficient as other cortical regions that are not considered prefrontal also receive input from MD such as premotor and motor areas (Groenewegen, 1988; Laubach et al., 2018; Preuss, 1995).

The PFC in primates is subdivided in different functional areas, the ventromedial (vmPFC), the ventrolateral (vlPFC), the dorsolateral (dlPFC), the dorsomedial (dmPFC) and the orbitofrontal (OFC) are distinguished (**Figure 1**A, B, Carlén, 2017). The anterior cingulate cortex (ACC) refers to the agranular part of the frontal regions and does classically not belong to the PFC (Laubach et al., 2018), although some consider it being prefrontal as it receives projections from MD (Preuss, 1995). The dlPFC receives special focus as other species do not receive MD input to their dorsolateral frontal areas. It is therefore often seen as a unique specialization in primates associated with higher order cognitive functions (Preuss, 1995; Preuss & Wise, 2022).

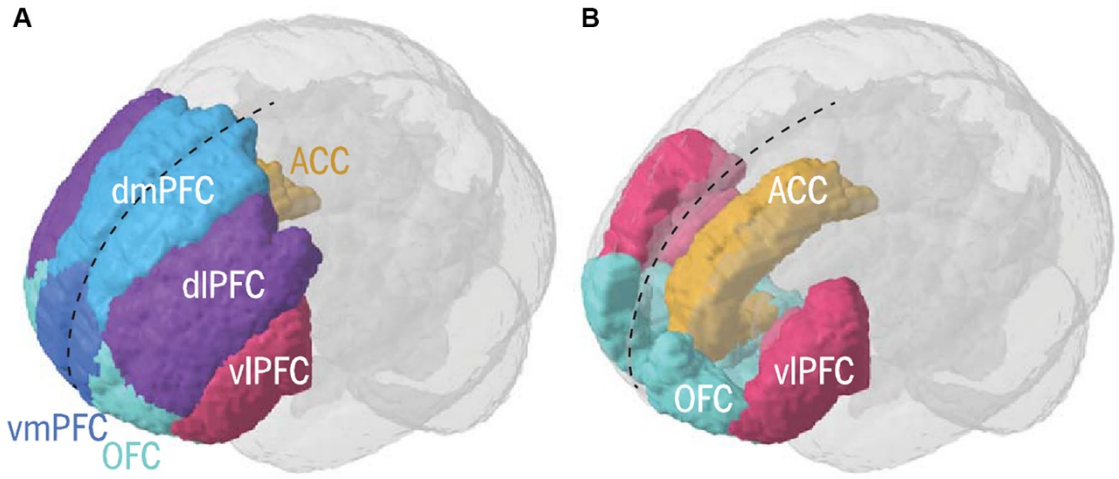

Figure 1: The prefrontal cortex in humans. **A**: 3D render of the human brain with different subregions in the PFC marked with different colors. **B**: As A but for medial and ventral regions. Dashed black lines indicate the midline. ACC: Anterior cingulate cortex, dlPFC: dorsolateral PFC, dmPFC: dorsomedial PFC, OFC: Orbitofrontal cortex, vlPFC, ventrolateral PFC, vmPFC: ventromedial PFC, (Figure from Carlén, 2017).

The medial prefrontal cortex in rodents

To what extent the rodents also have a PFC is widely debated as it lacks the typical granular structure of most primate PFC. While the PFC in primates spans across the whole frontal lobe,

in rodents it is lying mostly on the medial surface of the brain (Carlén, 2017). But the medial prefrontal cortex (mPFC) has some functional similarities with the PFC, especially the dlPFC, in primates. Therefore, the terms mPFC and "PFC" are used synonymously in rodent literature. But there are also clear differences in the definitions across species. While the majority does not consider the agranular ACC in primates as part of the PFC (Laubach et al., 2018), in rodents, the ACC is typically regarded as belonging to the mPFC.

The mPFC in rodents is organized in a laminar structure that differs from other cortical regions as it has no distinguishable layer IV. While in other cortices layer IV is mostly used as the input layer, in the rodent mPFC both deep and superficial layers receive long-range inputs (Hoover & Vertes, 2007). It is subdivided in the ACC, the prelimbic cortex (PL) and the infralimbic cortex (IL, **Figure 2**). Some also include the medial precentral area (PrCm), other terms for this area include medial agranular cortex (AGm), or secondary motor cortex (M2, Carlén, 2017).

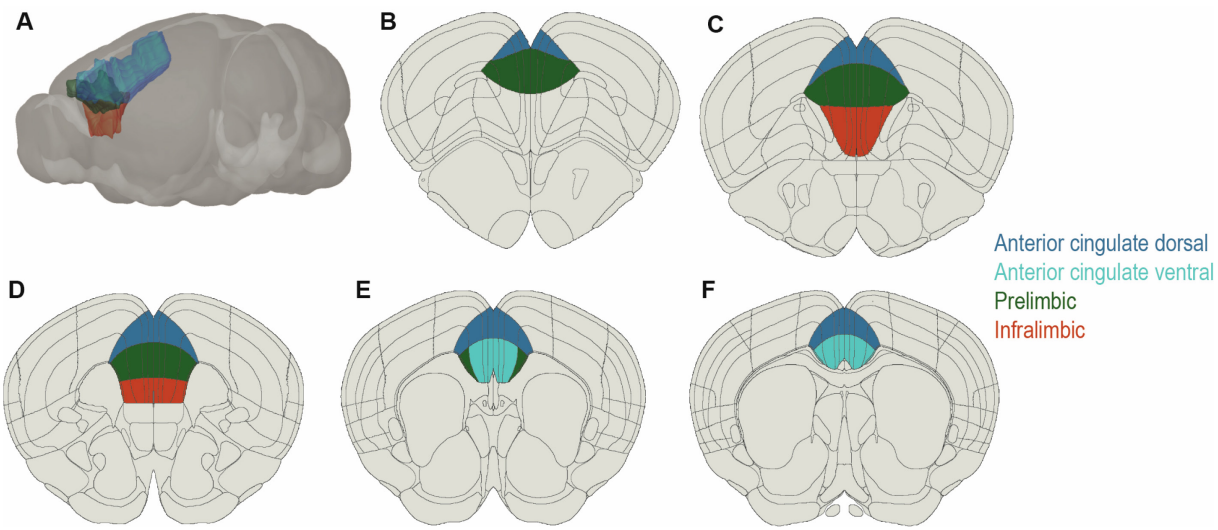

Figure 2: The medial prefrontal cortex in mice. **A**: 3D render of mouse brain with mPFC. **B-F** Coronal sections of mouse brain at different locations including parts of the mPFC, position given relative to Bregma. Anterior cingulate area dorsal part: dark blue; Anterior cingulate area ventral part: light blue; Prelimbic area: green; Infralimbic area: red. **B** Bregma +2.2 mm (Anterior to Bregma). **C** Bregma +1.9 mm. **D** Bregma +1.6 mm, **E** Bregma + 1.3 mm. **F** Bregma + 1 mm. Altered from Allen Adult mouse brain atlas (Lein et al., 2007).

Another widely used division is into the dorsal part (dmPFC), containing the ACC and the dorsal part of PL and the ventral part (vmPFC) with ventral PL and the IL region (Euston et al., 2012; Gabbott et al., 2005; Xu et al., 2019), although the exact limits differ between studies and authors (le Merre et al., 2021). These subregions can be divided by cytoarchitecture (van Eden & Uylings, 1985), different functions and by different afferent and efferent connection patterns (Euston et al., 2012; Gabbott et al., 2005; Heidbreder & Groenewegen, 2003; Hoover & Vertes, 2007; Sesack et al., 1989). Dorsal and ventral areas are distinguished by a functional

gradient with the dorsal part relevant for action control and the ventral areas more specialized for autonomic and emotional control. This is also partly reflected in their different connection patterns. The vmPFC for example has stronger reciprocal connections to the basolateral amygdala (BLA) which is important for emotional processes, the anterior insular area which is involved in pain processing and interoception and the hypothalamus, which is involved in autonomic and endocrine control. While the dorsal mPFC shares many of these connections, its connections to motor and premotor areas are stronger but it is not as well connected to areas of autonomic and emotional control (Euston et al., 2012; le Merre et al., 2021). Additionally, the dorsal areas mostly project to the dorsal striatum, while the ventral mPFC projects more to the ventral part of the striatum (Gabbott et al., 2005; Sesack et al., 1989). The mPFC consists mostly of excitatory pyramidal neurons, about 80-90% belong to this group. The remaining 10-20% are made of different types of inhibitory GABAergic interneurons which are important for local circuitry (Riga et al., 2014).

Similarities and differences between the rodent and primate prefrontal cortex

Although there is some clear functional similarity between some of the prefrontal regions in primates and rodents there is an ongoing debate over the extent of homology. Especially the presence of a structure homologous to the primate dlPFC in rodents is widely debated, with the mPFC as its prime candidate based on functional similarities (Laubach et al., 2018; Preuss, 1995; Uylings et al., 2003). One of the key problems that remains is that different nomenclature is used between primate and rodent studies. Together with unclear and inconsistent boundaries, even across two editions of the same brain atlas, this makes it difficult to compare across the different areas and species. Laubach et al. asked PFC researchers working with different species about different parts of rodent PFC belonging to different areas. They were surprised that just 20% of rodent and 40% of primate researchers considered PL being a part of the ACC as they could not find anatomical studies not considering PL as part of ACC. They also criticize the use of the terms dmPFC and vmPFC, as many researchers answered that PL is part of both structures and suggest rather using more precise terms (Laubach et al., 2018).

Based on Brodmann's definition requiring a granular layer IV for the PFC, rodents would not have a PFC. Using the more recent definition as cortical projection target of MD, rodents, like all mammals, would have a PFC but without a well-developed granular layer IV. And even in primates the PFC has dysgranular or agranular parts (Carlén, 2017). The appearance of a granular layer in primates was seen as an evolutionary development within the higher developed primates. But still no clear and common definition of PFC is used so which parts of the frontal areas would be considered PFC still changes depending on the author. One issue

is that the areas receiving essential inputs from MD in primates extend beyond that of the granular frontal cortex (Preuss, 1995). Additionally, other thalamic nuclei innervate the same areas, while originally it was proposed that all thalamic projections reaching the frontal fields originate in the MD (Carlén, 2017). Differences in input and structure of MD, which also varies across species, are also a bit problematic (Leonard, 1969; Preuss & Wise, 2022). Also, the position of the MD-projecting cortex in the rat is in the ventrolateral and medial surfaces and not at the dorsolateral part as in primates.

It is also debated what parts of the rodent cortex are considered prefrontal and again this is dependent on different definitions used. Some considered the dorsal cingulate and the PrCm as premotor areas and not prefrontal. It was argued that both areas only received sparse input from mediodorsal thalamus (Condé et al., 1990; Preuss, 1995; Uylings et al., 2003). But other studies show strong reciprocal connections between PrCm and MD or dorsal ACC and MD, respectively (Condé et al., 1990; Groenewegen, 1988; Krettek & Price, 1977; Reep & Corwin, 1999; Vertes, 2002). In combination the PrCm and dorsal ACC would show MD connection patterns that are “more prefrontal than premotor” (Uylings et al., 2003).

Because of the insufficient definition based on MD inputs further characteristics were added later like the necessity of the region for delayed response tasks (Preuss, 1995). Lesions of the rat mPFC produce deficits in delayed response tasks, similar to lesions of dlPFC in primates. Critics claim that the dlPFC is not the only structure involved in delayed response tasks in primates. At least infant primates can solve delayed response tasks directly after lesioning dlPFC (Preuss, 1995). But there are also other tasks that show more similarities, especially tasks that require behavioral flexibility like reversal learning or set shifting (Brown & Bowman, 2002). This leads to an idea that suggests that the mPFC of rodents is a mixture of the primate dlPFC and ACC. This is mostly based on functional overlap between the two areas (Seamans et al., 2008; Uylings et al., 2003). This view is criticized by Preuss and Wise, claiming there are no properties in rodent mPFC that are not also in primate ACC (Preuss & Wise, 2022). They claim the granular dlPFC is a specialization in primates, as it has structural and functional properties that are unique to it.

Apart from functional similarities there are also some similarities in the connections with other brain structures apart from MD. One early addition were dopaminergic inputs. Both, primates and rodent prefrontal areas receive strong dopaminergic inputs from brainstem nuclei, but dopaminergic inputs are widely distributed across the brain (Preuss, 1995). Likewise, other areas in the frontal lobe receive inputs from dopaminergic midbrain nuclei so also this criterion is not sufficient to define the PFC.

In both, rodents, and primates most of the input comes from different cortical areas, mostly on the ipsilateral side. Similarly, there are high similarities between basal ganglia-thalamocortical circuits in rodents and primates (Bonelli & Cummings, 2007; Uylings et al., 2003). Prefrontal cortical areas in rats and primates receive input from the amygdala. Of those, the dlPFC in primates has the weakest input from the amygdala, in rats the dorsal ACC and the PrCm receive the least input (Uylings et al., 2003). It is known that there are some areas within the striatum that project to specific other brain regions and are well-preserved across species. Heilbronner et al. used the connections between the mPFC and these areas in the striatum to identify resemblances between rodents and non-human primates. With that they identified the IL of rats to likely be homologous to area 25, a structure in the ventromedial PFC in primates, as they shared similar projection patterns (Heilbronner et al., 2016). Their results for PL and cingulate areas (Cg) are less clear, while they report similarities between PL and area 32, they also find parts of PL to be homologous with parts of area 24. But both these areas, 24 and 32 are also part of the ventromedial PFC. Cg on the other hand is most similar with caudal area 24 but also has commonalities with rostral area 24. The homology between rodent PL and non-human primate area 32 is supported by different other features like a similar receptor density and binding properties across different receptors within the superficial or deep layers or the cytoarchitecture, although there are also differences (Vogt et al., 2013).

Overall, it is noteworthy that there is no specific evidence for the absence of a dlPFC homologue, just no clear evidence for the existence of such a structure (Preuss, 1995). This might also not be necessary to draw useful conclusions from rodent research. To achieve this, precise definitions and consistent terminology are needed, to be able to compare across studies and species (Carlén, 2017). As rodents are cognitively less-complex organisms, it might even be better to understand elemental psychological or neural processes and then later extrapolate to dlPFC functions (Brown & Bowman, 2002). While the rodent mPFC is not the anatomical equivalent of the PFC in primates it still fulfills similar functions, as we will discuss in the next sections.

Now the question remains whether and to what extent studies in rodents can be used to understand PFC function in primates (Carlén, 2017). This question is very relevant as the PFC is not only considered the area relevant for higher cognitive function, but its dysfunction is also implicated in many psychiatric disorders like schizophrenia, Parkinson’s disease, depression, anxiety, and others (Xu et al., 2019).

The prefrontal cortex is required for working memory in primates

Remembering information over short time periods is a critical mechanism for most species. Holding information in mind and being able to process this information is a key feature in

decision making and action planning. This form of short-term memory that allows active manipulation to guide behaviors is called working memory (WM). For many animals it is mostly spatial information or visual and auditory cues, for example locations of transitory food sources or the call, sound or view of a predator. Humans use working memory in different and more complex processes such as language processing or mathematical operations. To test WM in animals, spatial working memory (SWM) tasks are often used. In those the test subjects are required to remember specific spatial locations over a delay.

After the early finding from Jacobsen (Jacobsen, 1935) that lesioning the PFC worsens performance in a delayed response task which requires WM, many studies investigated the role of different PFC subregions or how neurons code for different aspects of WM. In the delayed response task, a monkey observes the baiting of one of two food wells during the cue period. Both food wells get covered and a screen is lowered so the animal can't see the food wells for a short delay. After a delay period of varying length, the screen is lifted again, and the animal should choose the baited food well to retrieve the reward (match-to-sample).

First recordings in monkey prefrontal cortex revealed different activity patterns in prefrontal neurons during a delayed response task with neurons showing responses to cues or the onset of the delay period while some cells showed sustained activity throughout the delay (Fuster & Alexander, 1971; Kubota & Niki, 1971). Looking at this delay activity in greater detail revealed different types of delay activity, most strikingly cells that increase their activity with cue display, either gradual or abruptly, and did not return to baseline before the response period. Other cells were inhibited for the whole duration of the delay. Another group of cells was inhibited during the cue period but increased their firing during the delay (Fuster, 1973). Further investigations showed that the patterns seen are often fixed but about one third of the neurons shift in relation to the length of the delay period (Kojima & Goldman-Rakic, 1982). Delay activity could be, if different between the stimuli or targets used, sufficient for successful task performance. Indeed, such stimulus specific activity has been reported in monkeys for both delayed response tasks and delayed alternation, but not if the cue was present during the delay (Kojima & Goldman-Rakic, 1984; Niki, 1974a, 1974b; Sobotka et al., 2005). Disrupting PFC activity during the delay period was correlated with decreasing task performance (Sobotka et al., 2005). This delay activity coding is not limited to spatial locations or locations of visual cues but also to other properties like colors, shapes, and real-life images, but also to other modalities like auditory cues and even between associations of multiple modalities like combinations of specific tones and colors (Funahashi et al., 1989; Fuster et al., 2000; Hoshi et al., 2000; Miller et al., 1996).

Another typical working memory task that is done in monkeys is an oculomotor delayed response task where the animal has to remember a cued location on a screen and make a saccadic eye movement to the location. Again, delay period activity has been reported, representing more than two different location options (Funahashi et al., 1989, 1993). In error trials the delay period activity was reduced. More than half of the cells showed stimulus dependent activity which could be an indicator for integration of cue information and future response, which could allow associative learning (Asaad et al., 1998). When using stimuli of different luminance neurons code for the luminance of the cue during the delay period without the cue being present and not purely for the following choice, a further indication that the activity is not just motor planning but still coding for the sensory information (Constantinidis et al., 2001). Increasing task complexity by making the animal remember multiple cue locations and the order of cue presentation also revealed cells coding not only for the specific cues but also in which order they were presented (Funahashi et al., 1997).

The role of the rodent mPFC in working memory

Like the PFC in monkeys, the mPFC in rodents is also involved in WM. While in monkeys mostly visually guided WM tasks are used, where the subject responds with levers, joysticks, eye movements, or direct interactions, for example choosing one of two food wells, in rodents mostly spatially guided tasks are used, where the animal has to move to specific locations, although response tasks involving lever pressing, licking and other types also exist (Dudchenko, 2004; van Haaren et al., 1988). Often maze based tasks with mazes of different shapes are used to test SWM in rodents. A commonly used maze type is the T-maze that consists of a stem and two goal arms (Figure 3A). Small variations in Y-form, M-form (mirrored W-form respectively) or figure-eight form also exist (Figure 3A). Typically, the animal must move from the stem into one of the two goal locations to retrieve a reward. The animal has to follow different types of rules like in a continuous alternation task, where the animal always has to switch between the two goal arms or a discrete trial non-matching-to-sample (NMS) or matching-to-sample task, where the goal location is changing not continuously but based on a specific schedule (Figure 3C-E). For this the animal is forced into one of the two goal arms in the first phase of the trial, returns to the start and has to choose the opposite arm in the second phase. Both, continuous alternation and discrete trial tasks can be done with different delay lengths by keeping the animal in the start arm, additionally to the time the animal needs in the stem. With this the WM load can be altered. In the figure-eight maze different errors can be distinguished, a WM error, if the animal revisits the same arm it previously visited. If it enters the opposite goal arm during return from one goal it is considered a reference memory error, as the animal makes a mistake in the task structure (Figure 3F).

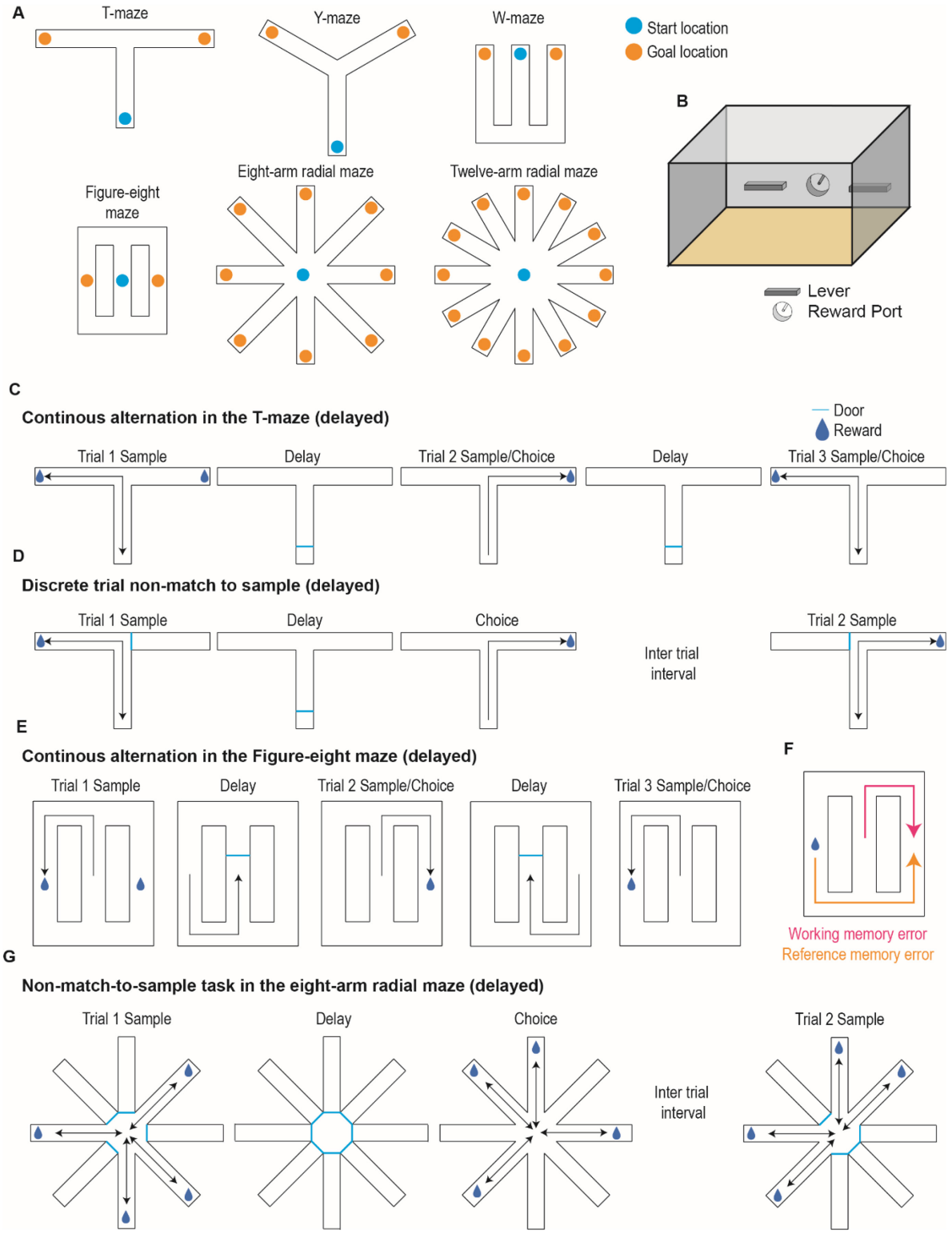

Figure 3: Testing SWM in rodents. **A**: Different mazes to test working memory in rodents. **B**: Operant chamber with two retractable levers and a reward port to test working memory in rodents. **C**: Continuous alternation task in the T-maze. In the first trial the animal can choose freely which arm to enter and returns the same way to the start. Afterwards it always must visit the opposite arm to retrieve a reward. **D**: Discrete trial non-match-to-sample task in the T-maze. The animal is forced in one arm during the sample phase and must visit the opposite arm after the delay to retrieve a reward. **E**: Continuous alternation in the figure-eight maze. Like B but the animal does not return the same way it moved to the goal location. **F**: Error types in the figure-eight maze. If the animal starts from the start location and turns into the wrong arm it is considered a working memory error. If the animal does not return to the start arm but visits the other goal arm, it is a reference memory error. **G**: Non-match-to-

sample task in the eight-arm radial maze. The animal visits all four arms freely during the sample phase and returns to the start platform. After a delay it must visit the other arms in the choice phase to retrieve rewards.

Rats and mice with lesions or inactivation of the PFC show deficits in both tasks (Brito & Brito, 1990; Larsen & Divac, 1978; Maharjan et al., 2018; Nonneman & Kolb, 1979). These deficits were partially dependent on the duration of the delay and were manifested as impaired learning. Although a clear drop in performance could be seen, most animals still performed above chance level, again dependent on the duration of the delay (Aultman & Moghaddam, 2001; Brito & Brito, 1990; Granon et al., 1994; Nonneman & Kolb, 1979; Yoon et al., 2008). Interestingly, in adult rats with neonatal (p6) mPFC lesions no performance effect could be found, while rats with lesions during adulthood showed a deficiency, indicating some rescue mechanism during maturation (Brabander et al., 1991).

Bilateral inactivation of the mPFC also impaired performance of spatial alternation in a W-maze without an extra delay, apart from the time the animal spends in the stem. Interestingly there also was a significant drop in performance, if the mPFC was unilaterally inhibited, if the contralateral Hippocampus (HPC) was also silenced (Maharjan et al., 2018). Ipsilateral inhibition of mPFC and HPC had no effect, indicating that the HPC-mPFC interactions are necessary. If those interactions are altered by inactivating either of the two in both hemispheres, task performance drops. If the interactions are still possible in one hemisphere there is no effect on task performance.

Similarly, lever-based delayed spatial alternation tasks, in which rats must alternately press one of two retractable levers (Figure 3B), are negatively affected by PFC lesion (Aggleton et al., 1995; Dunnett et al., 1999; M. Jones, 2002; van Haaren et al., 1988).

Following findings in primates that DA plays a role in working memory (Brozoski et al., 1979; Sawaguchi & Goldman-Rakic, 1991), a similar effect was found in rats. After lesioning DA terminals in the mPFC, rats were impaired during delayed alternation in the T-maze and in the RAM, whereas no effect was found during spontaneous alternation in the RAM. These results indicate a role for DA specifically during the delay of these tasks (Bubser & Schmidt, 1990). Reducing the amount of DA utilization in the mPFC also led to a delay duration dependent decrease in performance of a delayed alternation task, but not with no delay, further strengthening the role of prefrontal DA during working memory (Jentsch et al., 1997). On the other hand, infusion of different dopamine receptor antagonists in the ventromedial or dorsomedial PFC did not lead to specific memory effects in rats, in contrast to infusions of the muscarinic receptor antagonist scopolamine, that led to a drop in performance. Impairments were stronger with increased scopolamine dose or a longer delay time, indicating that these mechanisms are directly involved in working memory. (Broersen et al., 1994, 1995).

The PFC seems to play different roles during task learning and well-trained execution. In an odor guided Go-/NoGo task two different odors are presented with a delay between both, if two different odors are presented the mouse should respond (non-match-to-sample) if the same odor is presented twice (match-to-sample) the mouse should not respond (NoGo). Inactivating the mPFC led to performance impairments (Liu et al., 2014). Phase specific inhibition just had a delay-phase specific effect on learning but not in well-trained animals. This indicates that the mPFC is not necessary for task execution but to learn the task successfully. Interestingly, the representation of the two odors during the delay in the mPFC was different during training but not in well trained animals.

Working memory is differently affected by inactivation of specific subregions of the PFC and often dependent on delay length. Lesioning either ACC and PrCm or PL and IL regions negatively affects different forms of WM (Kesner, 2000). A clear role for the PL and IL subregions can be seen for SWM. While rats with a lesioned PL showed no deficits in spontaneous alternation in a Y-maze with a 10 s delay, performance dropped with longer delays (Delatour & Gisquet-Verrier, 1996). A similar delay length dependent effect was seen in a light cue guided Y-maze task, where either a slow- or a fast-flashing light indicated which of the arms rats had to enter (Delatour & Gisquet-Verrier, 1999). Here the learning of the task after PL/IL inactivation was not affected with short delays but with longer delays animals took more time to learn. These results suggest that the PL/IL regions are necessary for the working memory component of the task but not for the appropriate response selection. Another maze type that is commonly used to test spatial working memory is the radial arm maze (RAM) (Figure 3A). These mazes consist of a central platform and varying number of equal arms extending from there, typically eight or twelve. Different types of working memory tasks can be done in those, in a Go-/NoGo version the animals are always allowed to visit one arm at a time. The first time they visit each arm they will receive a reward (Go; Ragozzino et al., 1998). If they are allowed to visit an already visited arm again, they will not receive a reward and therefore should not enter but stay in the center of the maze (NoGo). This task is also dependent on an intact PL. Another option is that a specific number of arms is available and baited during the sample phase. After a delay all arms are made available and either the previously visited arms (match-to-sample) or the previously not visited (non-match-to-sample) should now be visited for a reward (Figure 3G). Inactivation led to an increased number of errors in the non-match-to-sample version of the task, both separately for the PL and the ACC subregion (Seamans et al., 1995).

One of the advantages of the discrete trial WM task is that different phases of working memory can be clearly distinguished. During the sample phase the animal must encode the memory about the arm it visits. During the delay phase the animal must maintain that information and

during the choice phase the animal retrieves the information and acts accordingly. Phase specific silencing approaches using optogenetics give the option to probe for which phases the mPFC is necessary. Silencing pyramidal neurons in the PFC of mice using the proton pump Archaerhodopsin (ArchT) during each phase independently was sufficient to impair performance during the task, indicating that the PFC is necessary for all three phases of WM (Vogel, **Hahn** et al., 2022). Another study silenced the HPC terminals in the mPFC in the different phases of the task and this alone was sufficient to impair behavior, but only during the sample phase, indicating that the HPC inputs to the mPFC are necessary for goal encoding (Spellman et al., 2015). In a similar study investigating the role of the connection between the mediodorsal thalamus (MD) and the mPFC the authors found a deficit for both, MD terminal inhibition in the mPFC but also inhibition of mPFC terminals in the MD. Notably, deficits were found with a 60 s delay while there was no effect with 10 s. While delay phase inhibition of the MD to mPFC projection was sufficient to disrupt behavior and inhibition during the other phases did not affect behavior, the effect of mPFC to MD projections was limited to the choice phase (Bolkan et al., 2017).

Many recording and imaging studies investigated neural correlates for working memory during these tasks. Recordings from rat mPFC during both an eight-arm radial maze or a figure-eight delayed spatial alternation tasks did not show goal specific delay activity (Jung et al., 1998). Nevertheless, while the animal was returning to the central arm, differential activity could be found. In contrast, recordings in rats during a continuous delayed alternation task in a figure-eight maze revealed an increasing amount of information about either the previous or the future goal using goal decoding during the delay. Goal decoding was already possible during initial learning in the early delay period and after training throughout the whole delay (Baeg et al., 2003). The authors speculate that during the early delay phase the past goal is represented better and during the later delay phase this switches to the future goal, as decoding during the early delay phase of error trials corresponds to the past goal, similar as in correct trials. Later the activity between correct and incorrect trials diverges, so it could be an increasing representation of the future goal, the choice of the animal, that is different in incorrect trials. Others also have shown differential activity dependent on the current or past goal during SWM (Yang et al., 2015). For a Y-maze delayed alternation task in rats they report sequential activation of different neurons instead of the sustained activity throughout the delay found in monkeys. Similar trajectory dependent firing was also found in another study in rats in figure-eight maze for continuous alternation (Ito et al., 2015a). Cells in the PFC already showed diverging activity between left and right turns at the base of the stem before the actual choice becomes visible. During a later introduced delay of 10 s at the base of the stem, decoding accuracy quickly dropped to chance, during the second half of the delay neither past nor future

goal could be decoded. Introducing the delay, the authors claim that they find evidence for prospective coding of the future goal, as they see diminishing retrospect decoding during the delay and increasing prospective coding when the animal is within the stem. Another odor guided task would be an odor-place matching task where rodents move to a specific location in a maze, dependent on a previously presented odor. Neurons in the mPFC code for different locations along the path, dependent on the future left or right choice of the animal (Fujisawa et al., 2008). But again no clear discrimination between prospective or retrospective coding can be made.

Another study used a slightly altered version of the T-maze in which the goal arms were subdivided into two compartments, to distinguish between prospective and retrospective coding. Like in the standard T-maze task, during the sample phase mice were forced in one of the four goal locations (Spellman et al., 2015). During the choice phase this goal location and one other goal location was opened, the animal had to visit the other location to retrieve a reward (delayed non-match-to-sample, DNMS). With this alteration, the animal could not possibly know the arm it has to visit during the choice phase while it is in sample or delay phase, so no decoding of the future goal can be expected. Additionally, decoding of the sample goal location was only possible after the animal entered the goal arm and only till it was back in the start box, so no retrospective coding during the delay was found. Decoding the sample goal during the choice run from mPFC activity was also not possible, although the animal could not know the future goal location, because of the four different goal arms. This indicates that the past goal should be represented somewhere else. Similar to this, there is also another study that cannot find evidence for memory maintenance in the mPFC during the delay (Bolkan et al., 2017). Neurons that show elevated delay phase activity and neurons that are spatially tuned are mostly mutually exclusive. Interestingly the delay phase elevated units show lower activity in incorrect trials, this difference is mostly gone if the MD to mPFC terminals are inhibited. Further they are affected by MD to mPFC terminal inhibition during the delay phase and show lower, but still elevated, activity. On the other hand, the spatially tuned units are affected by silencing the ventral HPC to mPFC inputs, strongest during the sample phase. One important influencer of delay phase activity seems to be the duration and predictability of the delay phase. In a delayed response task in head-fixed mice where the animals had to lick at one of two reward spouts, either coming from the left or right. During the sample phase one of the rewards spouts was present, during the choice phase with both spouts present they had to lick at the same spout (delayed match-to-sample). The activity in the mPFC was dependent on whether the delay phase was fixed at 4 s or if it was variable between 1 and 7 s. How neurons were active was more dependent on the session type than on the identity of the sample goal. Sample goal decoding during the delay phase was higher during random delay

sessions than during fixed delay sessions, but above chance for both session types indicating goal selective activity (Park et al., 2019). This could indicate a higher working memory demand for this variable delay, where additional neurons in the mPFC are recruited to allow successful task performance.

Specifically recording either optical tagged parvalbumin positive (PV) or somatostatin positive (SOM) neurons in a discrete trial delayed SWM task with a fixed three second delay in a figure-eight maze showed, that SOM neurons showed higher sample goal arm specific delay activity than PV neurons, but above chance decoding of the sample goal was possible in both neuron types. In error trials sample goal decoding was significantly lower in SOM neurons and stimulating SOM neurons led to behavioral deficits, but only with a 10 s delay (Kim et al., 2016). Also, in a different study using Neuropixels probes to record hundreds of single units while rats performed a more complex task using three different start and goal locations and unpredictable routes between them no evidence for goal selective delay activity could be found in any of the mPFC subregions (Bohm & Lee, 2020). Using calcium imaging to identify goal coding in the mPFC during the T-maze DNMS task enables, similar to probe recordings, a high number of simultaneously recorded cells that could be useful for goal decoding. In one study, cells coded differently for the left and the right arm during both, sample, and choice phase and also dependent on running direction (Vogel, **Hahn** et al., 2022). Differences were also observed in the stem, when the animal returned from the sample goal leading to above chance goal decoding. Decoding the current goal was also possible while the animal still was in the stem of the maze during the choice phase, but not during the delay. This indicates that information about the future goal is either transferred back to the mPFC at that phase or still present but not detected during the delay. Overall, these contrasting findings might indicate a role of the specific task design, like if a specific delay was used (Kim et al., 2016; Yang et al., 2015) or if the factual delay was just the time the animal needed to run in the central arm and for reward consumption (Baeg et al., 2003; Jung et al., 1998). Additionally, the length of the delay might play a role if goal specific delay activity can be found in the mPFC or not, with a trend to lower goal representation in tasks with longer delays. Also, the complexity of the task, like the number of possible goal locations, seems to be important.

Apart from cue or goal related coding, different other task related variables like spatial position, reward, running direction and others are encoded in the PFC. While some cells code specifically for single variables many of them also code for multiple variables (Jung et al., 1998; Vogel, **Hahn** et al., 2022; Yang et al., 2015). Calcium imaging of mouse PFC pyramidal cells during the T-maze DNMS task and subsequent linear modeling with different task variables revealed that the position of the animal in the maze is a strong influencer on neural activity.

Hereby position alone is not the driver of this activity but position together with other factors such as the running direction and the current goal (Vogel, **Hahn** et al., 2022).

Together this indicates that the mPFC in rodents as well as the dlPFC in monkeys is highly involved in WM. Inactivation studies show the necessity of the PFC to perform WM tasks successfully but with different restraints. Hereby the PFC and its integrity within its circuit is necessary during all task phases. Neural correlates of the PFC are WM task-specific and while some reports, especially in monkeys, show a clear decision specific delay activity this area is less clear in rodents, where for some tasks no clear delay activity can be identified. Overall representations of different cues, goals and the current spatial location can be seen, that are a necessity to successfully perform those tasks. Representations seem to depend on the specific task structure including the identity of cues and the length of the delay.

The prefrontal cortex plays a role in anxiety processing and fear learning

Anxiety and, with that, avoidance of threatening situations is a key factor in survival. Learning which situations are safe and which must be avoided is crucial to prevent harm or even death. Unfortunately, there are also many disorders that are linked to inadequate anxiety processing in humans like post-traumatic stress disorder (PTSD) or phobias.

Classic tests of anxiety and fear in rodents include the elevated plus maze (EPM) or fear conditioning (FC). While the EPM is a spontaneous behavior test where the innate avoidance of open and exposed areas is tested (Hogg, 1996), FC is a classical conditioning paradigm where a previously neutral stimulus, in most cases a tone (conditioned stimulus, CS) is paired in time with a noxious stimulus (unconditioned stimulus, US), normally a foot shock. In response to this threat rodents react with phases of immobility (freezing) but also changes in cardiovascular, respiratory, or endocrine activity (unconditioned response). In the laboratory freezing is often used as the behavioral readout as it can be noninvasively measured (McClelland & Colman, 1967). Other behavioral readouts like changes in cardiovascular or respiratory activity require further, mostly invasive, measurement devices and are therefore less used. After presentation of multiple CS-US combinations the animal will learn the association between the two. If the animal gets probed afterwards a CS presentation alone will elicit the same behavioral responses (conditioned response, CR). After presenting the CS without the US for multiple times animals will start to extinguish and will reduce the CR. This seems to be another form of learning by forming a new extinction memory in contrast to simply forgetting or erasing the CS-US association, as there are different forms of spontaneous recovery of this association (Bouton, 1994). The key region for these emotional processes in the brain is the amygdala (LeDoux, 2000) but also the PFC is involved in those processes (Giustino & Maren, 2015).

The EPM on the other hand does not require any learning. It was first described by Handley & Mithani (Handley & Mithani, 1984) and classically consists of four narrow arms of equal length outgoing from a center platform in a ‘plus’ configuration. All arms are equally highly elevated from the ground and two opposing arms are either surrounded by a high wall (closed arms) or just consist of the arms (open arms), sometimes with a small railing. The test utilizes the innate fear in rodents of open and elevated spaces and the clear preference for dark and enclosed areas in contrast to their innate motivation to explore novel environments (Walf & Frye, 2007). Untreated animals put in the maze for free exploration tend to spend more time in the closed arms and make fewer entries to the open arms with the difference depending on species, sex, and other factors (Baran et al., 2010; Tucker & McCabe, 2017).

Inactivation studies have shown diverse results after lesioning the mPFC of rats. One study that lesioned the IL and PL subregions of the mPFC specifically found a reduced time spent in the open arms (Jinks & McGregor, 1997) indicating an increase in anxiety. In line with that another study inactivating mainly to the prelimbic subregion showed the same effect, the rats reduced their time in the open arms in comparison to control animals (de Visser et al., 2011). In contradiction to that one study showed an increased time spent in the open arms and more entries to the open arms in comparison to untreated controls after bilateral lesions (Shah & Treit, 2003). Another study even reported a hemisphere specific effect. Lesioning of the right hemisphere led to increased exploration in the open arms while lesioning the left or both hemispheres had no effect in comparison to control animals (Sullivan & Gratton, 2002). Stern and colleagues also reported an increased time spent in the open arms after temporary PL inactivation both during first and second exposure to the EPM; but inactivation during first exposure had no effect on untreated exploration during a second exposure (Stern et al., 2010). These diverse results further indicate that the specific mPFC subregion, the extent and type of the lesion can have very different and even contradictory effects hinting at a diverse role in anxiety processing. Single unit recordings in the mPFC hint in a similar direction: Two groups of cells can be found that show an increased activity related to anxiogenic features of the maze (Adhikari et al., 2011). While one group increases their firing rate while the mice are in either of the two open arms the other group gets activated in both closed arms. This indicates a general role in anxiety processing and no clear coding for just threat or safety. Similar types of cells can also be seen in an open field (OF), where some cells tend to fire more in the center, where the mouse is exposed and others are more active while the animal is in the corners or close to the wall (Weible et al., 2009a).

Studies on conditioned fear learning also point in diverse directions with results seemingly contradicting each other. Electric lesions of the mPFC prior to fear learning led to longer time needed for extinction learning (Morgan et al., 1993). The same group later specifically lesioned

the PL part of the mPFC and found an increase in freezing levels and additionally a longer time needed for extinction (Morgan & LeDoux, 1995). Similarly, using muscimol for mPFC inactivation directly before extinction training, the mPFC has been shown to be necessary for the expression of fear memories after both, two and thirty days (Blum et al., 2006). Another group could not find an effect of electrolytic mPFC lesions, either happening before fear conditioning or after a first extinction session, on fear extinction memories (Garcia et al., 2006).

Two opposing roles during fear expression and extinction for the IL and PL subregions have been suggested. The PL in general is seen as a driver of fear expression and IL as a regulator for fear extinction with many studies supporting that view, but also studies that show other results. In support of a bifurcated distribution of tasks between the PL and IL, IL inactivation during fear extinction impairs extinction learning. The impairment in extinction occurred both during the extinction learning session and an extinction test on the following day, indicating a role for extinction memory (Akirav et al., 2006; Sierra-Mercado et al., 2011). PL inactivation in contrast led to a decrease in fear expression but no change in the formation of fear memory (Sierra-Mercado et al., 2011). Brief microstimulation at the beginning of a paired CS presentation to mimic neuronal tone responses during extinction learning in the PL subregion reduced fear extinction learning while stimulating the IL subregion during extinction enhanced fear extinction learning (Milad & Quirk, 2002; Vidal-Gonzalez et al., 2006).

Some of these seemingly contradictory results might be explained by off-target effects of the methods used. Pharmacological inactivation is hard to limit to the area of a specific prefrontal subregion. Similarly, electrolytic lesions or electrical stimulation can also affect neighboring regions, can influence fibers of passage and stimulations can also lead to ortho- and antidromic activation in other brain regions. In contrast direct recordings of neural activity can be mapped precisely to specific subregions but can only lead to neural correlates of behaviors that lack information if the regions are necessary to perform those behaviors.

Recordings in the IL of rats during fear conditioning showed increased spiking in response to the CS only in a second extinction session but not during habituation, conditioning or the first extinction session (Milad & Quirk, 2002). This increase was correlated with reduced freezing behavior during that second extinction session. The activity of PL or medial orbital cortex neurons was not modulated by tone onset in those sessions. In contrast, other studies reported that across PL and IL 75% of single units responded to the CS (Baeg et al., 2001). The activity of those neurons was correlated to freezing levels during fear extinction. If a delay between the CS and the US was introduced, many of the cells recorded showed delay specific activity that was terminated at the time point of the expected US. Another study found responsive cells in IL and PL as well. IL responses were already seen to the tone onset in baseline conditions

and during early extinction training but also a clear CS response in PL neurons has been found (Chang et al., 2010). The number of neurons responding to the CS more than doubles from habituation to conditioning and early extinction, while it returns to baseline conditions during late extinction (Burgos-Robles et al., 2009). Most of these responses are excitatory and the activity in the PL was correlated to the amount of freezing. Animals that showed higher fear levels during an extinction recall on the following day had a higher increase in PL activity and a higher percentage of tone-responsive neurons. This higher proportion was already detectable during conditioning and extinction training, where freezing levels were similar.

An extinction deficient mouse strain (Camp et al., 2009), showed increased single unit activity compared with C57BL/6J mice in the PL during an extinction retrieval phase in response to CS presentation (Fitzgerald et al., 2014). Surprisingly vmPFC (including IL) activity was higher than in control mice during early extinction training. Fear levels could be reduced by giving chronic fluoxetine, a clinically relevant pharmacological treatment, that led to lower fear levels during extinction retrieval but did not increase vmPFC activity in that phase. In contrast to that the expression of the immediate-early gene Zif268 was increased (indicating activity in those neurons) specifically in layer II of IL after extinction retrieval, but it remains unclear if that is a FC phase dependent effect of the treatment. In this study they also report a difference between animals that successfully extinguish that have a separation between conditioning and extinction of 24h. They show a decrease in activity in response to the tone during the late phase of the extinction session. In contrast to a separate group of animals that received extinction sessions immediately after conditioning and did not extinguish, where no firing difference between early and late extinction was found (Chang et al., 2010). Additionally, briefly stimulating IL neurons electrically facilitated extinction learning already in the first extinction session that also led to better extinction memory in a second test session (Milad & Quirk, 2002).

The prefrontal cortex is required for social processing

Most animals interact with conspecifics daily, often for mutual benefits. Many live together in social groups and cooperate when searching for food or shelter, all with sexual reproduction need a partner to beget offspring. Others compete and fight for limited resources like territories, food, or sexual partners. Adequate reactions when meeting known or unknown conspecifics, caring, mating, fight, or flight, must be chosen flexibly in order to survive. There is accumulating evidence for involvement of the mPFC in these behaviors.

An early study looking at rats in different social behaviors found an increased emotionality score after lesioning the mPFC (Kolb, 1974). The animals showed an increased escape behavior in comparison with sham operated control rats by interactions with humans while no

general loss in sociability or change in aggression was found. More recently tests for sociability are often social exploration tests, during which the test-animal can move around freely and interact with different social and non-social targets, sometimes behind a grid. Constraining the social target limits its ability to influence the interaction. If there is no grid to constrain the social target mouse normally OF are used. Lesioning the PL area during social interaction led to an increased duration of social contacts while novelty exploration per se was not altered (Avale et al., 2011). The authors speculate that this increase in social behavior could be due to the inability to disengage from social contacts. In this line, increasing the excitability of mPFC neurons reversibly led to a decrease in social interaction duration as animals disengaged earlier than control animals (Ferenczi et al., 2016).

Another typical social interaction test example is a three-chamber test, where the test mouse can move freely between the three chambers, one contains a wire mesh cup with a conspecific, the center chamber is empty and the other one contains an empty mesh cup or a mesh cup with an object. This context is now often used slightly altered as an elongated box with one compartment at each side. WT mice prefer the compartment with the conspecific over the compartment with the empty mesh or object. The preference for the social target is gone after optogenetically overexciting the mPFC (Yizhar et al., 2011). Similarly, after lesioning the PFC, mice showed no preference for a social target over an empty compartment anymore and did not discriminate between a novel social target in comparison to a familiar one (Liang et al., 2018; Murray et al., 2015).

Neurons in the mPFC seem to be activated by social interactions. The PL region of socially deprived mice was specifically activated during social interactions in an OF as revealed by increased c-Fos expression (Avale et al., 2011; Kim et al., 2015). For the IL region this effect is not as clear. Although the region showed increased c-Fos expression after social interactions, the cells were similarly activated as by novel objects, hinting to a role during general novelty processing and not social interaction specific (Avale et al., 2011) but another study reported increased c-Fos expression for both, novel and familiar conspecifics in comparison to a novel object interaction (Gutzeit et al., 2020). Increased mPFC activation was confirmed in another study using electrophysiology during social interactions between rats in an OF (Jodo et al., 2010). Similar to the effects in the OF, single-photon calcium imaging has shown that cells in the mPFC of mice increase their activity when the test mouse interacts with a conspecific compared to an empty grid compartment or a grid with an object behind it (Lee et al., 2016; Liang et al., 2018). These differences were most prominent during the early interactions as well as in interactions with a second, novel conspecific, indicating a role in novelty as well. This effect is not purely driven by spatial coding as there are neurons responding to social interactions if the position of the social target and the object is switched

(Lee et al., 2016). Two distinct, stable populations of neurons can be identified that increase or decrease their activity relative to the onset of the social target exploration (Liang et al., 2018). Both populations are of similar size and are not responsive in every exploration epoch but are highly correlated to behavior as a group. These ensembles get partly disrupted by acute phencyclidine (PCP) administration together with a decrease in social exploration. PCP is a N-methyl-D-aspartate (NMDA) receptor antagonist.

But the mPFC is not the only brain structure that is involved in social interactions. The amygdala and the nucleus accumbens (NAc), among others, are two structures involved in social behaviors, but they also have direct connections to the mPFC. Specifically stimulating the terminals of PL neurons in the NAc optogenetically reduced the time spent with the social target, indicating a crucial role for this connection (Murugan et al., 2017). This effect was observable both in an altered three-chamber test as well as during free social interaction in the home cage. Interestingly this also led to a learning effect. Mice spent less time in an area that had a social target paired with PL-NAc cells inhibition, even on the day following the exposure with no social targets present. The opposite was observable by stimulating these cells while mice explored one of two social targets, mice developed a clear preference for the target that was paired with PL-NAc activation, even on the next day without the targets present. As inhibition in that zone without targets had no effect on the behavior there seems to be a social learning related effect facilitated by the PL to NAc projections. Imaging the PL neurons projecting to NAc some neurons that respond to social targets can be identified, although there are also some neurons that are clearly place coding or just coding for the social target at a specific position (Murugan et al., 2017). Interestingly, for the PL-BLA connection, inhibition had no effect, but activation led to a decrease in social exploration, an effect opposite to that observed after stimulating the PL-NAc connection. Inhibiting the opposite direction, BLA terminals projecting to the mPFC, led to an increase in social exploration (Felix-Ortiz et al., 2016). Murugan et al. also could not find an effect of PL-BLA activation by using a three-minute continuous stimulation protocol while Huang et al. limited the stimulation to the immediate duration of social exploration (Huang et al., 2020; Murugan et al., 2017). But using the same inactivation in the IL-BLA connection led to a deficit in sociability while here activation didn't show an effect (Huang et al., 2020). These differences in behavioral outcomes are likely due to the distinct BLA populations targeted by the two mPFC substructures. They could either directly alter social behaviors or might also in general modulate emotional states, which then lead to differences in those behaviors.

Not only are positive social experiences encoded in the PFC, but there are also neural correlates of competitive behavior (Kingsbury et al., 2019; Wang et al., 2011) or aggression (Takahashi et al., 2014). In the tube test two mice walk from opposite directions in a tube that

is too narrow for them to turn. If one mouse pushes forward the other mouse must retreat backwards in the tube, the non-preferred behavior in such a situation. Both mice push and retreat till the dominant mouse pushes the subordinate out of the tube. After completing the tube test, dominant mice show higher c-Fos expression in the PL. They also have stronger excitatory synapses and manipulating this could change their social status bilaterally (Wang et al., 2011). Additionally, clear neural correlates in the dlPFC to the different behaviors in this test, pushing, retreating, or approaching can be identified (Kingsbury et al., 2019). It seems that not the PFC is not only involved in but also defining the social structure between animals.

Most of these studies just look at the neural activity of a single animal and often have different restrictions for the recorded and the target conspecific. Imaging the PFCs of two mice simultaneously while they interact freely revealed that on the population level the activity in the mPFC is highly correlated. This is true for both free interaction as well as in the tube test described above, but not if there is no direct interaction between the two mice due to a plastic separator. But not only on the population level, also on the single cell level many of the neurons show high correlations between the two animals. Interestingly this is not just because of correlated behaviors but also cells that clearly encode the behavior of the interaction partner. Hereby the behaviors were asymmetrically encoded, the more dominant partner showed a stronger representation of its own behavior and higher mPFC activation overall while in the subordinate stronger encoding of the behavior of the opponent could be seen (Garcia-Font et al., 2022; Kingsbury et al., 2019). Together this suggests that during social interactions not only the interaction itself but also the behavior of the conspecific as well as hierarchy are represented in the PFC. Social behaviors including dominance between conspecifics seem to be well represented within the mPFC with not only a representation of one's individuals' actions but also with representation of the conspecific, and changes of sociability after inactivation.

Novelty and familiarity are encoded in the prefrontal cortex

Novel environments, situations or objects present opportunities and risks in our daily lives. Many animals including humans have an innate curiosity to explore those novel stimuli extensively. Evolutionary this can be advantageous, identifying threats as well as new opportunities like food sources or shelter is beneficial for survival. On a neural basis it seems that novelty itself already has a rewarding value, even without directly rewarding features (Reed et al., 1996). Rodents also show this innate preference for novelty which is used in novel object recognition tests (Ennaceur & Delacour, 1988). In the first phase, the sample phase, two identical objects are presented at specific locations, in the second phase either one of them is replaced with a novel object or one of them is put to a new location. Both changes lead

to an increased exploration duration of the animal at the novel object or the familiar object at the novel location (Chao et al., 2020; Wang et al., 2021; Weible et al., 2009a).

To detect if a stimulus is novel, its identity must be detected and compared with already stored information about previous stimuli. It has been shown in primates that PFC neurons can code for object identity and location (Rainer et al., 1998). Early lesion studies reported that neither the ACC nor the more frontal parts of rat mPFC are necessary for this novel object preferring behavior with short delays (Barker et al., 2007; Ennaceur et al., 1997; Hannesson et al., 2004). It was claimed that while the frontal parts of the mPFC are also not necessary to discriminate between novel and known locations of objects, the ACC is only required for novel location memory (Ennaceur et al., 1997). However, more recent studies show that recognition memory retrieval is impaired by ACC inactivation (Pezze et al., 2017). These differences might originate in adaptive processes after permanent lesioning in comparison to short-term inactivation. The effect of ACC inactivation was restricted to the retrieval of the memory as inactivation prior to the sample phase had no effect (Pezze et al., 2017). In contrast, another study showed temporary inactivation of the mPFC directly after the sample phase led to impaired object recognition hinting more to an effect in memory encoding or consolidation (Tuscher et al., 2018). These conflicting results might indicate that different subregions of the mPFC might be differently involved in novelty processing. Another study also points to a time dependency of the inactivation. Different drugs led to an effect after 24 h but not after 3 h. Again, the drug administration was reported to be time sensitive, infusion shortly after the sample phase is crucial for it to be effective (Akirav & Maroun, 2006). This shows that the timing of the inactivation is important and the role of the mPFC might be restricted to memory formation or retrieval dependent on different substructures.

Changing the concentration of neuromodulators in the mPFC led to contrasting results. Stimulating dopamine D1 receptors in the PL before the sample phase did reduce recognition performance after a delay (Pezze et al., 2015). On the other side, using a D1 antagonist in the PL led to the same effect with a comparable delay between the phases (Clausen et al., 2011). In another study only long-term memory was affected by, but not shorter memory (Nagai et al., 2007). This indicates that the dopaminergic input to the mPFC plays a role in either encoding or retrieval of this object memory and that the right balance is necessary for successful memory storage or recall. Hereby the effect is dependent on the dose and spread of inactivation.

Overall neural activity in the mPFC seems to increase with novelty explorations. c-Fos expression was increased in the mPFC of mice immediately after exposure to novel objects (Nagai et al., 2007; Tanimizu et al., 2018; Wang et al., 2021). Hereby just observing the novel objects was sufficient for increased c-Fos expression in comparison to the observation of

familiar objects (Zhu et al., 1995). This indicates that mPFC cells are activated by novel object presentation. Although there are only a few studies recording neural activity in the PFC during object recognition, there are some clear neural object- and novelty-correlates found. Most cells in the ACC changed their firing rate in response to an object location in an OF. The majority increased their activity if an object was present, but some cells also showed a decrease. While some responded to both objects, others just responded to one of the objects, even if they are the same. Many of these responses were also stable across multiple sessions. Interestingly, many cells started to respond only after changes in object identity or location. This occurs for both, the familiar as well as for the novel objects and at familiar and novel locations, interestingly also at the now vacant position (Weible et al., 2009a). A similar increase in activity during novel object recognition was reported for the PL region. Interestingly, while PCP treatment did not alter mPFC activity per se, activity during novel object exploration was indistinguishable from familiar object exploration after PCP treatment. This came together with a behavioral effect: The PCP treated rats did not prefer the novel object (Asif-Malik et al., 2017). Wang and colleagues draw a more detailed picture, although they also record neurons increasing their firing rate, they see more cells that decrease their activity (Wang et al., 2021). They report that more putative fast spiking interneurons increase the activity, while a higher proportion of principal cells decrease their activity which could lead to a net effect of increased overall activity. Overall, it seems that the mPFC has some relevance in processing novel object information but that other structures can replace the mPFC when it is dysfunctional. Replacement seems to be impossible for some specific cases of object memory, for example the retrieval after longer, in most cases 24 h delays.

Stable encoding of different behaviors in contrast to flexible action selection

Together these results show that the mPFC of rodents is involved in the execution of different, basic behaviors. For some of those behavioral tasks the mPFC is necessary for successful execution, for others like some forms of novelty recognition it just codes for specific variables without being essential. But very little is known how the same neurons are activated across multiple sessions of the same task, and how the execution of other behaviors in between may influence the coding. While some features of the behaviors overlap, for example different relevancies of locations, others are specific to single behaviors, like the reaction of a social partner or the texture of an object.

Stable codes for similar task features might be beneficial as fewer cells would be necessary to code during different behaviors. To code for the exact context the specific activation patterns of multiple cells would be required which is called “distributed coding”. Every cell could then code for different task features in a nonlinear way. The combination of activation patterns then

would code for the information, which is known as “mixed selectivity” (Rigotti et al., 2013). The other extreme would be the grandmother cell, sometimes also called “Jennifer Aniston cell”, a cell that codes very specifically to one specific feature, landmark, object, or person, in this case, very different pictures of the actor Jennifer Aniston but not other actors, famous people, objects or landmarks, not even Jennifer Aniston together with other people in one picture (Quiroga et al., 2005). Even the written name of the feature could activate the cell in some cases. This would be an extreme example of “sparse coding”, where one item is encoded in one cell. Sparse coding would require a high number of cells but only a few cells would need to be activated together. To achieve flexibility, it is likely that the PFC shows distributed coding with mixed selectivity rather than sparse coding, as novel stimuli would always require new cells, or the previously coded information would be lost.

But how different task related information within the same neurons is represented in the PFC still remains unknown. Jung and colleagues recorded from PFC single units in rats while they performed an eight-arm radial maze spatial working memory task and a delayed spatial alternation task one after the other (Jung et al., 1998). Only slightly above 10% of the recorded neurons showed similar correlates to related behaviors like “goal approach” or “at goal”, but they also had additional correlates that were not common across the tasks. They speculate that the representations in the mPFC are not just defined by sensory information or motor output but by abstract task phases and rules. Additionally, it remains possible that the relevant and overlapping task features like positional coding were not extracted well enough to find correlated activity across the tasks or that the features in the task were not similar enough to elicit the same code. Also, for the primate PFC there are already reports for stable across task representations. One study showed stable representations across three different tasks within one session in the PFC of monkeys for cues and other task periods, indicating that task features are stably represented across different behaviors (Asaad et al., 2000). But this is just done within one session, so it is unclear if these representations stay stable over longer time periods.

Imaging neurons in the amygdala in mice across three behavioral tasks revealed two ensembles of neurons coding for specific task features across the different tasks. In one ensemble which Gründemann and colleagues call “exploratory” they group the neurons that show excitation while the animal in in the safer corner of the OF, in the non-preferred (both open, one closed) arms of the EPM and when the animals stopped freezing after FC. The other group that they call “non-exploratory” was activated when the animals started freezing, while the animal was in the preferred closed arm and in the center of the OF (Gründemann et al., 2019). This example shows that, at least in another brain region, the amygdala, there is a relationship in neuronal ensemble activation across different tasks, with groups of neurons

responding in a similar way to specific task features. Although tasks are not repeated multiple times, the emergence of ensembles that code for specific variables across multiple tasks and days suggests that their activation is somewhat stable.

It is already known for a long time that some other cells in the brain show stable representations for specific features over days and months. One of the earliest reported examples of stable patterns is the presence of place cells in the HPC. Place cells get consistently activated when the animal is in a specific location and this activation can be stable over multiple sessions, if the environment does not change (Thompson & Best, 1990). More recently this view is a bit less clear, although there is some stability in place cell coding, drift between sessions has been reported (Kentros et al., 2004; Mankin et al., 2012; Rubin et al., 2015), whereas high stability in spatial coding was observed in the dentate gyrus (Hainmueller & Bartos, 2018). Not only in those regions, but also in other brain areas including the PFC, stable representations are reported. Assad et al. recorded the same neurons from the lateral PFC in monkeys during three different behavioral tasks repeated multiple times but within one session. They found that the baseline activity of more than half of the recorded neurons changed depending on the current task the animal had to follow, consistent across different repetitions of the same task (Asaad et al., 2000). About one quarter of the cells showed task-specific stimulus activity. This indicates that there is some stability across different tasks, both after returning to the same task as well as coding for the same stimulus across tasks.

Another study in monkey PFC also showed stable responses for task selective cells across two days during different Go/No-Go tasks (Greenberg & Wilson, 2004). Additionally, there are also examples of stability in the PFC of rodents. During the tube test many PFC neurons show neural correlates for pushing, resisting, retreating but also for stillness, moving forward and withdrawal. Cells identified across different sessions show some consistency in their task related coding, about 20% code uniquely for the different task variables across different sessions (Garcia-Font et al., 2022). About 30% of the cells that code uniquely for one of the tested task variables code for any task variable uniquely during the other sessions. This indicates that although some of the cells code stably for a specific variable, others change their task related activity.

In this study, only task related correlates are measured but others like the position of the animal are not tested, although spatial coding is a common feature across many behavioral tasks. Stable position coding has been shown for PL neurons during a spatial navigation task. Spatial cell activity in an altered figure-eight maze was correlated across sessions with about 40% of cells having a correlation coefficient of 0.8 or higher, compared to less than 5% for random cell pairs (Powell & David Redish, 2014). Another study showed that neurons in the mPFC of mice

that explore a track in a virtual environment also show some spatial tuning. If they are getting exposed to a novel virtual environment afterwards, these cells remap to a novel code but after returning to the old environment, part of the original coding is reinstated (Sauer et al., 2022). These codes appear in the absence of a specific task or reward but the exposure to the environments happened within one day, so no statement about long term stability can be made. Though, for other brain regions than the mPFC, including the HPC or sensory areas "representational drift", the change of neural representations over time, has been reported (Rule et al., 2019).

Investigating the stability and flexibility of medial prefrontal cortex neurons during different behaviors

In this study we build on this previous work and systematically investigate stability and flexibility of neural codes in the mPFC. We image the same neurons in the mPFC of mice during learning and execution of different behaviors. To be able to image the same neurons over multiple days in freely moving animals we use the Miniscope, a miniature microscope, and image calcium fluctuations in pyramidal cells selectively. We let the animals perform five different behaviors, a SWM task, three spontaneous tests of innate behaviors, and one discriminatory aversive learning paradigm using classical FC. With this we investigate how prefrontal neurons that code for task-specific features in one task respond to other, sometimes similar features in another task. We also investigate more general behavioral variables like spatial coding or movement speed to determine if they are consistently encoded within the same task, as well as whether the same cells encode them across various tasks. Additionally, we aim to investigate how exposure to other tasks alters these representations.

Methods

Animals

Thirteen male C57BL/6N mice (Charles River Laboratories, Wilmington, MA, United States) aged 8-10 weeks at delivery were used for the calcium imaging experiments. The mice were housed in groups of up to four in acrylic cages (35 cm x 19 cm x 14 cm) prior to their first surgery. The cages floor was covered with bedding material (Aspen animal bedding, Abedd SIA, Kalnciems, Latvia) and the animals received nesting material (Sizzlenest, Scanbur Technologies, Karlslunde, Denmark) as well as a red acrylic mouse house (mouse house, Tecniplast, Province of Varese, Italy) for enrichment. Food pellets (Ssniff Spezialdiäten GmbH, Soest, Germany) and a water bottle containing tap water were provided ad libitum in a metal grid below the filtertop of the cage. After the initial surgery animals were single housed in an acrylic cage (35 cm x 14 cm x 12 cm) and the house as well as the metal grid were removed to reduce the risk of injury with the implant. Ad libitum food (see above) was provided on the cage floor and a small water bottle was fixed to the cage lid. During behavioral experiments the animals were food restricted and the amount of food the mice received was limited. Animals' health and body weight were monitored daily after initial surgery.

The cages were kept in ventilated animal scantainers (Scanbur Technologies, Karlslunde, Denmark) with a 12h dark/light schedule. All experiments were conducted during the light cycle. All procedures were approved by the local animal care committee (TVA FU-1038 and FU-1256, Regierungspräsidium Darmstadt, Germany).

Surgical procedures

Prior to all surgeries mice were placed in a small box flooded with 4-5% isoflurane (Forane, AbbVie, North Chicago, IL, United States) in oxygen for anesthesia initiation. When the respiratory frequency was below 1 Hz animals were placed in a stereotactic frame (Model 940 or Model 1900, KOPF, David Kopf Instruments, Tujunga, Canada) on a closed loop-controlled heating pad to maintain body temperature. The head was placed in an inhalation mask where they received a continuous level of 1-2% isoflurane in oxygen at a rate of 0.35 l/min to keep them anesthetized. Respiration rate was monitored during the surgery and isoflurane concentration was adjusted to maintain a breathing rate of 1-2 Hz. To avoid corneal dehydration eye cream (Vidisic, Bausch & Lomb GmbH, Heidelberg, Germany) was applied at the beginning of the surgery and renewed afterwards if necessary. Small parts of examination gloves were put over the eyes to protect them from the later applied ultraviolet (UV) light. During the invasive surgeries Lidocaine (EMLA cream, AstraZeneca GmbH, Wedel, Germany) was applied to the scalp as a local anesthetic to the area of the incisions. Additionally, the

animals were injected subcutaneously into the neck with Carprofen (4 mg/kg; Rimadyl, Pfizer, New York, NY, United States) as general analgesic and dexamethasone (2 mg/kg; Dexa 8 mg inject, Jenapharm, Jena, Germany) to avoid inflammation. Fifty µl of atropine solution (1:10 in saline; Atropinsulfat 0.5 mg/ml, B.Braun, Melsungen, Germany) were injected intraperitoneally as a bronchodilator and 800 µl ringer solution (2*400 µl, Ringer-Injektionslösung, B.Braun, Melsungen, Germany) were injected subcutaneously on both sides of the abdomen for maintenance of the fluid balance.

The head was fixed in the stereotactic frame using head or ear bars and an incision was made to expose the skull. The skull was leveled between bregma and lambda as well as between the left and right half to allow for precise use of brain coordinates. A small part of skin was removed, and the skull was cleaned and scraped with a scalpel. Three small holes were drilled into the skull for skull screws (two on the right/left side between bregma and lambda and one on the right side behind lambda) and a larger craniotomy was made above the left mPFC (center at -1.95 mm anterior to bregma, 0.35 mm left to the midline). Skull screws were sterilized in ethanol and screwed for ~2 turns into their holes. A small drop of medical-grade superglue (Loctite 4011, Henkel, Herts, United Kingdom) was applied to the threads to increase screw-bone bonding. The screws were then turned an additional ~1 turn, without contacting the brain surface below, and protruded from the skull to enable subsequent fixation of the implant and enhance stability. Medical glue (see above) was applied to the edges between skull and skin to seal the wound.

For virus infusion a Hamilton syringe (NanoFil syringe, 10µl, World Precision Instruments, Sarasota, United States) with a 35-gauge needle (NanoFil, NF35BL, 35 GA BLUNT NEEDLE, World precision Instruments, Sarasota, United States) was filled with a AAV1-CaMKII-GCaMP6f (AV-1-PV3435, UPENN Vector core; titer 2.3*10^13) viral construct diluted 1:10 in artificial cerebrospinal fluid (Artificial CSF, 59-7316, Harvard apparatus, Holliston, MA, United States). The needle was slowly lowered into the left mPFC (coordinates as above, depth 1.5 mm with respect to brain surface and 500 nl of virus solution was infused at a rate of 50 nl/min controlled by a micro-syringe pump controller (Ultra Microsyringe Pump, Micro4, World Precision Instruments, Sarasota, United States). To allow proper diffusion of the virus in the target area the needle was left in place for 10 minutes after completed infusion, retracted for 50 µm and kept there for another 5 minutes before retracting it completely from the brain.

Following the virus infusion, a 0.5 mm diameter gradient refractive index (GRIN) lens (4 mm long; #002181, Inscopix or #CLHS050W002055NN, GoFoton) was placed at the same location. The lens was fixed on a specifically designed GRIN lens holder and slowly lowered into the left mPFC (coordinates as above). After the target depth was reached the lens was

fixed to the skull and skull screws using UV-light curing glue (Permaplast LH Viscous Flow, M+W Select, Büdingen, Germany). Afterwards a small headbar (Headpost small – S, or Headpost Dovetail – M, both Luigs & Neumann, Ratingen, Germany) was fixed using a superglue gel (Pattex Sekundenkleber GEL MINI TRIO, Henkel AG & Co. KGaA, Düsseldorf, Germany). For increased stability dental acrylic (Paladur, Kulzer GmbH, Hanau, Germany) was used to secure the lens and the headpost to the skull. The acrylic was stained black by mixing it with black oil paint (Lukas Studio 382 Elfenbeinschwarz, Lukas-Nerchau, Düsseldorf, Germany) to avoid spreading of the excitation light and to avoid picking up ambient light during the experiments. The GRIN lens was covered with a silicone elastomer (Kwik-Sil, World Precision Instruments, Sarasota, United States) for protection. The mice were removed from the stereotactic frame, weighed, and placed on a heating pad in their home cage. They were provided with oats and a small cup containing water for easier availability to ease surgical recovery. After the animals showed free mobility the heating pad was removed, and the cage was returned to the scantainer.

After about three weeks the animals were habituated to being held tightly and afterwards to head fixation. To this end the head post on the implant was placed in a matching head post holder (Headpost holder – dovetail type, Luigs & Neumann, Ratingen, Germany) on a custom-made head fixation platform. A screwable adapter (Adapter plate TYPE 1, Luigs & Neumann, Ratingen, Germany) was first attached to animals implanted with a ‘Headpost small – S’ to fit into the holder. To ensure animals’ comfort during head-fixation they were placed on a soft foam platform enclosed by custom made plastic walls inside a dark chamber. This procedure was repeated 2-3 times on separate days for increased habituation to head-fixation.

Approximately four weeks after surgery and after successful habituation to head-fixation a miniaturized microscope (“Miniscope”, UCLA Miniscope v3.2 or v4) was lowered above the GRIN lens using a stereotactic arm while the animals were head-fixed. The miniscope was connected via a 50 Ohm coaxial cable to a miniscope data acquisition system (DAQ, custom made using Miniscope DAQ PCB, v2.3, Labmaker, Berlin, Germany, designed after Miniscope DAQ, miniscope.org) running firmware v2.01 or 3.2 (both https://github.com/Aharoni-Lab/Miniscope-DAQ-Cypress-firmware). The DAQ was connected to a computer running the miniscope software (MiniScopeControl v1 2.3, https://github.com/daharoni/Miniscope_DAQ_Software or Miniscope DAQ Software Version 1.1, https://github.com/Aharoni-Lab/Miniscope-DAQ-QT-Software) to visualize the video stream and adjust the excitation settings. The brain area below the GRIN lens was imaged continuously at 20 Hz to identify the optimal field of view (FOV). If clear calcium activity could be seen a screenshot was taken at that location to identify landmarks like blood vessels of the area for later baseplate fixation. The baseplates were used to connect the miniscope to the

skull and keep it in position during the imaging sessions. Later that day animals were again anesthetized with isoflurane (anesthesia and stereotactic procedures as during initial surgery). Apart from eye cream no further medication was given to the animals. The silicone gel cap was removed from the GRIN lens and the lens as well as the surface of the implant was cleaned using 70% ethanol. A small metal baseplate (MS_Baseplatev3; Shylo Stiteler, UCLA, for miniscope v3.2 or Miniscope v4 Base Plate Variant 2, open ephys, Carnaxide, Portugal, for miniscope v4) was fixed to the miniscope with a small set screw and lowered above the implanted GRIN lens and moved to the position where the same FOV as during awake head-fixed recording could be seen. Several layers of UV-light curing glue were used to fix the baseplate to the implant created during the last surgery. After a stable connection was formed it was fortified with blackened dental acrylic to avoid light spread. When the acrylic was hardened the miniscope was detached and silicone gel was applied (v3.2) or a cap was fixed (v4) to the baseplate to cover the opening that enables imaging and avoid dust or bedding material on the lens.

After at least three more days of recovery the animals were food restricted to ~85% of their ad libitum body weight over a period of one week. During that week the animals were further habituated to handling and the mounting procedure of the miniscope. To this end animals were held tightly in one hand and the silicone gel was removed from the baseplate using forceps (v3.2) or the cap was removed loosening the set screw (v4). The miniscope was moved into the groove of the baseplate and held into place by small magnets on the miniscope bottom and the baseplate (miniscope v3.2) or just by the tight fit between baseplate and miniscope bottom (v4). The set screw was fixed to stabilize the miniscope in the baseplate. To ensure imaging of the same field of view the previously recorded landmarks were used. The focus was adjusted, if necessary, by moving the focusing slider in miniscope v3.2 or electrically by using the electrowetting lens on the miniscope v4.

Behavioral testing

General procedures

Animals were kept in a scantainer (see above) in the same room where the experiments were conducted. During experiments that involved sound learning (FC) animals that were not currently tested were placed in a different room in their home cage to avoid sound exposure during testing of the other animals. EPM exploration and the OF exploration and NO recognition were done on one day as well as the habituation and conditioning phase of fear conditioning, apart from that only one session was conducted per day.

All behavioral arenas were placed in the center of the same room. Light conditions were dimmed using red light by a light emitting diode (LED) strip placed about 80-100 cm above the

environments leading to an even illumination of about 8-10 Lux. A metal rod mounted to the ceiling was used to hold three cameras, the led strip, an infrared (IR) light source as well as a commutator for the miniscope. The commutator was connected to the DAQ (see above) which was connected to a computer to record the miniscope videos at 20 Hz. Digital TTL pulses were sent from the DAQ to a recording system (Digital LYNX system, Neuralynx, Bozeman, MT, United States) to align the miniscope signal to behavior control signals and behavioral cameras. One of the behavioral cameras was directly connected to the Neuralynx system to track the 2D position of a red LED on the top of the miniscope mounted on the animal. The system was connected to a dedicated computer to save the timestamps of the TTL pulses, the behavioral X/Y position and the video recorded with the Neuralynx camera. The second camera (Manta G 125 C, allied Vision, Stadtroda, Germany) was used to image IR light for better recording quality in the dimmed light conditions also recording at 20 Hz. This camera also sent TTL pulses to the Neuralynx system to align the acquired frames to the behavior.

The third camera was a standard webcam (Logitech C615, Logitech, Lausanne, Switzerland) to record videos of animal's behaviors. This camera was connected to a third computer that was also used to control the behavioral tasks using an Arduino microcontroller (the automated T-maze and FC). To align the behavior to the videos the microcontroller also sent TTL pulses to the Neuralynx system for specific behavioral events such as nosepokes, door movements or tones.

Prior to all experiments the animal was removed from the home cage. The silicone elastomer covering the lens was removed from the baseplate using forceps (Miniscope v3.2) or the plastic cap was removed by hand (Miniscope v4) and the miniscope was mounted on the head of the animal. Hereby the FOV was set to the same FOV as in the previous sessions. The animal was placed in an empty home cage containing only bedding material without nesting material to avoid getting caught with the cable. Focus and excitation LED intensity were adjusted as necessary. Afterwards the recordings were started, and the animals were placed in the respective behavioral environment. After the experiments the miniscope was dismounted from the animal and the hole in the baseplate was covered with silicone gel (Miniscope v3.2) or with a protective plastic cap (Miniscope v4) to protect the lens. The animal was weighed, and food pellets were placed in the home cage of the animal to maintain the animal at about 85% of its original body weight. Afterwards it was returned to the scantainer.

Spatial working memory in the automated T-maze (SWM)

The automated T-maze consisted of three wooden arms, the central arm (stem) was 40 cm long and 4.5 cm wide while the two goal arms were 36 cm long meeting at a 4.5 cm by 4.5 cm area (choice point). The arms were surrounded by a 4 cm high wooden wall. At the bottom of

the central arm was a 16 x 12 cm wooden start box surrounded by 24.5 cm high plastic walls (**Figure 4**A, B). Part of the start box was not accessible as it contained the reward port. Three plastic doors, one between the start box and the central arm as well as two between the center and the two goal arms were used to control access to the arms. Reward ports at the end of the two goal arms and in the start box were used to deliver sweetened condensed milk (Milch Mädchen gezuckerte Kondensmilch, Nestlé, Frankfurt, Germany) diluted 1:3 in tap water. Therefore, a solenoid was connected to a milk reservoir and a blunt needle in each of the reward ports. For reward delivery the solenoid was opened for 100-300 ms to ensure reward delivery of about 10µl per reward.

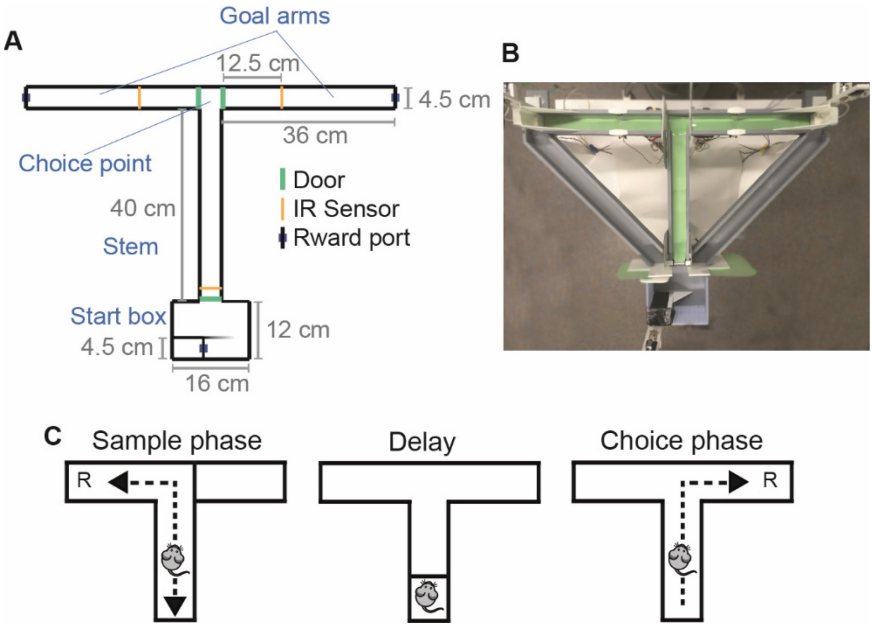

Figure 4: Spatial working memory in the T-maze. **A**: Schematic of the T-maze with doors and IR sensors. **B**: Picture of the automated T-maze that was used during the experiments. **C**: Schematic of the task phases, during the sample phase the animal is forced in one of the goal arms, after returning to the start box the delay phase starts. After the delay the animal can choose freely between both goal arms and has to select the opposite arm to retrieve a reward.

The maze was controlled using an Arduino microcontroller (Arduino Mega, Arduino.cc). The doors were moved automatically using Arduino controlled servo motors (Modelcraft Standard-Servo RS-22 YMB, Hirschau, Germany) to rotate the doors in and out of the maze. Infrared (IR) sensors close to the base of the stem and close to the center in the goal arms were used to detect the animal's position while IR sensors in the reward ports were used to trigger reward delivery.

Animals were trained on a delayed NMS SWM task (Figure 4C). At the start of the experiment the mouse was placed in the start box with the start box door closed. The animal initiated the session by poking into the noseport in the start box which triggered reward delivery. After a delay of 40 s the sample phase started, and the start door was opened. Only one of the two

goal arm doors was opened, limiting the animal's entry to only one of the two arms. Poking in the reward port led to reward delivery and the animal could return to the start box. A nose poke in the start box again led to reward delivery and triggered the closing of the start door for the duration of the delay period (15 s normal delay or 60 s long delay). After the delay period the start door opened, and the choice phase started. In the choice phase both goal arm doors were opened so the animal could choose between both goal arms. After entering one of the goal arms the door to the opposite goal arm was closed. If the animal visited the correct goal arm (opposite to the goal arm visited during the sample phase) a nosepoke at the reward port would lead to reward delivery, no reward was delivered if the animal made the incorrect choice. In both cases the animal could return to the start box and initiate the inter-trial interval (ITI) with a nosepoke in the reward port there. This poke only was rewarded if the previous choice of goal arm entry was correct but always ended the trial and closed the start box door. After the ITI of 40 s the next trial was started with a new sample phase. Sample phase goal arms were pseudo randomly counterbalanced between left and right with a maximum of two same arms in a row. During testing sessions 40 trials were conducted. Prior to testing sessions, the animals were habituated and trained on the task. Initially, they were exposed to the maze and the reward ports for 15 min on two consecutive days. They could explore the maze freely without any doors but could get rewards at any noseport. To get subsequent rewards at one specific noseport the animal first had to leave the corresponding area. After two habituation sessions two shaping sessions with 10 trials each were conducted, where the animal learned the task structure. Sample and delay phase as well as the ITI were the same as during the testing sessions, but during the choice phase the sample goal arm was blocked with the door, so the animal could only enter the correct goal arm. Afterwards the animals were trained on the task with 10 - 20 trials until they did at least 80% correct trials within one session.

Exploration of elevated plus-maze (EPM)

The EPM was made from wood and consisted of four 30 cm long and 5 cm wide arms plus an additional center area of 5 cm x 5 cm. The two opposing arms were either surrounded by 15 cm high walls (closed arms), or no walls at all (open arms) and the maze was elevated 40 cm from the 50 cm high platform it rested on (**Figure 5**A, B). The room light was dimmed even further to about 1 Lux, and the computer screens were switched off to avoid uneven lighting in the maze. The animal was placed in the center of the maze facing one of the open arms and the experimenter left the room to avoid any influences on the behavior. The animal could explore the maze freely for 10 minutes and was removed from the maze afterwards.

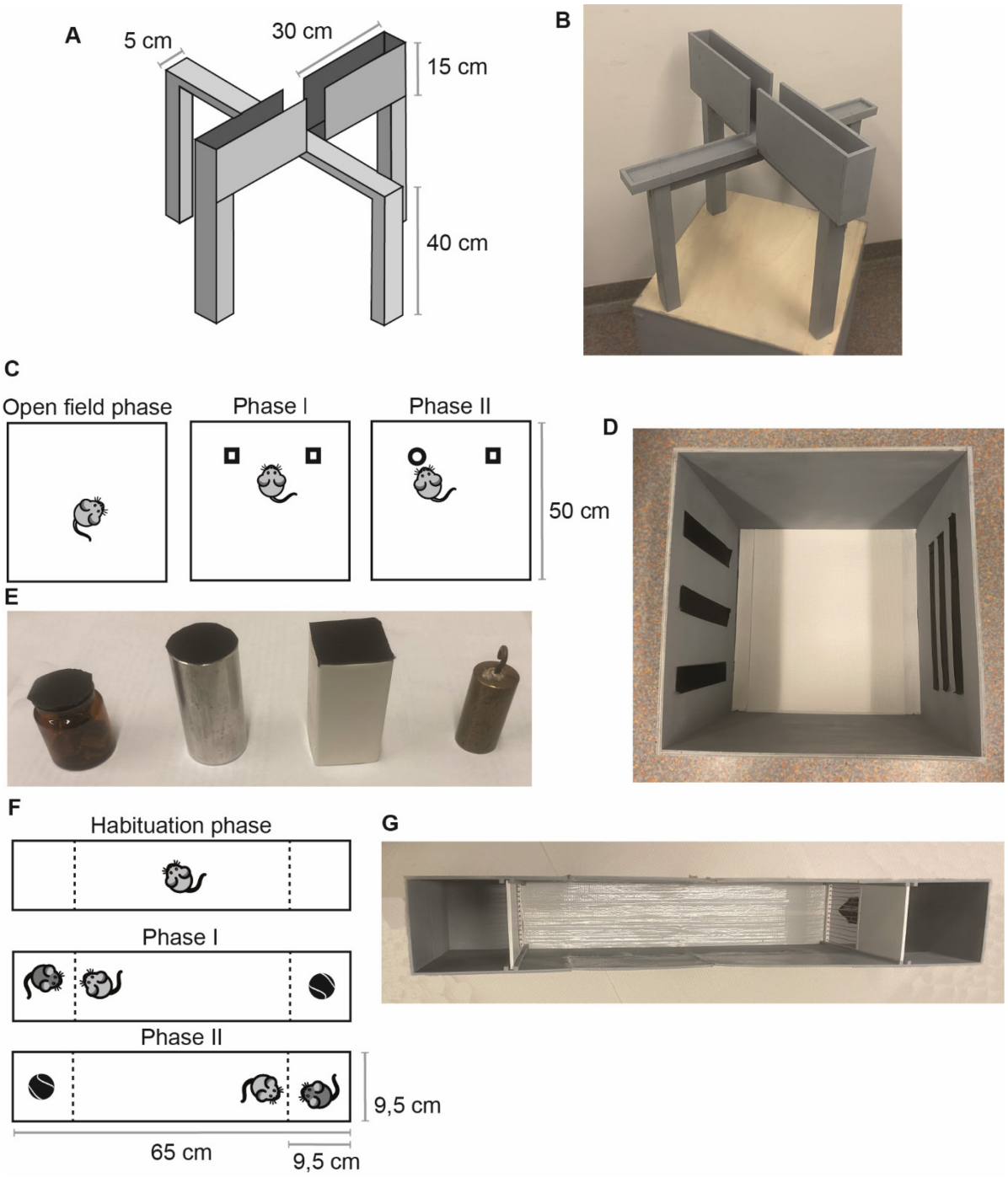

Figure 5: Spontaneous behavior contexts. **A**: Schematic of the EPM. **B**: Picture of the EPM. **C**: Schematic of the three task phases of the novel object recognition task. After 10 minutes of exploring the empty OF two identical objects were placed in the OF. After another 10 minutes, one of the objects was replaced with a novel object. **D**: Picture of the OF. **E**: Objects used for NO. **F**: Schematic of the SI task phases. After 10 minutes of free exploration a conspecific and an object were placed in the box in opposite compartments. After an additional 10 minutes, the conspecific and object switched places. **G**: Picture of the SI box.

Open-field exploration and novel object recognition (NO)

The OF box was 50 x 50 cm wide with 50 cm high wooden walls (**Figure 5**D). The floor was covered with a white lab soaker mat (Nalgene Versi-Dry Surface Protectors, Thermo Scientific,

Waltham, MA, United States). The walls were painted gray and two opposing walls were covered with 5 cm wide black stripes, either three vertically or four horizontally as orientation cues for the animal. The task consisted of 3 phases of 10 minutes each conducted directly after each other (**Figure 5** A). For all phases the animal was placed in the box in the middle of the quarter closest to the wall with the horizontal stripes facing the wall. After each phase the animal was removed from the box and placed back in the empty home cage for 1-2 minutes to prepare the next phase. The OF phase was a free exploration of the empty OF box, afterwards followed by two NO phases (phase I with two identical objects and phase II with one novel object and one familiar object). After the OF phase two identical copies of four possible objects were placed in the box with 10 cm distance to the wall with the vertical stripes and the other two walls respectively. Again, the animal was placed in the box and could explore the box and the objects freely. The objects were either a silver metallic cylinder (**Figure 5**E, radius: 1.5 cm, height: 6 cm), a metallic cuboid with white plastic covering around the long edges (area: 3 cm x 3 cm, height: 6 cm), a small glass bottle (radius: 1.6 cm, height: 4 cm) or a golden metallic cylinder (radius: 1 cm, height: 4 cm) with a hook on top (1.5 cm). The top of the objects was covered with black non-reflective tape to avoid reflections. Directly before placing the objects in the box, they were cleaned with 70% ethanol. Objects were counterbalanced between animals and always novel to the animal during the phase they were presented for the first time. For the second NO phase one of the identical objects was replaced with a different one, again both objects were freshly cleaned with ethanol to avoid odor traces from the previous phase.

Social Interaction test (SI)

The social interaction box was 65 cm long, 9.5 cm wide with a 20 cm high wall and consisted of three compartments separated by a 10 cm high metal grid with a solid wall on top. The box was made from white plastic, the inside of the box was colored gray while the walls separating the compartments were white and the grid was copper metallic (**Figure 5**F, G). The two compartments on the edges were 9.5 cm by 9.5 cm wide while the center compartment was 45 cm by 9.5 cm. The task consisted of 3 phases of 10 minutes each conducted directly after each other. Between the phases the test animal was placed in the empty home cage. Before each phase the box was cleaned using 70% ethanol. The test animal was always placed in the middle of the center compartment facing one of the walls. During the habituation phase the two compartments on the sides were left empty. In the first SI phase another mouse, the social target that was novel to the test mouse (male, aged 10-13 weeks) was placed in one of the side compartments and a black abstract plastic mouse (3D printed with PLA), the object, was placed in the other side compartment. For the second social phase the position of the social target (same mouse as in second phase) and the object were switched. In all phases the test mouse could explore the center compartment freely. It could poke its nose through the metal

grid and interact with the social target mouse through it, but it could not enter the side compartments.

Discriminatory auditory fear conditioning (FC)

Discriminatory auditory FC consisted of four phases, the habituation phase, the conditioning phase and two extinction phases. The respective chamber was placed within the OF described before to avoid the influences of the surroundings on the behavior of the animal. A speaker was placed 30 cm above the behavior chamber to play the computer-generated tones, either a 4 kHz sinusoidal pure tone or white noise. Tone duration was set to 10 s at 70 dB SPL and they were used as either CS+ (stimulus followed by foot shock during conditioning) or CS- (neutral stimulus as control not followed by foot shock) and counterbalanced between animals. Context A was used for habituation and conditioning and consisted of a standard mouse operant chamber 15 cm x 14 cm (ENV-307A-CT, Med associates, Fairfax, VT, United States) without lid but increased wall height by an additional 15 cm (**Figure 6**A, B). The walls on the shorter side were silver metallic rods with white plastic sliders while the other two walls were transparent Plexiglas. The custom-made extension on top was from white plastic all around the box. The mouse was placed on a metal grid within the chamber with a removable drawer below. The metal grid could be electrified using an aversive stimulator (ENV-414S, Med associates inc, Fairfax, VT, United States).

Context B was used for the extinction sessions and consisted of a circular arena (radius: 10 cm). The floor was covered with a lab soaker mat with bedding material on top. A custom programmed Arduino microcontroller with an Audio Shield (Adafruit Wave Shield Kit for Arduino, Adafruit, New York City, NY, United States) was used to play the tones and for shock delivery.

During the habituation session the animal was placed in context A and the CS- and CS+ were played in alternating order starting with a CS- (**Figure 6**C). Each tone was repeated 10 times with a pseudo-random inter tone interval of 40 – 70 s leading to a total session duration of 30 minutes. Later that day the animal was put again in context A for the conditioning session and five of each tone were presented, again starting with a CS-. After each CS+ the animal now received a mild (0.48 - 0.5 mA) foot shock for 1 s through the grid. The time between tones was pseudo randomly set to between 40 and 120 s leading to a total session time of about 30 minutes. On the two following days two extinction sessions were conducted. For those the animal was placed in context B and the tones were presented in the order of 5 CS-, 10 CS+,

2 CS-, 10 CS+, 2 CS-, 10 CS+, 1 CS-. The time between tones was pseudo randomly set between 40 and 90 s leading to a total session time of about 50 minutes.

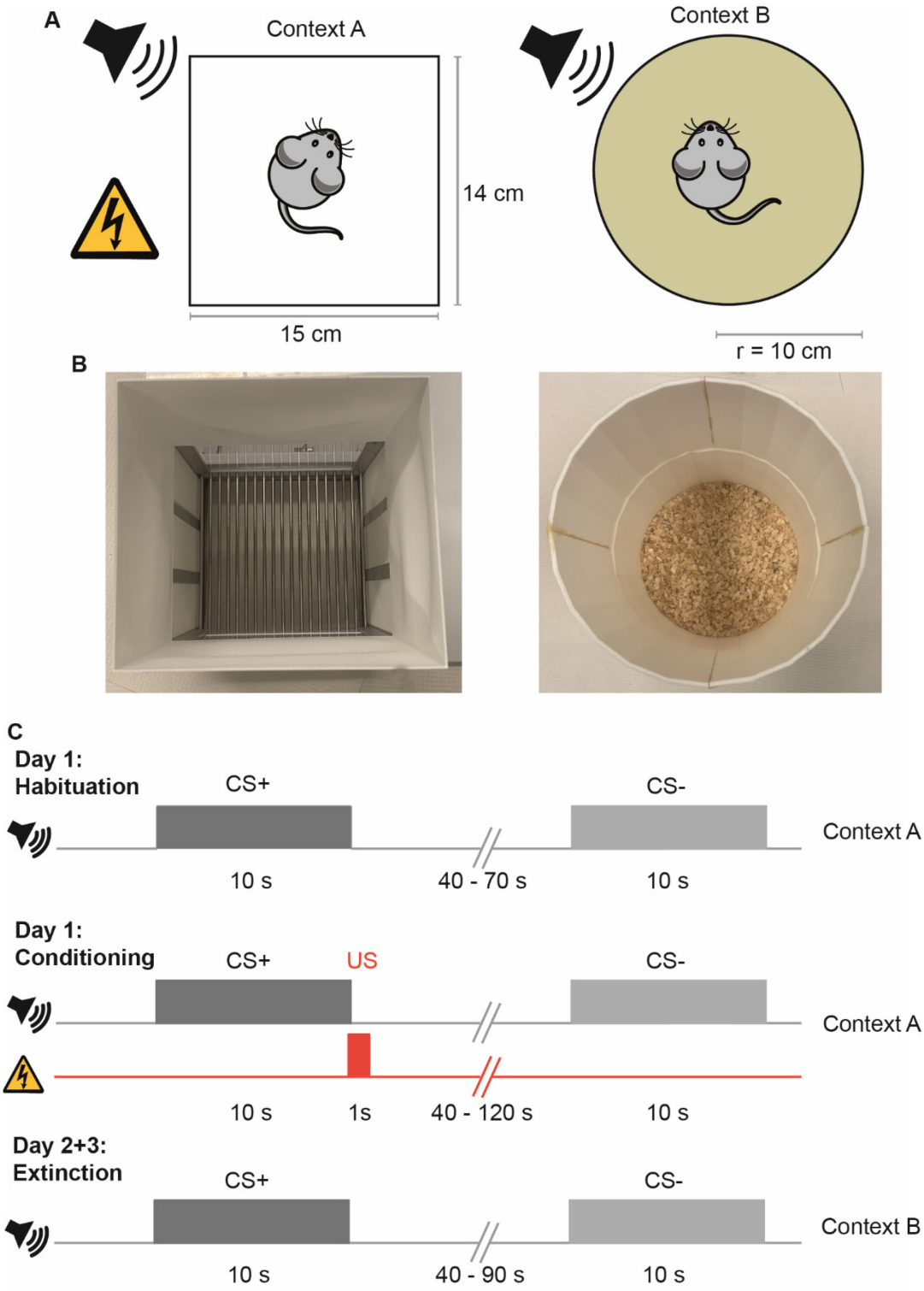

Figure 6: Discriminatory fear conditioning. **A**: Schematic of the different FC contexts, left: context A, right: context B. **B**: Pictures of the FC contexts like in A. **C**: Task structure for discriminatory FC.

Training schedule

Eight animals were first trained on the SWM in the T-maze, and at least two testing sessions, one with a short and one with the long delay were performed (Table 1). Afterwards they did a first block of spontaneous behaviors (EPM, NO, SI) and a first re-testing session in the SWM. After a second block of spontaneous behaviors another re-testing session was conducted followed by FC and the third re-testing session. The remaining animals also first got trained on the SWM task, afterwards on a discriminatory auditory reward task, then in the EPM, another SWM task in a RAM interleaved by NO and SI followed by FC and SWM re-testing. Two of those animals had two additional re-testing sessions after the auditory reward task and the SWM task in the RAM. Both the auditory reward task and the WM task in the RAM were discontinued after the first animals to reduce the number of training and recording sessions per animal and increase cell alignment across the other tasks. The number of animals tested in those tasks and data quality were not sufficient to be included in this thesis. Instead, a second round of spontaneous behaviors was introduced to be able to identify stability measures also in those tasks. Due to better cell alignment quality only the miniscope v4 animals were used for the across task analysis.

Table 1: Behavioral tasks training schedule

# animals	3	2	2	6
Miniscope	v3.2	v3.2	v3.2	v4
Across session analysis	-	-	-	included
T-maze WM	Training & testing 1 re-testing session	Training & testing 3 re-testing sessions	Training & testing 3 re-testing sessions	Training & testing 3 re-testing sessions
Auditory reward conditioning	Training & testing	Training & testing	-	-
Spontaneous behaviors	1 round	1 round	2 rounds	2 rounds
Radial arm maze WM	Training & testing	Training & testing	-	-
Fear conditioning	Conditioning & extinction learning	Conditioning & extinction learning	Conditioning & extinction learning	Conditioning & extinction learning

Analysis of calcium imaging data

Cell extraction from video data

To identify the cells in the imaged video we used a custom adapted version of the miniscope analysis framework (https://github.com/etterguillaume/MiniscopeAnalysis) written in MATLAB. Every recording session was analyzed individually. First all frames were aligned using non-rigid motion correction with the NoRMCorre algorithm (Pnevmatikakis & Giovannucci, 2017). Non-rigid motion correction was used to avoid the correction being influenced by the border of the lens which would influence the motion estimate. First the frames were high pass filtered using a gaussian filter with kernel size of 16 pixels and a standard deviation of 3 pixels. Then non-rigid motion correction was performed on overlapping patches of the video. The resulting frames were saved in a new video file. Afterwards constraint non-negative matrix factorization was performed to extract the cells. To this end the motion corrected video file was passed on to the CNMF-E algorithm (Zhou et al., 2018). This algorithm tries to iteratively find and update cells as well as the background in the video by following the constraints that pixels within a cell are correlated with each other across time and have a high signal-to-noise ratio while other pixels should not be correlated, and the signal-to-noise ratio should be low. It is iteratively estimating the background followed by cellular activity and shape, that is then removed from the video for the next iteration. The algorithm results in two separate matrices, one containing the spatial footprints of the cells (x_pixels X y_pixels X cells) and one containing the traces (time X cells). The resulting cell candidates are visually inspected manually with custom written scripts for trace and cell shape plausibility. Cells with abnormal shapes or transients not resembling calcium transients, like fast negative peaks, are marked and excluded from further analysis.

Cell Registration across sessions

We used the CellReg (CellReg v1.5.3, https://github.com/zivlab/CellReg) algorithm to identify the same cells across multiple sessions (Figure 8E-I, Sheintuch et al., 2017). The algorithm works by aligning (moving, transforming, rotating) the spatial footprints of all cells within a session to the spatial footprints of a reference session to achieve the highest spatial correlation across sessions. Sessions without sufficient spatial overlap (2D correlation of all spatial footprints across 2 sessions <0.25) were excluded. After alignment all cells within 14 µm distance (distance between center of the cells, centroid distance) to each other across all sessions were used as cell pair candidates. The correlation of the spatial footprint (spatial correlation) of all candidate pairs was calculated, and for both, the centroid distance as well as for the spatial correlation two independent distributions were fitted, one for the nearest neighbor of each cell (being same cell candidates) and one for all other neighbors (Figure 8E-H). A weighted sum of both distributions was then used to fit the combined data. Every cell-

pair candidate then got a probability assigned that these are the same cells based on the fit for nearest and other neighbors. Afterwards cell pair candidates from every session with the highest probability (minimum of 0.95) were clustered together and assumed to be the same cell.

Behavioral analysis and analysis of task-specific neural correlates

Pose estimation using DeepLabCut

We employed the pose estimation algorithm DeepLabCut (DLC, Deeplabcut v2.2.03, Mathis et al., 2018) to identify animals' 2D position and head direction in the tasks where the IR camera video was recorded (all tasks except the T-maze SWM). We trained the deep learning algorithm to detect five spots on the animal, the Miniscope (Center Head position), the left and right ear, the center of the back of the animal and the base of the tail. For increased accuracy an independent model was trained and used for every task individually because of variation in distance to the camera and lighting. All models were trained and tested multiple times with an increasing number of manually labeled frames (20-50 labeled frames per session in 10-20 sessions per task), until the accuracy of the algorithmically labeled frames was sufficient by manual observation. The models were trained on a local computer or in the cloud using the NeuroCAAS (https://neurocaas.com/) online service. Analyzing the videos (using the models to extract the body part positions) was done on the local computer. Apart from the position also a likelihood of each body part being at this position was given as a measure how confident the algorithm was in its position. The resulting 2D positions together with the likelihood for all body parts and every frame were saved in a CSV file and imported to MATLAB. Two new positions were calculated there, the head position as the average of miniscope, left and right ear positions and the body position as the average of the base of the tail, left and right ear positions. The head direction of the animal was defined as the vector orthogonal to the line between the two ears and pointing to the snout. Speed (in pixels per frame) was calculated as the average two-dimensional movement of the detected body parts with a likelihood above 0.95.

General Behavior analysis

All behavioral analysis was conducted in MATLAB using custom written scripts. First, the data from the Neuralynx system containing timestamps of all behavioral events, timestamps of each frame recorded for both the calcium imaging as well as the IR camera and the 2D position of the tracker LED were imported. Every calcium sample was aligned to the tracker position sample closest in time and every IR camera frame was assigned to the calcium sample closest in time. With that the body part positions as well as head direction and movement speed identified with DLC were also assigned to every calcium sample if applicable.

Spatial working memory in the automated T-maze

Behavior in the automated T-maze was logged automatically in human-readable text form on the computer that controlled the Arduino microcontroller. These text files were imported into MATLAB and the events were aligned to the TTL pulses sent to the Neuralynx system for additional information, for example whether a nosepoke was rewarded. Different events were created for the start and end of sample phase and choice phase, the breaking of the IR beams in the stem as well as in the arms and nosepokes in the individual noseports. The path the animal was taking after leaving the start box and entering the goal location was specifically linearized from 1 to 100 for the outbound runs (running from the start box to the goal arm) and the path after leaving the goal location and the entry in the start box (inbound run) was linearized from 100 to 1 (for spatial correlations between the left and the right runs). Every position of the animal was linearized in cm between -15 (being the distal end of the start box) and 80 (being the distal end of either goal arm) for linear modeling. Every calcium sample was assigned to the current trial the animal was in, whether it was in the sample, choice or delay phase, the linearized positions and maze location, if the animal was currently in an outbound or inbound run or consuming the reward at the goal location, which goal the animal was going to or coming from in that moment, which choice the animal would make in that trial and whether the trial was correct or not.

Performance of the animal was calculated as the number of correct goal arm entries during the choice phase divided by the total number of trials in that session. Additionally, the number of rewards collected as well as the number of additional nose pokes was recorded. Running times were calculated as the time the animal needed to reach the goal location after leaving the start box in that phase. Trial and phase durations were calculated as the difference between start box door opening and closing.

To identify spatial firing patterns across the maze we binned the linearized position further into nine bins (see Figure 10A, bin 1: start box, bin 2-5: central arm, bins 6-9: goal arms). We averaged the z-scored activity in those bins in each phase and running direction (sample outbound, sample inbound, delay, choice outbound, note that the animal is only in position bin 1 during delay) for each trial and calculated the average over trials. These averages were concatenated to get an activity vector for each cell. Runs with a duration above 25 s were excluded (<3% of runs).

To compare goal arm dependent activity, we separately averaged the fluorescence over left and right trials by the goal arm the animal visited in that phase. For the delay phase we used the arm the animal returned from in the sample phase. We compared the neural activity

between left and right trials with the Wilcoxon rank sum test for each bin to get the fraction of neurons with significant differences.

We performed population decoding of the goal location at each position-phase bin by using 'pseudo-simultaneous' population activity (Meyers et al., 2008). We randomly sampled eight left and eight right trials from the first testing session with above 80% performance of each animal to get 16 pseudo-simultaneous population vectors containing data combined from all animals. We trained a linear classifier on seven of the left and seven of the right population vectors and tested the classifier using the two remaining population vectors. We repeated this eight times with each population vector being used once for testing (8-fold cross-validation). The average performance of these classifiers (correct classifications divided by number of predictions) was then calculated at each position. We repeated this 100 times using different random population vectors to get a distribution of decoding performance for each position-phase bin. This was compared with a shuffled distribution we retrieved with the same method but using randomly shuffled goal identities for the population vectors. To test for significance of the decoding performance we compared the actual and the shuffled distribution using the z-test.

Difference scores were calculated between the averaged activity during left and right trials in specific phases. They are calculated as the difference in averaged activity during the in- or outbound runs (excluding reward retrieval) specifically for sample and choice phase or during the delay phase (including reward retrieval). They were always calculated as the difference between the left and the right arm with positive scores indicating higher activity in the left arm.

Elevated plus maze

The time the animal spent in the different parts of the maze was automatically analyzed using the tracking LED. Regions of interest were marked manually around the closed arms and the center. Entries to both arm types were counted as entering one of the arms from the center and staying there for at least two seconds. We set a label for each calcium imaging frame in which arm the mouse was during that frame.

We calculated an EPM score for every cell to identify neurons that fire more similarly in both arms of the same type (open or closed) in comparison to both arms of the other type (Adhikari et al., 2011). The EPM score was calculated with the following formula:

$EPM\_Score = \frac{a-b}{a+b}$ with $a = \frac{1}{4}(|F_{O1} - F_{C1}| + |F_{O1} - F_{C2}| + |F_{O2} - F_{C2}| + |F_{O2} - F_{C2}|)$,

$b = \frac{1}{2}(|F_{O1} - F_{O2}| + |F_{C1} - F_{C2}|)$ and F_{O1}, F_{O2} being the averaged fluorescence in each open arm and F_{C1}, F_{C2} being the averaged fluorescence in each closed arm. A cell that would be

equally active in both arms of the same type but not at all in the other type would get a EPM Score of 1, a cell that would have the same fluorescence in one of the open arms and one of the closed arms and also the same activity between the other open arm and closed arm would get the minimal EPM score of $-0.\overline{3}$. Additionally, we calculated a difference score to identify the arm type in which cells with a high EPM score showed higher activity. For that we used the following formula:

$DifferenceScore_{EPM} = z(F_O) - z(F_C)$ with z(F_O) being the averaged z-scored fluorescence in the open arms and z(F_C) being the averaged z-scored fluorescence in the closed arms.

A positive difference score would indicate that this cell was more active in the open arms, a negative score would mean that the cell was more active in the closed arms. We calculated a shuffled distribution for both the EPM score and the difference score by randomly shifting the arm identity labels for each frame 1000 times and calculating the scores with the shuffled labels. We considered cells to be significant that had a difference score that was lower than 2.5% or higher than 97.5% of the shuffled difference score distribution. A cell with a difference score higher than the 97.5% of the shuffled distribution was considered an open arm cell while a cell with a difference score below 2.5% of the shuffled distribution was considered a closed arm cell. Heatmaps of cell activity were created by averaging the activity of the animals in different maze positions using binning of 40X40 bins (~1.6 cm/bin). The results were smoothed over a 4X4 bins (~6.5 cm x 6.5 cm) rectangle.

Novel object recognition

The OF phase of the novel object recognition task was specifically analyzed as free OF exploration. We distinguished three different zones in the arena, a center zone, a wall zone and a corner zone. For this we divided the area of the box into 16 equally sized squares, with the four center squares forming the center zone, the four corner squares building the corner zone and the remaining eight zones forming the wall zone (Figure 12A). Wall and corner zones together were defined as the periphery zone. We set a label for each calcium imaging frame in which zone the mouse was during that frame. We then analyzed the time the animal spent in the different areas of the box. To correct for the different sizes of the areas for periphery or wall in comparison to center and corner areas, we calculated an area corrected “time spent” value. For this we multiplied the time spent in the smaller area by the ratio of the larger area to the smaller area and divided it by the new total time.

We calculated an OF score analogous to the EPM score defined above. For this we compared all combinations of corner squares with all combinations of center squares.

$OF\_Score = \frac{a-b}{a+b}$ with

$a = \frac{1}{16}(|\mathrm{F_{Corner1}} - \mathrm{F_{Center1}}| + |\mathrm{F_{Corner1}} - \mathrm{F_{Center2}}| + |\mathrm{F_{Corner1}} - \mathrm{F_{Center3}}| + |\mathrm{F_{Corner1}} - \mathrm{F_{Center4}}| + |\mathrm{F_{Corner2}} - \mathrm{F_{Center1}}| + \cdots),$

$b = \frac{1}{12}(|\mathrm{F_{Corner1}} - \mathrm{F_{Corner2}}| + |\mathrm{F_{Corner1}} - \mathrm{F_{Corner3}}| + |\mathrm{F_{Corner1}} - \mathrm{F_{Corner4}}| + \cdots + |\mathrm{F_{Center1}} - \mathrm{F_{Center2}}| + \cdots)$ and $\mathrm{F_{Corner1}}$, $\mathrm{F_{Corner2}}$, $\mathrm{F_{Corner3}}$, $\mathrm{F_{Corner4}}$, being the averaged fluorescence in the four corners and $\mathrm{F_{Center1}}$, $\mathrm{F_{Center2,}}$ … being the averaged fluorescence in the Center areas.

If a cell only was active in all corner squares equally and not at all in the center it would get a OF score of 1, the minimum OF score is $-\frac{1}{7}$ if the cell was active in the same way across pairs of center and corner cells. We also calculated a difference score for the OF using the following formula: $DifferenceScore_{OF} = z(F_{Center}) - z(F_{Corner})$ with $\mathrm{z(F_{Center})}$ being the averaged z-scored fluorescence in the corner zone and $\mathrm{z(F_{Center})}$ being the averaged z-scored fluorescence in the center zone. We calculated a shuffled distribution for both the OF score and the difference score by randomly shifting the zone identity labels in time for a minimum of 500 frames and calculating the scores. This was repeated 1000 times with different shuffled labels. We considered cells to be significant that had a difference score that was lower than 2.5% or higher than 97.5% of the shuffled difference score distribution. A cell with a difference score higher than the 97.5% of the shuffled distribution was considered a center cell while a cell with a difference score below 2.5% of the shuffled distribution was considered a corner cell. Heatmaps of cell activity were created by averaging the activity of the animals in different maze positions using binning of 30X30 bins. The results were smoothed over a 2X2 rectangle. We also performed principal component analysis (PCA) on the heatmaps. For these we used 18X18 bins to avoid having bins the animal did not visit.

For the NO task we defined two zones of approximately 6X6 cm around the two object locations. For every frame we created a label if the animal was in one of the object zones. All further behavior analysis was limited to the first five minutes of each phase. We compared the time the animals spent in the two object zones across the different phases and counted the number of visits for each object. A visit was defined as staying in the object zone for at least one second. To compare both NO sessions we calculated a behavior modulation index for the time spent in the zones or the number of visits using the formula $modulation\ index = \frac{a-b}{a+b}$ with *a* being the time spent or number of visits in one object zone and *b* respectively for the other object zone during phase I. During phase II *a* was the time spent or the number of visits in the novel object zone and *b* respectively for the familiar object zone.

Heatmaps of position-averaged cell activity were created at 30X30 bins for the three phases independently. We created object-zone-variables for both object zones for every phase set to 1 when the animal was in that zone or 0 otherwise. These variables were correlated to the

calcium activity during each phase independently (Asif-Malik et al., 2017) for each cell. The correlation values were averaged over the different object positions (OF-phase and NO-phase I) or over object identity (novel or familiar, NO-phase II). We created a shuffled distribution by shifting the object-zone-variables 1000 times by random values with a minimum of 500 samples. We considered cells being significantly modulated by the object zone if the correlation value was higher than 97.5% or lower than 2.5% of the shuffled distribution. We calculated a difference score as the difference of the z-scored activity of each cell while the animal was in one of the two object zones.

Social interaction test

Two 7.7 cm wide interaction zones were defined in front of both grids, the social zone if the social target was behind the grid or the object zone if the object was behind the grid and created a zone variable indicating for each calcium imaging frame if the animal was in one of the zones. All further analysis was limited to the first five minutes of each phase. We averaged the time spent in each of these zones per phase. A visit was counted when the animal spent at least 2 seconds in one of the zones. We calculated a behavior modulation index for the time spent in the zones and the number of visits using the formula $modulation\ index = \frac{a-b}{a+b}$ with a being the time spent or number of visits in the social zone and b respectively for the object zone.

Heatmaps of position-averaged cell activity were created at 25X5 bins for the three phases independently. We calculated a difference score as the difference between the averaged z-scored fluorescence across the two zones, during the habituation phase we compared the left and right zone. A shuffled distribution was created by randomly shifting the zone vector 1000 times with a minimum of 500 samples and calculating the score in the same way. A cell was considered significantly coding for the social target if the difference score was higher than 97.5% or lower than 2.5% of the shuffled distribution.

Fear conditioning

Freezing behavior was analyzed using the animal position as tracked by DLC. First, the average movement of the five body parts tracked by DLC was calculated. Body parts with a likelihood below 0.95 at each behavioral sample were excluded from the average at this datapoint. Periods of at least 1 s with average movement across body parts of less than 1 pixel were considered freezing. This was manually confirmed by marking frames in the behavior video when the animal showed freezing according to the algorithm. Freezing levels were then analyzed for durations that either CS was played.

Cell responses were plotted as the average response across all CS of one type aligned to the onset of the CS. For illustrational purposes the CS response was normalized by the pre-CS

activity by dividing the difference of the CS response and the mean of the activity in the second before the CS by the standard deviation of the second before the CS.

We used two different measures to identify cells responding to the CS. We compared the average activity trial-wise between CS+ and CS- using the Wilcoxon rank sum test and for CS+ and CS- independently we compared the activity in the 1.5 s before onset to the activity in the first 1.5 s of the CS using the Wilcoxon signed-rank test with a p value below 0.05. We calculated difference scores both for the onset of either CS as the difference between the 1.5 s of the CS and the 1.5 s before CS onset and as the averaged activity difference of CS+ and CS-.

Generalized linear models

We used generalized linear models (GLM) to identify which task features influenced mPFC activity strongest. This enabled us to analyze the neural activity across neurons and multiple tasks in a common way. For every neuron we modeled its activity as the weighted sum of different behavioral variables (Figure 16A). GLMs were fit for every cell and session independently.

The fluorescent signal of each cell was downsampled with a factor two by averaging the fluorescence of two frames and selecting every other sample. We assigned a behavioral variable to every bin indicating if a specific event or variable was active in that bin and in which state. A different set of categorical variables and discrete event time points per task was used as regressors. Discrete events like reward time points, zone entries or on- and offsets of behaviors were convolved with splines to get a better representation over time. The onset often was set before the event happened until a few seconds after (for details see below and Table 2). Categorical variables were treated as multiple variables with a specific weight coefficient β_x for every unique entry. Continuous variables such as speed and position were discretized by binning and treated as categorical variables.

Two regressors were used across all tasks, position and speed. A third regressor, head direction, was used in all tasks but not in the T-maze working memory. All other regressors were specific for each task. For the position regressor we used similarly sized bins of the tracked LED on top of the miniscope. We kept the size of position bins similar across tasks using an area of about 20-25 cm² per bin. In the maze tasks we used linearized position bins. In the T-maze working memory task the same bin IDs were used for the left and right goal arm. Movement speed was binned into 5 bins using quintiles as limits for each session individually. Movement speed was calculated from the difference in LED tracking position across samples in the T-maze task and as the average difference of all body parts detected by DLC with a likelihood of above 0.95 for all other tasks. Head direction was detected by DLC as the vector

orthogonal to the line between the two ears pointing to the snout of the animal and was split into 9 bins 40° each.

Table 2: Overview over the different regressors for the GLM per task.

T-maze working memory	Reward	5 Splines	0.5 s before till 1.5 s after
	Arm entry	5 Splines	0.1 s before till 1 s after
	Door opening	5 Splines	0.5 s before till 1 s after
	Position	25 Bins	Linearized position in the maze
	Speed	5 Bins (Quintiles)	Movement speed of the animal
	Direction	[0 1]	Outward run / Inward run
	Goal	[0 1]	Left / Right
	Correct	[0 1]	Correct / incorrect trial
	Phase	[1 2 3]	Sample / Choice / Delay
Elevated plus maze	Position	29 Bins	Linearized position in the maze
	Speed	5 Bins (Quintiles)	Movement speed of the animal
	Head direction	9 Bins	Direction the animal is looking at
Novel object recognition	Position	10 x 10 Bins	Position in the box
	Speed	5 Bins (Quintiles)	Movement speed of the animal
	Head direction	9 Bins	Direction the animal is looking at
	Object	[0 1]	Left object / Right object
Social interaction	Left entry	5 Splines	Time around entry to left zone
	Right entry	5 Splines	Time around entry to right zone
	Position	9 x 2 Bins	Position in the box
	Speed	5 Bins (Quintiles)	Movement speed of the animal
	Head direction	9 Bins	Direction the animal is looking at
	Interaction	[0 1 2]	Interaction zone: Empty zone / social zone / object zone
Fear conditioning (Extinction)	Position	6 x 2 Bins	Radial bins, equal size
	Speed	5 Bins (Quintiles)	Movement speed of the animal
	Head direction	9 Bins	Direction the animal is looking at
	CS+	[0 1]	CS+ off / CS+ on
	CS-	[0 1]	CS- off / CS- on
	Freezing	[0 1]	Not freezing / Freezing

Seven other regressors were used in the T-maze WM task. Reward, arm entry and door opening time points were convolved with 5 splines (Matlab function create_bspline_basis;

http://psych.mcgill.ca/misc/fda/software.html). For the reward 2 seconds were used and shifted in time so the splines lasted from 0.5 s before till 1.5 s after reward delivery. For door opening and goal arm entry shorter time frames were used, 0.5 s before and 1 s after for goal arm entry and 0.1 s before till 1 s after for door opening as the door opening cannot be predicted precisely by the animal. The other variables were categorical with two or more states. The phase regressor had three values for in which phase the animal currently was (“sample”, “choice”, “delay”). Goal indicated which goal arm the animal had visited or would visit in that phase. For the delay phase it was set to the goal the animal would visit during the following choice phase. Direction indicated the running direction of the animal, whether it was on the outbound (start box to goal arm) or inbound (goal arm to start box) run. Correct indicated whether the whole trial was correct or incorrect.

The EPM GLM did not use any other regressors apart from position, head direction and speed. The GLM for the NO task used one additional regressor, object, which had two states for the object locations. The SI GLM had 3 additional regressors, a left and right zone entry, which marked the time points of the zone entry that were convolved with 5 splines lasting from 0.5 s before to 0.5 s after and a categorical regressor with 3 states indicating in which kind of zone the animal currently was (“empty” during habituation, “social” or “object” in phase I and II). Both the GLM for the NO task and the SI task were fit across all phases. For FC we used three additional predictor variables. One for both the CS+ and the CS– ranging from CS onset for the full duration and 2 s after CS offset. The third regressor was a binary variable indicating whether the animal was currently freezing. The speed variable was excluded for freezing periods.

We used 10-fold cross validation to avoid overfitting. For this we trained the model 10 times with different 90% of the data, the remaining 10% of the data were used as testing data. To create the training and testing data we split the whole session in two second long chunks and used 90% of the chunks for testing and 10% for training to keep training and testing samples independent because of the autocorrelation of the calcium signal. The average variance explained by the testing data was used for all further analysis.

To test for the influence of single behavioral variables multiple models were created. First, we created single variable models to see how much variance each variable explained on its own and a full model using all the variables together. Second, we used the full model and ran the model again, shuffling one of the variables from the model (reduced models) to identify the unique contribution of each behavioral variable. For this we calculated the difference of the explained variance of the full model from that of the reduced model for every variable. This was done to remove the amount of explained variance that could also be explained by other

variables. Last, we looked for the cells that significantly coded for a specific variable by testing if the real behavioral vector removed from the full model led to a larger drop in explained variance than in 95% of the cases after removing it from a shuffled behavioral vector for that variable 1000 times (Figure 16B-E, right column).

Across session analysis

Spatial correlation across sessions

To identify if cells coded stably for the same positions across multiple sessions of the same task, we correlated their averaged spatial activity across different bins pairwise. The number of bins was chosen in a way that every bin was visited at least once by every animal in every session. In the T-maze WM task we correlated the averaged linearized activity in inbound and outbound runs (Positions 1-100). In the EPM we created 13 bins (3 per arm + center), the NO box was divided into 3X3 equally sized bins and the SI box in 2X4 equally sized bins. For fear conditioning we just used the extinction sessions as a different environment was used for habituation and conditioning. We used a total of eight equally sized bins (two circles each divided into four sectors). The averaged activity in each bin was then correlated for each cell across session pairs. Pearson's r was compared for every task to a distribution of 1000 correlations of random cell pairs by shuffling the cell identity vector for the second session.

Correlation of task variables encoding across sessions

As a broader and task independent measure of coding for specific variables we correlated the unique explained variance (reduction of explained variance after removing specific variable) from our linear models. To do this we created two vectors for each task variable combination across two sessions of any task combination. Each vector contained the reduction of explained variance for a specific task variable for every cell that was recorded in a session pair with that task variable combination (also within each task) across all animals. Every nth data point contained the information from the same cell in both vectors. These two vectors were correlated, and the resulting Pearson's r was compared to a shuffled distribution where one of the vectors was randomly redistributed 20000 times leading to random cell pairs. To correlate the unique contribution of two different variables within the same task across sessions, each cell was used twice, once for each of the behavioral variables. This led to double the number of cells that were correlated in the same-task-different-variable-correlations compared to the same-task-same-variable-correlations.

To test how stable correlations of task variables were over time we performed an ANCOVA (Matlab function aoctool) with the across task correlation as the response variable, the time (in sessions) between the two tasks as predictor and grouped them in either two same tasks or

two different tasks. Every possible task-time difference combination was used as one datapoint.

Testing for correlations in task-relevant event coding

Similar to our approach testing for correlated task-coding from the GLM results we created vector pairs with the difference scores (for details see methods for specific tasks) we calculated for all task combinations across all animals. These vectors were correlated over cell pairs recorded across all sessions across all animals (also for the same task). This correlation was again compared to a shuffled distribution, where one of the vectors was randomly shuffled 20000 times (leading to random cell pairings).

Statistics

All statistical tests were calculated using Matlab 2022b. To compare two groups of paired data the Wilcoxon signed-rank test was used (Matlab function signrank). To compare two groups of unpaired data the Wilcoxon rank sum test was used (Matlab function ranksum). For comparison of proportions of binary variables, the binomial test was used (Matlab function binocdf to calculate binomial cumulative distribution function). Single data points were compared using shuffled distributions, usually the data was compared with 1000 shuffles, more if needed for corrected p-values. Calcium traces or behavior vectors were shifted in time to keep the temporal structure instead of random shuffling (Matlab function circshift). If not otherwise specified, we used a 5% significance level. Bonferroni correction for multiple comparisons was used if multiple independent statistical comparisons were performed together. Significances were marked with * for a significance level of $p<0.05$, ** for $p<0.01$ and *** for $p<0.001$. Summary statistics are given as mean ± s.e.m. if not otherwise stated.

Histological confirmation of GCaMP expression and lens location

After the experiments animals were deeply anesthetized using a lethal dose of sodium-pentobarbital (Narcoren, Merial GmbH, Hallbergmoos, Germany) and perfused transcardially using a cooled 4% paraformaldehyde 15% picric acid solution in phosphate-buffered saline (PBS) at a pH of 7.4. The brains were removed from the skull and placed in the perfusion solution overnight for post-fixation. Afterwards they were transferred to sucrose solution (50 g/500 ml sucrose and 0.25 g/500 ml sodium azide in PBS). The part of the brain containing the mPFC was cut on a vibratome (Leica VT1000S, Leica Biosystems, Nussloch, Germany) in 80 µm thick coronal sections. The sections were washed multiple times in PBS and nonspecific antibody binding sites were blocked using blocking solution (10% horse serum, 0.5% Triton X-100, and 0.2% bovine serum albumin in PBS) for one hour. Afterwards a primary GFP antibody (rabbit anti-GFP, 1:1000, Invitrogen, A11122) was added in carrier solution (1% horse serum, 0.5% Triton X-100, and 0.2% bovine serum albumin in PBS) overnight. The next day the slices

were washed again three times in PBS and a secondary green fluorescent antibody (anti-rabbit 488, 1:750, Invitrogen, A11008) in carrier solution was added. The next day the antibody solution was removed, and the slices were incubated in DAPI 1:5000 in PBS (Molecular Probes, #D1306) for five minutes. After three further washing steps in PBS the sections were mounted on a microscope slide and covered with a covering medium (VECTASHIELD, Vector Laboratories, Burlingame, CA, United States) and a glass cover slip. The edges of the cover slip were fixed to the microscope slide using nail polish. After drying the sections were examined under a confocal microscope to visualize the DAPI-stained nuclei as well as the GCaMP6 expression and the location of the lens.

Results

Calcium imaging in the prefrontal cortex

We confirmed successful virus expression and lens location histologically after the experiments. For this the animals were transcardially perfused and the brain was removed and sectioned. Sections were stained using DAPI to label the nuclei and GCaMP fluorescence was increased using a green fluorophore linked to a GFP antibody. Slices were inspected under a confocal fluorescence microscope and aligned to the Allen mouse brain atlas (Wang et al., 2020, see methods for details). GCaMP6 was well expressed in our target region in the mPFC without staining the nuclei (filled nuclei are associated with dysregulated Ca^{2+} dynamics, Y. Yang & Mailman, 2018), indicating good expression levels (Figure 7A). While most of the lenses were implanted at the intended location within the PL area of the mPFC centered at about 1.95 mm frontal to bregma two lenses were placed a bit more frontal at about 2.2 mm frontal to bregma and one was placed a bit more posterior just 1.3 mm frontal to bregma (Figure 7B). Nevertheless, all lenses were placed in the mPFC, all but one lens was centered in the PL area and one in the ventral ACC.

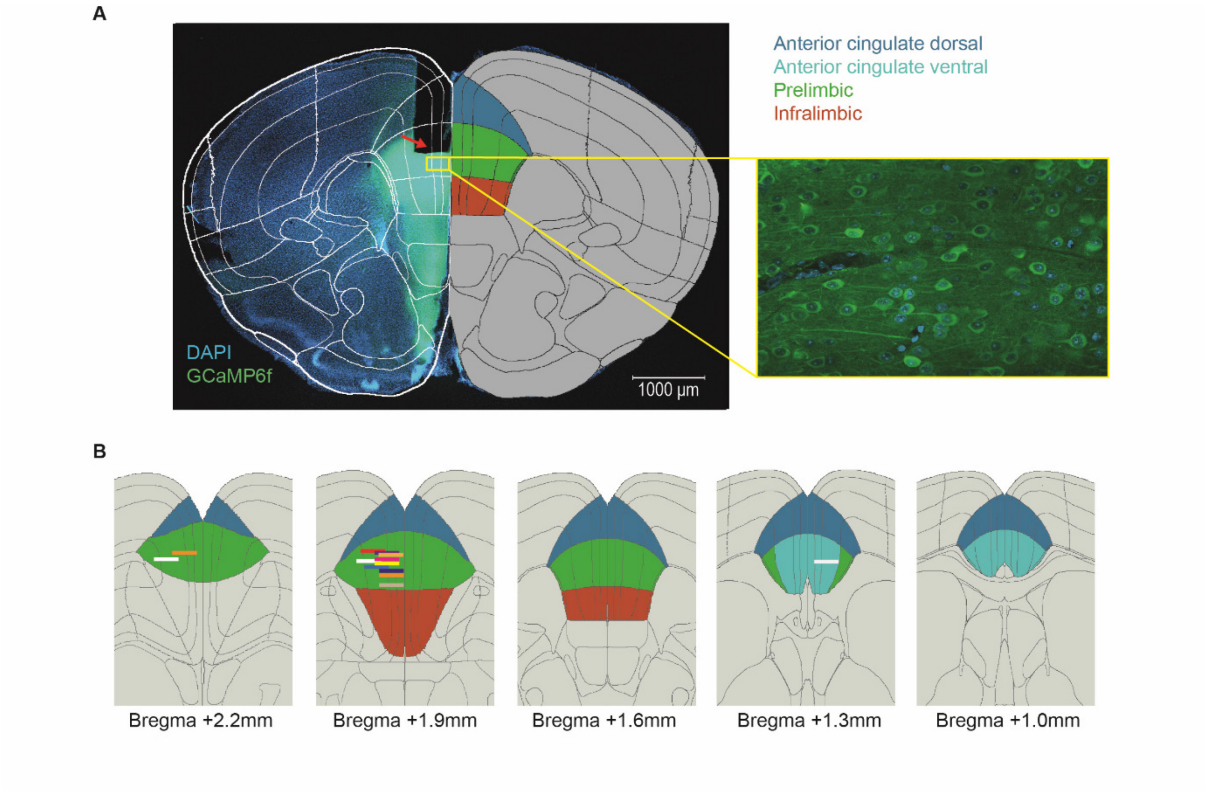

Figure 7: Histological confirmation of lens location. **A**: Histological image of mPFC with GCaMP positive cells (green) and DAPI stained nuclei (blue), coronal slice 1.9 mm anterior to bregma. Overlay shows brain regions in that section, altered from Allen mouse brain atlas with mPFC regions labeled in colors. Blue: Anterior cingulate cortex (dorsal/ventral), green: Prelimbic cortex, dark red: infralimbic cortex. Cutout shows larger magnification of GCaMP expressing cells excluding expression in the nucleus.

Arrow points to the tip of the implanted GRIN lens. **B**: Lens locations (tip of lens) for all imaged animals overlaid on coronal brain sections spanning the whole mPFC at 0.3mm steps. mPFC regions are labeled as in A (Allen mouse brain atlas, Wang et al., 2020).

We successfully imaged thirteen animals across our five behavioral tasks (Figure 8A, B). Hereby we identified 12225 cells from all 191 successful imaging sessions leading to an average of 64 ± 3 cells per session. Cell shapes (spatial footprints) and activity over time were extracted using CNMF-E and the results were plotted and checked manually (Figure 8C, D).

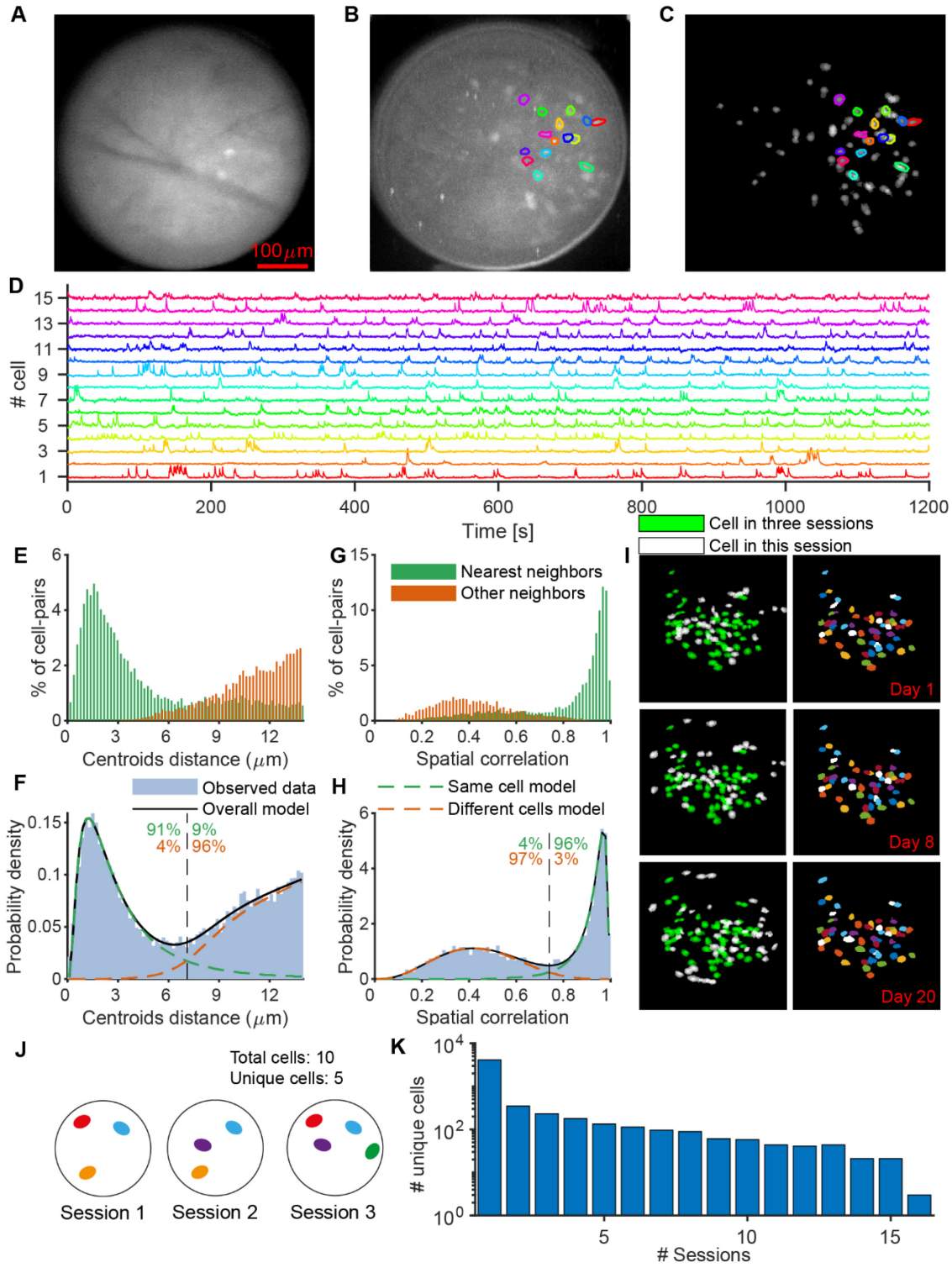

Figure 8: Miniscope imaging and identification of cells across sessions. **A**: Raw frame from a miniscope recording in mPFC. **B**: Maximum projection over time with background removed. Example mPFC neurons are marked with different colors. **C**: Spatial footprints of all neurons detected by CNMF-E within the same recording. Same neurons are marked as in B. **D**: Color coded fluorescence traces for cells marked in B&C. **E**: Centroid distance histogram for all cell pairs within 14 µm of each other across all sessions from one animal classified as nearest neighbors or other neighbors. **F**: Model based on distribution of centroid distances between nearest and other neighbors. **G, H**: As E, F but for spatial correlation. **I**: Spatial footprints from three example sessions in the T-maze WM task, up to 20 days apart. left: Cells detected in all three sessions (green) and cells not detected in all sessions (white). right: Cells detected across these three sessions color coded. **J**: Illustration of unique cells for a total of 5 unique cells detected across 3 sessions. The green cell is found in just one session, the blue cell is found in 3 sessions and the other cells are found in 2 sessions leading to a total cell count of 10. **K**: Most cells are found in just one session but many cells are found across multiple sessions for a total of up to 16 sessions.

As a next step, to identify the same cells across sessions, we used the CellReg algorithm (for details see methods). In brief, we took all cell pairs within 14 µm distance of each other across sessions as same-cell candidates and classified them as nearest or other neighbors. We compared the centroid distance and the spatial correlations of each pair candidate (Figure 8E, G). We modeled the nearest neighbor and other neighbor distributions to get the probability for each nearest neighbor candidate to be the same cell (Figure 8F, H, see Methods). Many cells were identified across multiple sessions up to 20 days apart (Figure 8I). Some of the cells were found in all sessions while others were found in fewer sessions or just one. Cells identified in more than one session would only be counted once for the number of unique cells (Figure 8J). After cell registration we identified 5537 unique cells that appeared at least in one session. A large proportion, 4055 cells, were only found in one session but 1482 of the unique cells were found at least across two sessions with cells being identified in up to 16 sessions (Figure 8K). Most of the cells registered just once were recorded in sessions that could not be aligned with other sessions (2902/4055 cells).

Behavioral performance and neural correlates in the mPFC during each behavior

In this first section of the results, we will discuss the behavioral performance of the animals as well as the neural correlates we recorded for each task individually. Next, we present the results of the linear modeling approach common for all behaviors to be able to compare neural coding across the different tasks. The last section will focus on the activity of the same neurons recorded across multiple sessions, both within each task as well as across the different tasks.

Task phase dependent goal coding during working memory in the T-maze

To test for SWM, an NMS task was conducted in an automated T-maze (see methods, Figure 4A, B). After a sample phase where the animals had to visit one of the two goal arms while the other arm was blocked the animal was held in the start box for a delay period of 15 or 60 s. After this period the animal had to enter the other goal arm not visited during the sample phase to retrieve a reward (see methods, **Figure 4**C). The animals learned the T-maze WM task well

within a few sessions. While most animals needed just one or two training sessions after the two shaping sessions, one animal needed three and one needed four sessions to reach criterion. Already during the training sessions after the shaping they performed with high accuracy (Figure 9A, 85.7 ± 3.5% correct, n=13, 1 session per animal). Performance stayed at that level for the following testing sessions with 40 trials (86.3 ± 1.6%, n=13, Training vs. Testing: p=0.88, Wilcoxon signed-rank test). Increasing the delay to 60 s instead of 15 s led to a significant drop in performance (67.3 ± 2.6%, n=10, Long delay vs Training: p=0.008, Long delay vs Testing: p=0.004) but it was still above chance ($p=4*10^{-6}$). The performance was again higher during later re-testing sessions with a 15 s delay (85.9 ± 1.6%, n=12, average over sessions per animal, Long delay vs Re-testing: p=0.0078), but comparable to the earlier session types, (Re-testing vs. Training p=0.75, Re-testing vs. Testing p=0.91) although other tasks were performed in between. The running time between the start box and the goal location was independent of the session type the animal was in or whether it was in the sample or choice phase (Figure 9B, ANOVA phase x session type, no main effect of phase p=0.063, no effect of session type p=0.136 or phase x session type interaction p=0.840). The total phase duration (time between start box door opening and closing after phase ended with start box nosepoke) was dependent on the different session types but not on the current phase (Figure 9C, ANOVA phase x session type, main effect of session type p=0.0097, no effect of phase p=0.119 or phase x session type interaction p=0.684). Post-hoc testing revealed a shorter duration in the long delay session than during testing (p=0.037, Wilcoxon rank sum test) or re-testing (p=0.0007), but not between testing and re-testing (p=0.312). Together with the similar running times this indicates that the animals spent less time at the reward port or in the start box during the long delay trials.

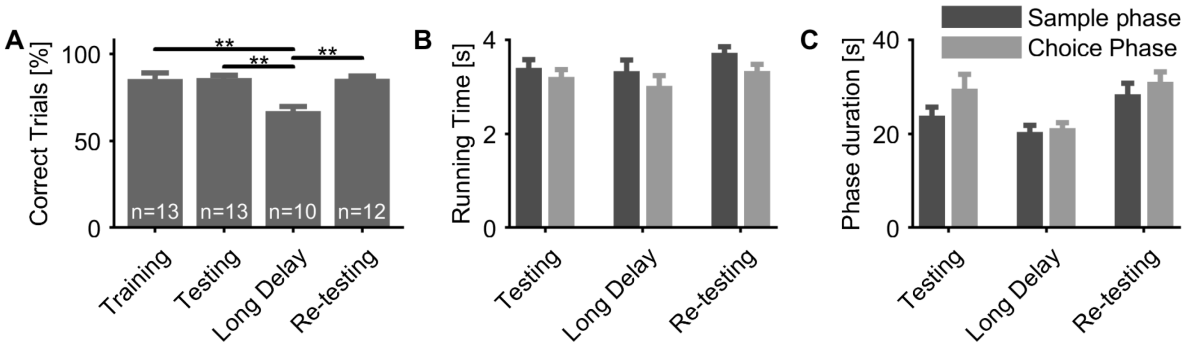

Figure 9: T-maze working memory performance. **A**: Performance of the animals in the T-maze working memory tasks is lower with 60 s delay compared to the 15 s delay but not influenced by the learning of other tasks in between the re-testing sessions. **B**: Running time does not differ across different testing stages or task phases. **C**: Phase duration was different across different session types but not between phases, ANOVA phase x session type, main effect of session type p=0.0097, no effect of phase p=0.119 or phase x session type interaction p=0.684). Post-hoc test: Testing vs Long delay: p=0.037, Long delay vs. Re-testing p=0.0007, Testing vs. Re-testing p=0.31. n=13 sessions (one per animal) for training and testing, n=10 sessions for long delay testing (not performed in all animals), n=12 animals, average over sessions per animal for those with more than one session, Wilcoxon signed-rank test, **p<0.01.

Similarly to what our group reported previously (Vogel, **Hahn** et al., 2022), we found many cells responding to various features of the SWM task. Most cells coded for positions in the maze in various ways (Figure 10A-C). Cells responded differently between outbound and inbound runs, but often coded similarly for both the sample and the choice outbound run. Other cells changed their activity profile in the inbound run, in comparison to the outbound run, for example firing in the goal arms in the outbound run but in the stem during the inbound run. Across all cells the similar firing profile between both outbound runs during sample and choice phase becomes visible, indicating it is a general feature across many neurons (Figure 10D).

Another often observed firing pattern is different activity profiles in left and right trials, again depending on specific maze positions (Figure 10E-G). While no differences in coding are found while the animal is in the stem of the outbound run, about one quarter of the cells show significant differences between the left and the right goal arm during the sample outbound run after reaching the goal arm (Figure 10H, $p<0.01$). This is reduced when the animal is returning to the start box to about 15-20% of the cells in the different maze areas of the inbound run. No differences in activity can be seen while the animal is waiting in the start box whether the animal was in the left or right goal arm during the sample phase. While the animal runs in the stem during the following outbound runs the number of neurons coding for the future arm is still at chance level. After the turn, this number increases again from about 8% to more than 26%.

To see whether we could predict the choice of the animal based on the neural recordings, we performed pseudo-simultaneous population decoding. To do this, we treated the cells recorded from different animals as if they were recorded within the same population. While goal decoding was not successful in the stem of the maze during the sample outbound run, as soon as the animal made the turn decoding accuracy increased up to nearly 100% in the goal arm (Figure 10I). It stayed high at about 85% while the animal was returning to the start box in the inbound run but dropped to chance level during the delay phase. As soon as the choice phase started, decoding accuracy increased to about 60% already in the stem of the maze predicting the future choice of the animal. In the goal arm decoding accuracy again reached up to 100%. Below chance goal decoding in the stem of the sample phase could originate in the animal encoding the previous choice goal during the sample run in combination with the pseudo-random trial structure, that makes it more likely that a left-in-choice-phase trial is followed by a left-in-sample-phase trial.

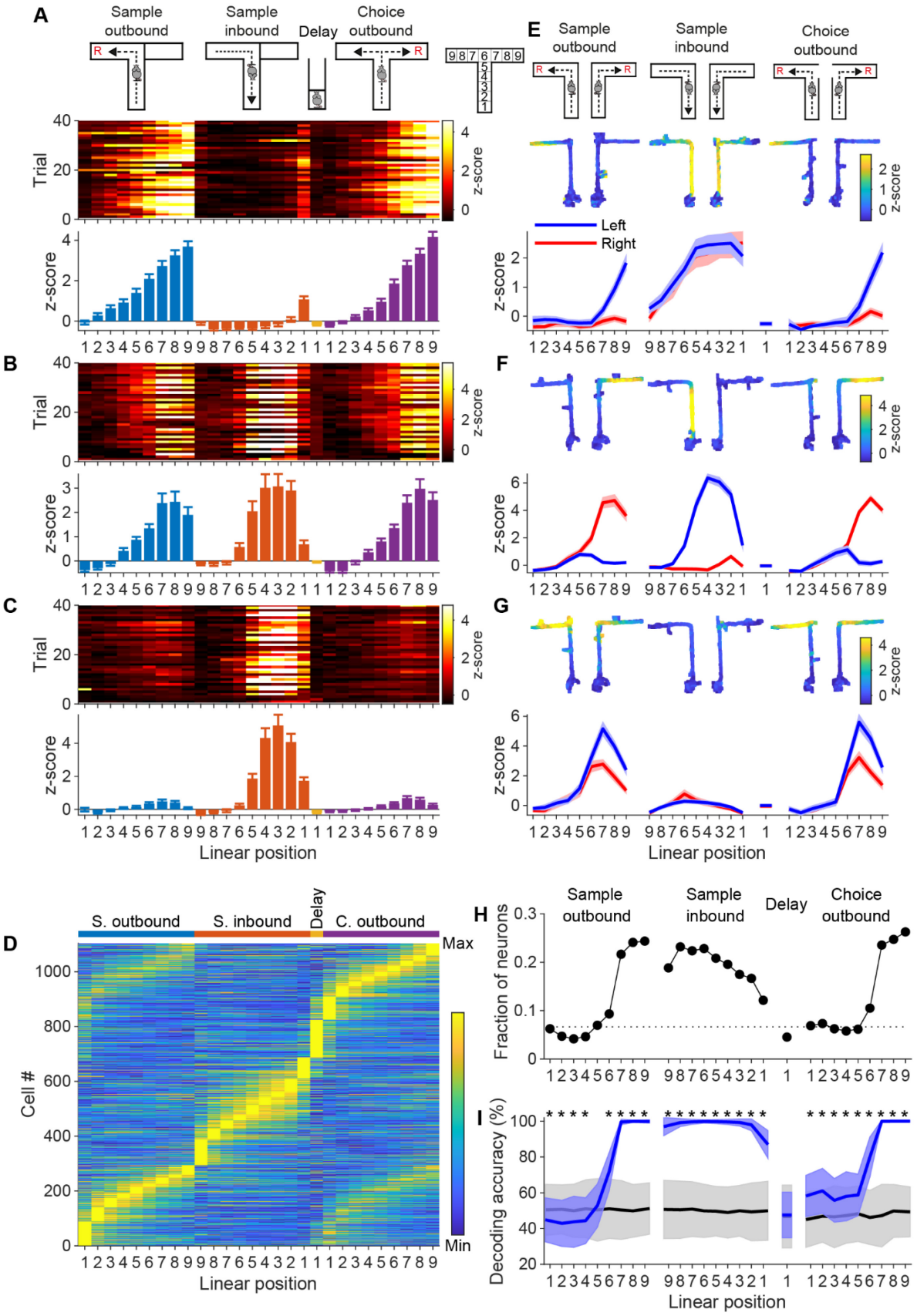
A
Sample outbound
Sample inbound
Delay
Choice outbound
Trial
z-score
Linear position
B
C
D
S. outbound
S. inbound
Delay
C. outbound
Max
Min
Cell #
E
Left
Right
F
G
H
Fraction of neurons
I
Decoding accuracy (%)

Figure 10: Encoding of task phase and goal-dependent spatial position. **A**: Example of a cell activated in both outbound runs. Top: Illustration of the task phase and maze linearization. Middle: Heatmap of trial-wise z-scored cell activity dependent on task phase, running direction and position. Bottom: activity averaged over all trials. **B**: like A, cell example activated in the goal arms during the outbound runs but in the stem during the inbound run. **C**: like A, cell example that is only activated during the inbound run. **D**: Activity map of cell activity like in A but averaged over all trials for all cells recorded during the first successful testing session, sorted by peak in activity. **E**: Example of a cell that shows different activation patterns at different positions dependent on the left or right goal location. Cell is more active in both outbound runs when the animal runs to the left goal arm and similarly activated in the return runs from both directions. Top: Heatmap of firing dependent on different maze positions separately for left or right trials. Bottom: activity vector for the same cell averaged for left and right trials independently. **F**: like E, example of a cell that shows high activation in the outbound runs to the right goal arm and high activation in the inbound runs when the animal returns from the left goal arm. **G**: like E, example of a cell that shows higher activation in the left goal arm during outbound runs but no activity in the inbound runs. **H**: Fraction of neurons that show significant differences ($p<0.05$, Wilcoxon rank sum test) between left and right trials at phase and running direction dependent locations. Dashed line represents the fraction expected by chance ($p=0.01$, binomial test). **I**: Goal decoding accuracy for pseudo-simultaneously recorded neurons at different positions dependent on trial phase and running direction. Real data in blue vs shuffled data in gray. Successful goal decoding at all locations ($p<0.05$) after entering the goal arm in the sample phase but not during the delay. Below chance decoding in the stem during the sample phase might depend on a combination of encoding of the previous trial direction and the pseudo-random goal selection (see discussion). Line: mean, shaded area: ± 1 SD, * mark significant differences between actual data and shuffle ($p<0.05$).

Preference for closed arms in the elevated plus-maze

During the EPM test the animal was placed in a standard EPM (Figure 5A, B) and was able to explore the maze freely for 10 minutes. The animals explored the different areas of the EPM (Figure 11A). As expected, they spent more time in the closed arms (Figure 11B, 61.4 ± 2.9%) in comparison to the open arms (25.0 ± 2.6%, $p<0.001$) or the small center area (13.6 ± 1%, $p<0.001$, Wilcoxon signed-rank test, Open arms vs. center: $p=0.0012$). They spent even less time in the open arms during the first five minutes of exploration (20.8 ± 3.3%, $p=0.017$) indicating a change in exploratory behavior. They also had nearly three times as many entries with a duration of more than two seconds into one of the closed arms (Figure 11C, 30.2 ± 1.6) in comparison to the open arms (12.6 ± 1.4, $p<0.001$, Wilcoxon signed-rank test). When comparing the first and the second exposure to the EPM (three days later, NO, SI and T-maze session in between, only in 8 animals) there was no difference in time spent in the different regions of the maze across sessions, the animals still spent more time in the closed than in the open arms (Figure 11D, ANOVA session x maze location, main effect of maze location $p<0.001$; no effect of session $p=1$ or session x maze location interaction $p=0.840$). Similarly, the number of entries to both arm types was similar between the first and the second session (Figure 11E, ANOVA session x maze location, main effect of maze location $p<0.001$; no effect of session $p=0.393$ or session x maze location interaction $p=0.314$). Likewise, there was no difference in the distance the animals traveled between the first (data not shown, 2872 ± 156 cm) and the second session, (2726 ± 151 cm, $p=0.11$, Wilcoxon signed-rank test). This shows that although the animals explore the open arms less during the start of each session the duration of exploration does not differ between both sessions.

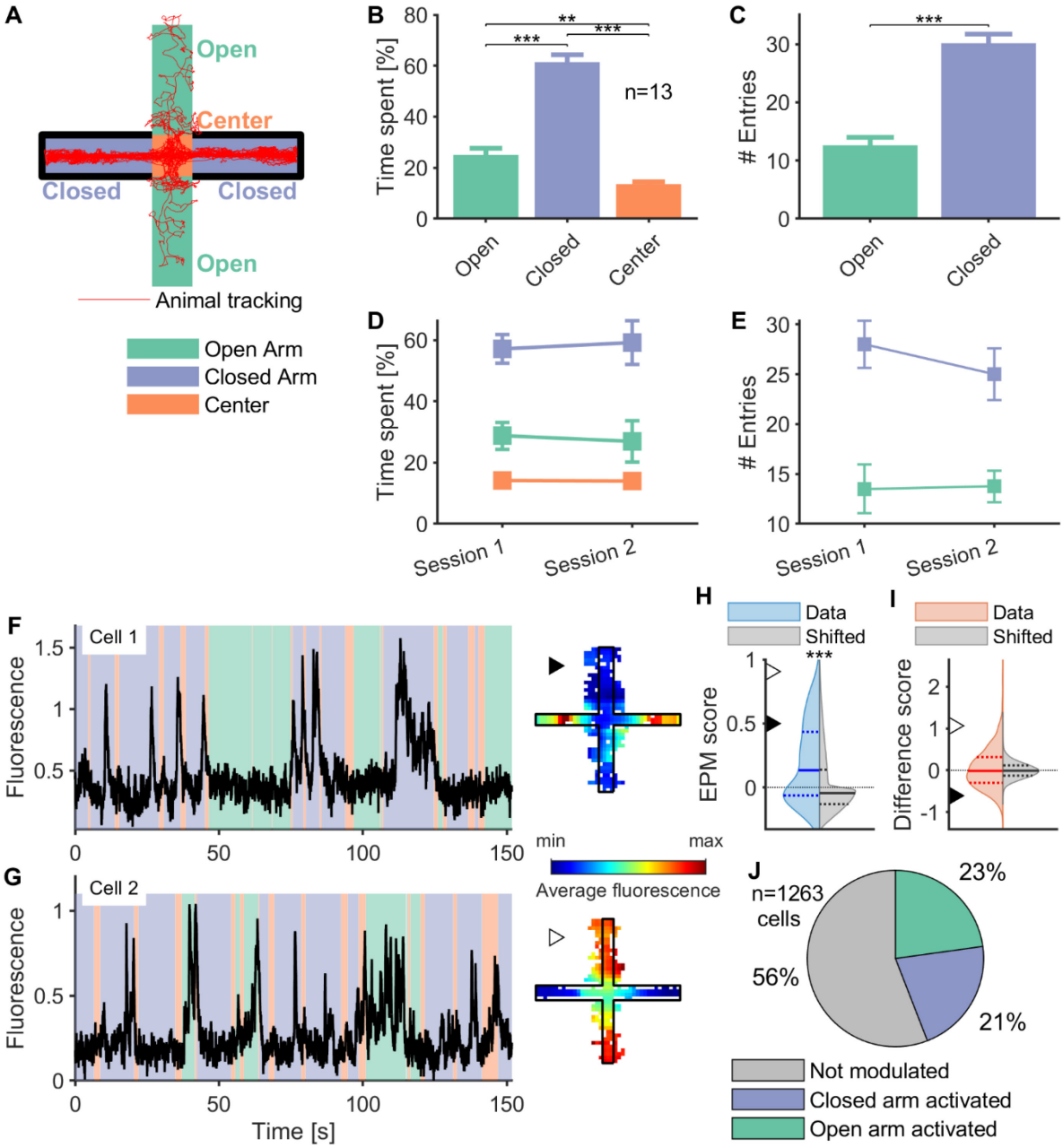

Figure 11: Neural coding of behavior in the elevated plus maze. **A**: Example tracking of a single mouse exploring the EPM for the first time. **B**: During the first session in the EPM animals spent more time in the closed arms than in the open arms. **C**: Animals entered the closed arms more often than the open arms. **D**: There is no difference between the time spent in the different maze regions between the first and second exposure to the EPM. **E**: Animals still had more entries to the closed arms during the second exploration of the EPM. **F**: Cell example showing stronger activation in the closed arms. Left: example transient for first 150 s of cell activity in the EPM. Right: Heatmap of averaged fluorescence at different positions in the EPM over the whole session. **G**: like F but a cell with higher activity in the open arms. **H**: Distribution of all EPM scores of all cells, many cells code the anxiolytic features of the EPM. Triangles indicate the values of the respective cell from F (filled) and G (open). **I**: The difference score distribution of all cells illustrates that groups of cells show stronger activation in both arm types. Triangles as in H. **J**: Number of neurons that are coding for the open or closed arms. B, C: n=13 animals, D, E: n=8 animals, H, I, J: n=1263 cells. *p<0.05, **p<0.01, ***p<0.001, Wilcoxon signed-rank test

Many of the neurons recorded in the EPM showed task-specific firing patterns. Different cells were found that showed higher activity for either both open arms or both of the closed arms

than for the other arm type. This can already be seen in the raw transients of example neurons as well as in an averaged fluorescence heat map over the whole session (Figure 11F, G). It was also represented in the EPM score (see methods), a measure for how similar the activity is between the two arms of the same type versus the activity in the arms of the other type. Most cells showed a positive EPM score indicating that the fluorescence in the same type of arms was more similar than in arms of different types (Figure 11H). The distribution of EPM scores was shifted to higher EPM scores compared to a shuffled distribution generated by randomly shifting the arm identity ($p<0.001$, Wilcoxon rank sum test, $n=1263$). As the EPM score does not give any information whether neurons were mostly activated or inhibited in either the open or closed arms, a difference score was calculated as the z-scored difference in activity between both arm types. There was no difference in the strength of the preference or number of neurons that preferred the open or the closed arms as indicated by the difference score (Figure 11I, difference in average activity in the open and closed arms) that was not different from zero ($p=0.335$, Wilcoxon signed-rank test), but also not different from the shuffled distribution ($p=0.772$, Wilcoxon rank sum test). More than 40% of the neurons had a difference score significantly different from chance, compared to a shuffled distribution (Figure 11J). There was no difference in the number of neurons being more active in the open arms (288) compared to the closed arms (269, $p=0.397$, Binomial test).

Discrimination between the center and corners in the open field

The OF and NO test was separated into three phases of 10 minutes each conducted directly after each other. During the first phase the mouse could explore the OF freely, in the following phases the objects were introduced (see methods, Figure 5C-E). This first test of free OF exploration is used as an anxiety test where untreated animals avoid being exposed in the open center and prefer the areas near the walls and especially the corners. During the first session of free exploration of the OF the mice preferred the periphery (Figure 12A, 90.2 ± 1.5%) over the center (9.7 ± 1.5%, $p<0.001$, Wilcoxon signed-rank test) of the arena. There was no difference in the time they spent in the corner areas (48.3 ± 3.1%) compared with the wall areas (41.9 ± 2.3%, $p=0.600$). Correcting for the larger area of the wall led to a significant difference between the time spent in the wall area (Figure 12C , 26.9 ± 1.9%) compared to the corner area (60.6 ± 3.2%, $p<0.001$), while the area-corrected periphery (76.4 ± 3.0%) was still preferred over the center (23.6 ± 3.0%, $p<0.001$). There was no difference in preferences between the first and the second session of OF exploration for the 8 animals imaged across two sessions for the time spent in the different zones (Figure 12D, ANOVA session x OF location for center and periphery, no main effect of session $p=1$; significant main effect of OF location $p<0.001$; no interaction effect session x OF location $p=0.313$ and ANOVA session x OF location for wall and corner, no main effect of session, $p=0.785$; no main effect of location

p=0.081 and no interaction effect session x OF location p=0.6747). Also if corrected for the different area sizes no difference between the session can be detected (Figure 12E, ANOVA on area corrected data, session x OF location for center and periphery or for wall and corner, no main effect of session p≥0.526 for both; significant main effect of OF location, p<0.001; no interaction effect session x OF location p≥0.270).

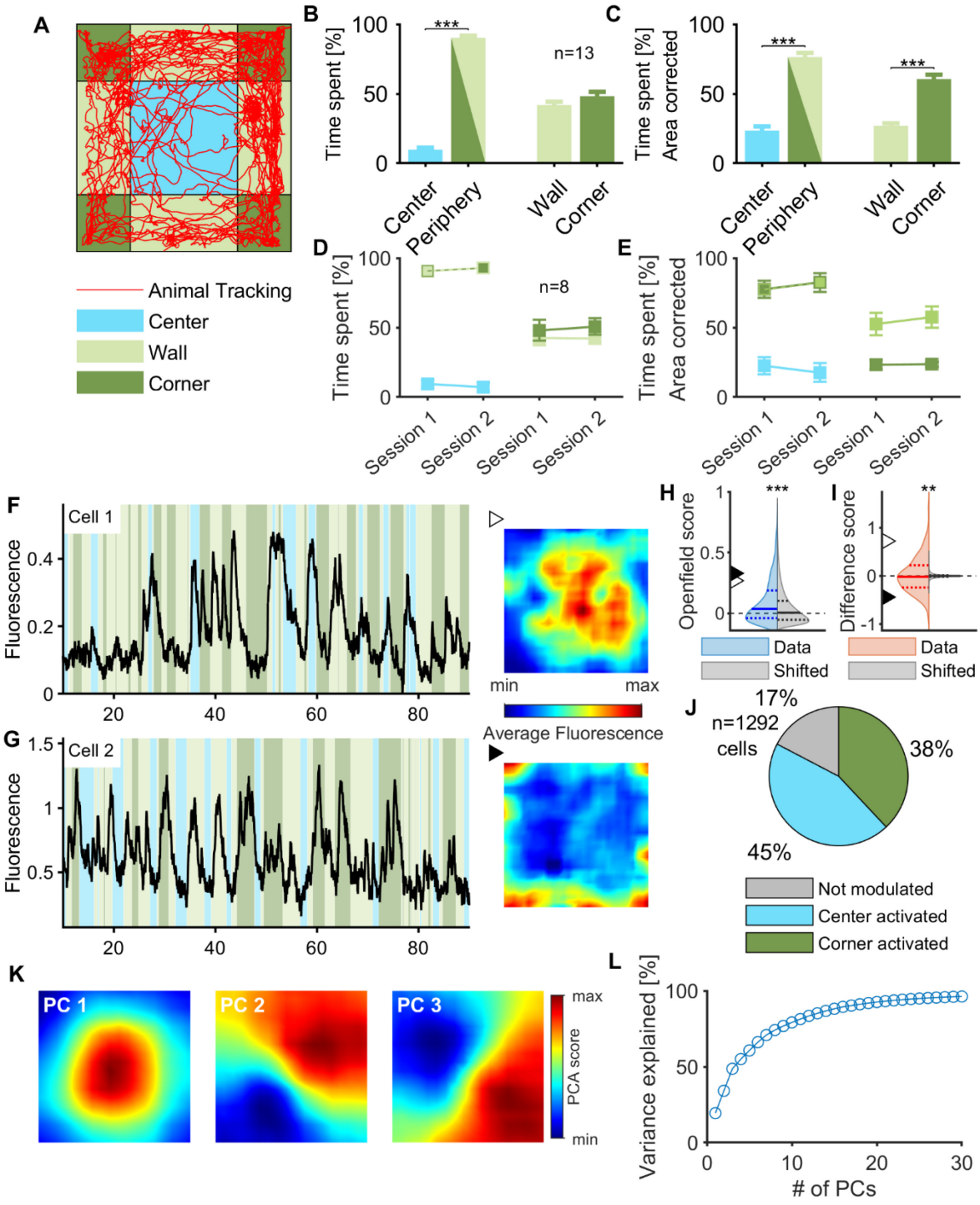

Figure 12: Neural codes for anxiogenic features during OF exploration. **A**: Example tracking of a single mouse in the OF and illustration of the different OF zones. **B**: Comparison of the time the animals spent in the different zones of the OF. **C**: Area corrected time the animals spent in the zones of the OF. **D**:

Like B but a comparison of session 1 and 2 of OF exploration. **E**: Like C but a comparison of session 1 and 2. **F**: Example of a cell that is more active in the center of the OF. Left: Raw fluorescence trace with color coded zones in the background. Right: Heatmap of cell activity over the full OF phase. **G**: Like F but a cell that is activated in the corners. **H**: Distribution of the OF scores of all cells imaged in the OF vs a shuffled distribution. **I**: Like H but showing the difference score. **J**: Distribution of cells with significant differences between center and corner activity. **K**: Heatmap of first three PCs of OF activity. **L**: Cumulative sum of variance explained by the number of PCs.

Many of the 1292 neurons imaged during the OF sessions were differently activated depending on the current zone the animal was in, clear differences could be found especially between the center and the corner areas (Figure 12F, G). Analogous to the EPM score we calculated an OF score based on how similar the activity in the four corners or the four quadrants of the center was to each other compared to the other zone type. The distribution of OF scores was significantly different from a shuffled distribution (Figure 12H, $p<0.001$, Wilcoxon rank sum test). The difference score distribution was similarly spread around 0 (Figure 12I, $p=0.729$, Wilcoxon signed-rank test) indicating that some cells preferred the center while others preferred the corner areas. But the distribution was significantly different from a shuffled distribution ($p=0.004$, Wilcoxon rank sum test). About 83% of the neurons showed significant preferences for either the center or the corner of the OF ($p<0.05$ compared to a shifted zone vector). Fewer neurons showed higher activation in the corner (491, 38%) than in the center (577, 45%, Figure 12J; Binomial test, $p=0.0077$). We then performed PCA on the activity maps to identify common spatial patterns across neurons. The first three components explained about 50% of the variance with 17 components explaining 90%, indicating a relatively high dimensional representation of space in those neurons (Figure 12K, L).

Neural correlates for novel object exploration

After 10 minutes of free OF exploration the objects (Figure 5E) were introduced (phase I), first two identical objects and after 10 minutes of exploration one of them was replaced with a novel object at the same location (Figure 13A, phase II). The animals showed clear interest in the objects after they were added to the OF, especially at the beginning of each phase. In the first 5 minutes they spent with 15.7 ± 7.9% nearly double as much time exploring the objects as in the last 5 minutes (8.1 ± 6.0%, $p=0.0012$). Therefore we limited the further behavioral analysis of the NO task to the first 5 minutes of each phase. After adding objects to the empty field in NO phase I animals explored the area around the objects more than three times as much as the same area during free OF exploration (15.7% objects, 5.0% empty zones, $p<0.001$, Wilcoxon signed-rank test, data not shown). While both objects were visited similarly during phase I the novel object was highly preferred during phase II (Figure 13B, phase I: $p=0.273$, phase II: $p<0.001$, Wilcoxon signed-rank test). This effect was driven by an increased visit duration for the novel object ($p=0.048$) and a decreased duration with the familiar object ($p=0.005$), while the total time in the zones was similar between phase I and phase II ($p=0.689$,

Wilcoxon signed-rank test, data not shown). A similar effect could be observed in the number of visits that was higher for the novel object than for the familiar object (Figure 13C, $p<0.001$) and similar for the same objects in phase I ($p=0.370$, Wilcoxon signed-rank test). Here the effect was driven by a decrease in the number of visits for the familiar object during phase II to either object in phase I ($p<0.001$), while the number of visits to the novel object was similar to that of either object in phase I ($p=0.935$, Wilcoxon signed-rank test).

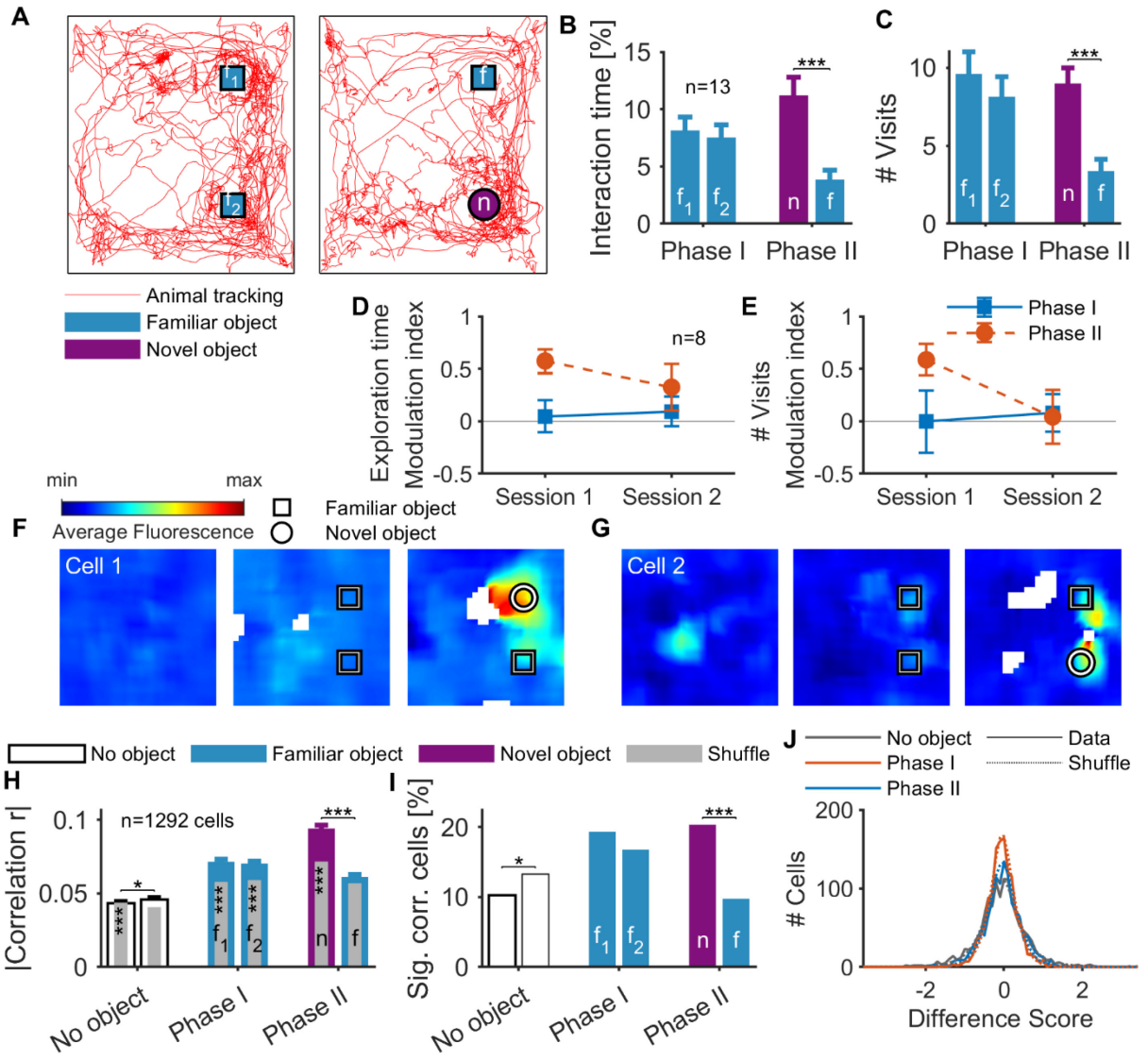

Figure 13: Preferences for novel objects coded in mPFC activity. **A**: Single animal tracking of the first five minutes during the object recognition task. Left: Phase I with two identical objects. Right: Phase II, one of the objects gets exchanged with a novel object. f_1, f_2 and n indicate the object locations of the familiar (f) or novel (n) objects. **B**: Animals spend more time investigating the novel object than the familiar one. **C**: Animals have more visits to the novel object compared to the familiar one. **D**: Preference for the novel object was gone in the second session of NO. Modulation index of exploration time, comparing the times spent at the two object locations in each phase. Phase I: values different from zero indicate preference for one of the objects. Phase II: positive values: preference for novel object, negative values: preference for familiar object. **E**: The number of visits to either object is equal in both phases of the second NO session. Modulation index as in D. **F**: Example of a cell that prefers the novel object in

phase II but shows no object preference in phase I. **G**: Example of a cell showing clear object coding in phase II, but very little preference in phase I. **H**: Neurons show higher encoding for the novel object than for the familiar object during phase II. Encoding in phase I is higher than expected by chance for both objects. Gray bars: correlation to shuffle, stars in gray bars indicate significance. **I**: More cells are significantly correlated to the novel object during phase II. **J**: Distribution of difference scores between the two object locations for the three phases. A, B, H: *p<0.05, ***p<0.001, Wilcoxon signed-rank, I *p<0.05, ***p<0.001 Binomial test.

To compare the first and second session of the novel object interaction task we calculated a modulation index comparing the time spent with either object. A positive modulation index in phase II would indicate a preference for the novel object while a modulation index of zero would indicate no preference for any object. While there was no preference for either object during phase I (Figure 13D, p>0.461 for both sessions, Wilcoxon signed-rank test) the mice showed a clear preference for the novel object in phase II during session 1 (p=0.008) as indicated by an increased visit duration but not session 2 (p=0.109). While the modulation index was higher in phase II than phase I during session 1 (p=0.008) there was no difference between the phases during session 2 (p=0.109). The number of visits to the novel object was also higher during session 1 in comparison to the familiar object (p=0.008) but again, no difference could be found in session 2 (p=0.844). Similarly, the modulation index for the number of visits was higher in phase II than I (p=0.0078) indicating a preference for the novel object during session 1 but no difference could be found during the second session (p=0.101). Together this indicates that the preference for the novel object is gone after the first NO session.

Some of the neurons recorded in the NO task showed clear preferences for the object locations specifically during the second phase, when one of the objects was exchanged (Figure 13F, G). We correlated the activity vectors of the neurons with binary behavior vectors for both objects independently (1 for animal in object zone, 0 otherwise) and found an increased neural coding for both object locations during phase I (Figure 13H, p<0.001) in comparison to chance. During phase II we found increased coding only for the novel object location (p<0.001) but no difference for the familiar object (p=0.604, n=1292 cells, Wilcoxon signed-rank test). No difference between the coding for the same objects in phase I was found (p=0.879), but during phase II the strength of coding for the novel object was increased (p<0.001, Wilcoxon signed-rank test). Surprisingly there was also a slight difference in the OF phase between both object locations, although no object was present. We found a small difference in coding between the locations (p=0.026), while coding for only one of the two locations was different from chance (p<0.001 and p=0.082, Wilcoxon ranked sum test). Similarly, the number of cells significantly coding for the object locations was slightly higher for one side during the OF phase (Figure 13I; p=0.019). Again, no difference could be found between the number of cells that coded significantly for either object during phase I (p=0.116) but more than double as many cells

coded for the novel object (20.4%) in comparison to the familiar object in phase II (9.8%, p<0.001, Binomial test). Additionally, no difference could be found between the distribution of difference scores, the z-scored differences between the activity in both object locations across the three phases (p>0.1154 for all, Wilcoxon signed-rank test). This indicates that there is encoding for the objects and also for novelty in some neurons and while some neurons are excited at the object locations others are inhibited.

Transient preference for social target during social interaction

To test for preferences in social contact over an object a SI test was conducted (**Figure 5**F, G). It was split in three phases of 10 minutes each. After a habituation phase with both compartments empty two social interaction test phases were carried out. In phase I another mouse was placed in one compartment (social compartment) while an inanimate object was placed in the other compartment (object compartment). For phase II the locations of the inanimate object and the conspecific were switched to control for effects of position. During all three phases the animals visited all areas of the social interaction box (Figure 14A). While they spent a similar time at both compartments during habituation (p=0.339, data not shown, Wilcoxon signed-rank test) they preferred the social compartment during phase I during their first session (p<0.001, data not shown). The proportion of time they spent in the social compartment in comparison to the object compartment was much higher in the beginning of the phase (57.4 ± 2.1%, Figure 14B, during first 5 minutes) compared to the last 5 minutes (28.5 ± 3.9%, p<0.001, data not shown), so we limited all further behavioral analysis to the first five minutes of each phase. The time they spent at the social compartment was significantly higher than at the object compartment in the first 5 minutes of phase I (p<0.001), but during phase II no difference could be observed (p=0.094, Wilcoxon signed-rank test). The same effect could be seen in the number of visits with nearly twice as many visits to the social compartment during phase I (Figure 14C, p<0.001) and no difference during phase II (p=0.525, Wilcoxon signed-rank test). This shows a clear but only transient preference for the social target during the first SI session.

To identify whether the behavior was stable across sessions, both sessions of SI were compared. The sessions were separated by three days with a T-maze WM session, an EPM session and a NO session in between. To compare stability a modulation index was calculated as the ratio between the time spent or the number of visits to each compartment respectively (Figure 14D, E). While the eight animals recorded across two sessions preferred the social target over the object (p=0.008) in phase I during session 1, there was no clear preference for either target during session 2 in the same phase (p=0.109). During phase II no preference could be seen (p>0.383 for both sessions). Preference for the social target was higher during phase I than II in session 1 (p=0.008) but not during session 2 (p=0.195, Wilcoxon signed-rank

test). Similar to novel object preference during the NO test preference for social exploration seems to be limited to the first session of the SI test.

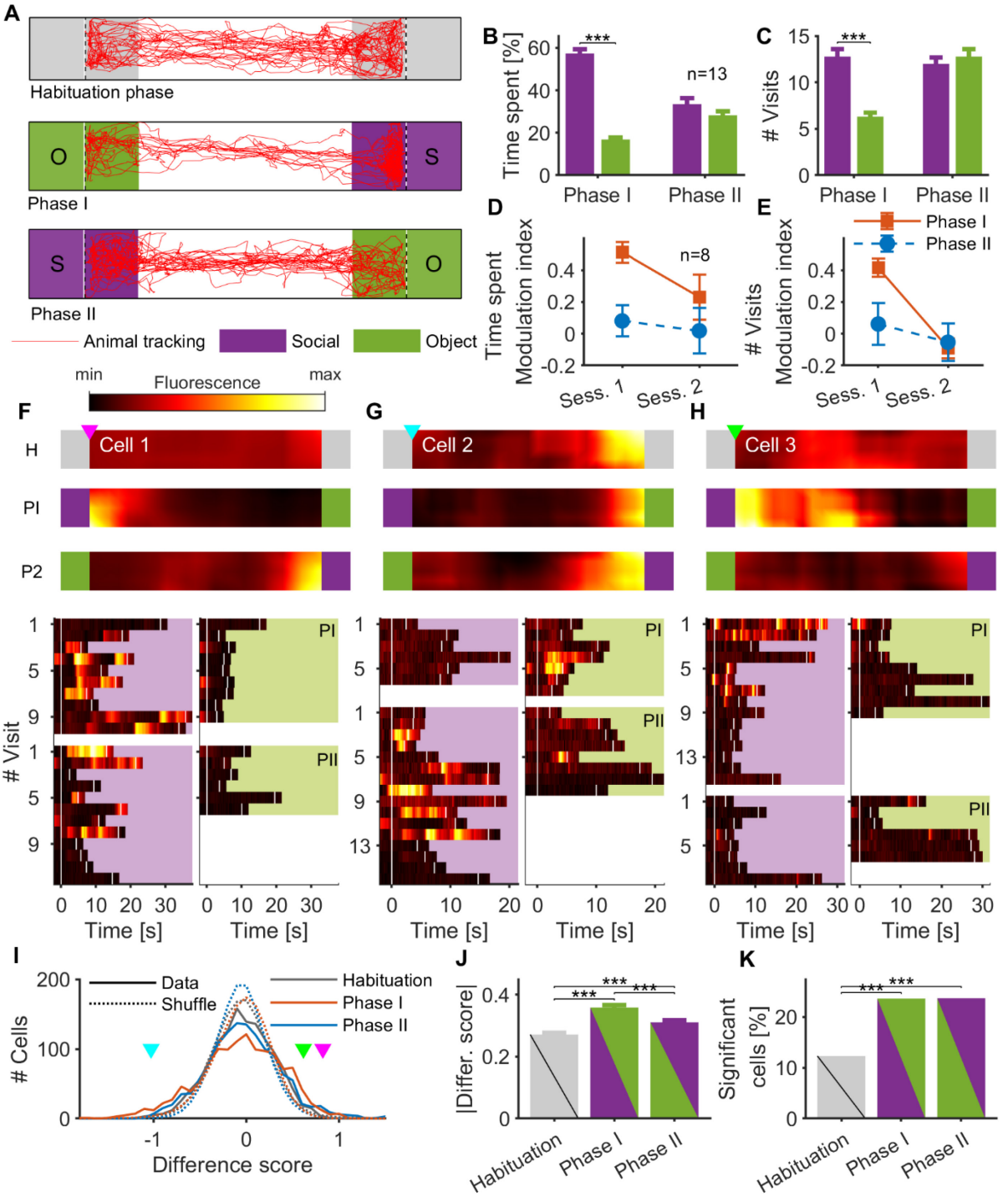

Figure 14: Neurons in the mPFC respond to social interactions. **A**: Mice explore the social interaction box across three phases. In phase I a clear preference for the social compartment is seen. **B**: Preference for the social target area in comparison to the object area during phase I which disappears in phase II. **C**: Mice visit the social compartment more often than the object compartment during phase I but not phase II. **D**: The animals do not prefer the social target over the object during session 2 in either phase. Positive values: more time spent with the social target, zero: same time with both targets, negative

values: more time with the object. **E**: The number of visits to the social compartment and the object compartment during phase I are similar during session 2. **F**: Example of a cell that prefers the social compartment to the object compartment in both social phases ('social cell'). Top: individual heatmaps of cell activity across the interaction box for the three phases. Bottom: Heatmaps of the activity of the same cell as above for all visits to either compartment during phase I (top) or phase II (bottom), sorted by social (left) or object compartment (right). White lines indicate the entry and exit of each visit, activity is shown for 2 seconds before and after each visit. **G**: Like F, cell with place coding that always is active at the right compartment in all three phases. **H**: Like F, cell that transiently gets activated in phase I during the first visits of the social target. **I**: The difference score distribution does not change across sessions. Colored triangles mark the three cell examples from F, G, H during phase I. **J**: The absolute difference score is highest during phase I and higher in phase II then during habituation, indicating bigger cell activity differences between both compartments. **K**: The number of cells with significant compartment differences is higher during phase I or II than during habituation. B, C, J: *** $p<0.001$, Wilcoxon signed-rank test; K: Binomial test. B-E: Error bars: mean ± s.e.m over animals, J: Error bars mean ± s.e.m over cells.

As a next step the neural correlates in the mPFC for these social interactions were analyzed. Many cells coded for different features in the social interaction box with most of them roughly categorizable into one of three groups. Some of the cells showed activation in the social zone (see Methods, area in front of the compartment with the social target) across both phases with the social target and object present and also across most individual visits of the social zone (Figure 14F, social cell). Some cells showed activation always in either the right or left zone (area in front of the right or left compartment), independent from the identity of the compartment (Figure 14G, position cell). Another group of cells showed transient activation for the social target, only during the first visits in the first phase of the social interaction task (Figure 14H, transient social cell). To identify further patterns in activity we calculated a difference score as the z-scored difference in activity between both zones. We could not find differences between the different distributions of difference scores across the phases (Figure 14I, $p>0.271$ for all combinations, Wilcoxon signed-rank test). By taking the absolute values ignoring the sign of the difference score we found that there are bigger differences during phase I than during habituation (Figure 14J, $p<0.001$) or phase II ($p<0.001$), with phase II also showing bigger differences than habituation ($p<0.001$ for all three, Wilcoxon signed-rank test). The number of cells that discriminated significantly between both compartments was similar during phase I and phase II (Figure 14K, $p=1$). There were more significant cells during either of that phase than during habituation ($p<0.001$ for both, Binomial test). This indicates that although there is no preference for the social target during phase II, many PFC neurons still code for the differences between the compartments, but not as strongly as during phase I.

Clear CS+ correlates during fear conditioning

The last test that was conducted was discriminatory auditory FC (**Figure 6**A-C). Two different tones were presented where one of them was paired in time with a mild foot shock. Afterwards both tones were tested during two extinction learning sessions. All mice learned the CS+ and US association successfully. While they did not show freezing to either CS during the

habituation session, freezing levels were higher during the conditioning session (Figure 15A, $p<0.002$ for both tones, Wilcoxon signed-rank test). Here the animals generalized and did not discriminate between the CS+ and the CS- ($p=0.102$). During the following two extinction sessions freezing to the CS+ was much higher than to the CS- ($p<0.001$ for both). After the first extinction session CS+ freezing was lower in the second extinction sessions ($p=0.043$). Within the first extinction session freezing did not decrease substantially between the first and the last 10 CS+ (Figure 15B, $p=0.970$) and also was still at similar levels at the beginning of the second extinction session ($p=0.622$). But during the last 10 CS+ of the second session freezing levels were substantially lower than during the first session ($p=0.002$, Wilcoxon signed-rank test).

To identify neural correlates to the different CS and the US during fear conditioning the neural responses were aligned to those events. Many of the recorded neurons showed responses to either the US during the conditioning or the CS+ during extinction with different response types. Some neurons responded to the US onset during the conditioning session (Figure 15C). During extinction training most neural responses were seen in response to the CS+. Some cells showed transient responses, strongest to the onset of the CS+ (Figure 15D), while others showed more persistent responses, often with a ramp down after a high onset response (Figure 15E). Very few cells were found that responded to the CS- exclusively, but some showed similar responses to the CS+ but with much smaller amplitude. Overall, only few cells responded to either CS during the conditioning sessions (Figure 15F), but quite many showed either activation or inhibition to the US (Figure 15G). During the extinction session many cells showed a response to the CS+ (Figure 15H, I). The number of CS+ responsive cells was higher during extinction than during the other phases (Figure 15J). Although the number of CS+ onset responsive cells dropped between the two extinction sessions ($p<0.001$) it was still much higher than the number of cells responding to the CS- or expected by chance ($p<0.001$, Binomial test). It should be noted that the number of CS+ and CS- responsive cells for the extinction sessions cannot be directly compared here due to the different number of CSs, which leads to lower statistical power for the CS-. Additionally, the different session types can also not directly be compared due to the different number of CS+ and CS- between habituation, conditioning, and extinction.

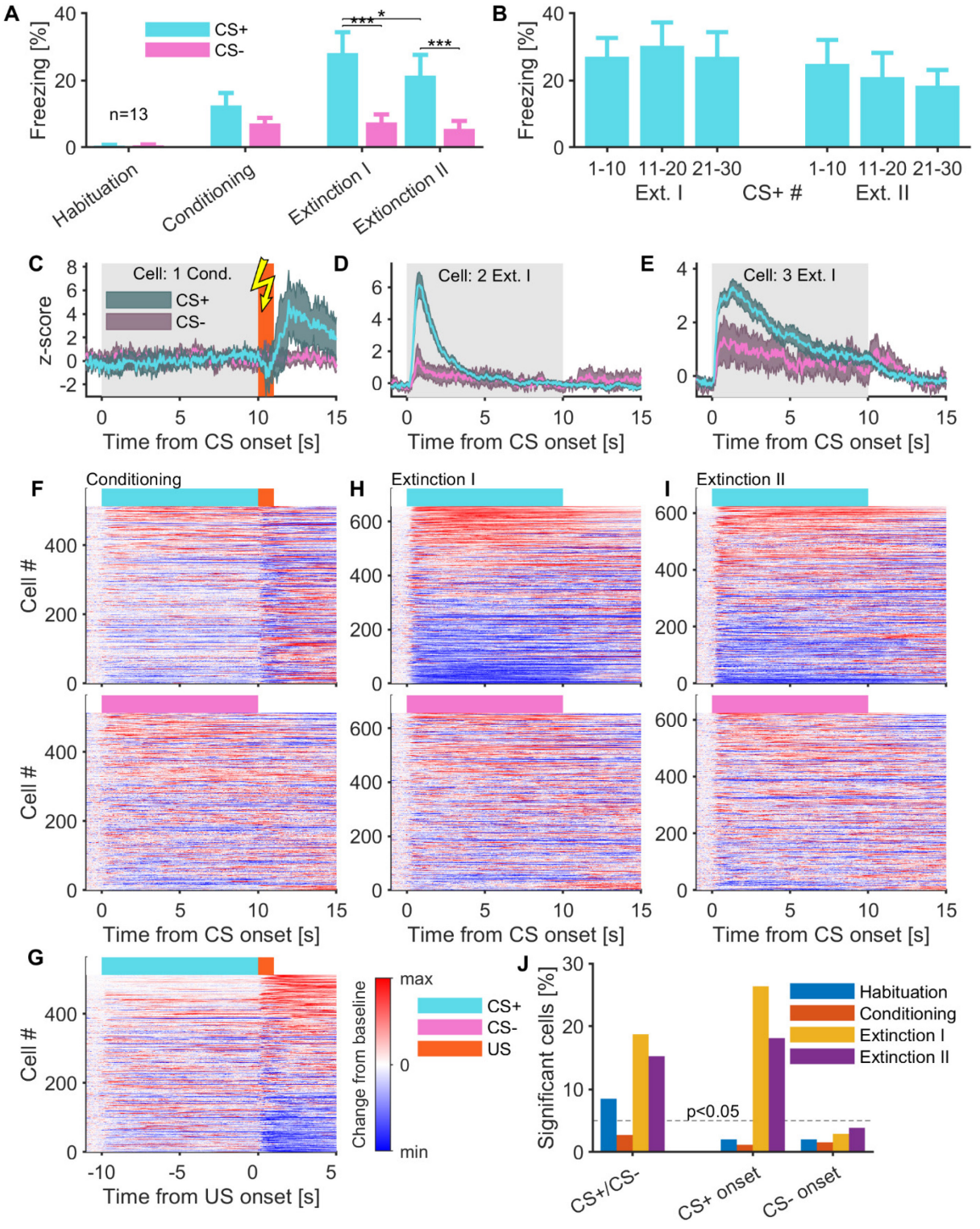

Figure 15: CS representations during fear conditioning in the mPFC of mice. **A**: Freezing levels increase after fear conditioning most prominently during the CS+ and get reduced in the second extinction training session. **B**: Freezing levels stay high during Ext. I and are reduced at the end of Ext II. **C**: Example of a cell showing an increase in activity after US offset during conditioning. The gray area marks the CS duration, the orange area the US duration (only after CS+). **D**: Like C, example of a cell showing a transient response to the onset of the CS+ but not to the CS- during Extinction I. **E**: Like C, example of a cell showing a ramp-down response during the CS+ and a much weaker response to the CS- during

Extinction I. **F**: Average response to the CS of all cells recorded during the fear conditioning session sorted by their average CS+ response (top) or CS- response (bottom). Activity is normalized to the pre-CS period and divided by the absolute maximum per cell. **G**: Average response to the US of all cells recorded during the fear conditioning session sorted by their average US response (US duration + 4 seconds afterwards). Normalization like F. **H**: Like F but for the first extinction session. **I**: Like F but for the second extinction session. **J**: Cells with significant CS responses during the 4 session types. Left: Fraction of cells showing significant differences between CS+ and CS- responses. right: Fraction of cells showing significant differences before and after CS onset for CS+ (center) and CS- (right) comparing 1.5 s before CS onset with the 1.5 s after CS onset. Wilcoxon rank sum test, threshold $p<0.05$. ***$p<0.001$, *$p<0.05$. A, B Error bars mean ± s.e.m. over animals, C-E: Error bars mean ± s.e.m. over CS presentations.

Linear modeling to analyze mPFC coding for different task features

In a next step we used generalized linear models to identify which task features influenced mPFC activity strongest. This enabled us to analyze the neural activity across neurons and multiple tasks in a common way. For every neuron we modeled its activity as the weighted sum of different behavioral variables (Figure 16A). First the fluorescence got binned into 100 ms bins (as the average fluorescence of two frames). We assigned a behavioral vector to every bin indicating the value of each variable in that bin. The model is trained 10 times with different 90% of the data and 10% of the data is used as testing data (10-fold cross validation). Discrete events like reward, door opening, and arm entry are convolved to get a better representation over time. Categorical variables are treated as multiple variables with a specific weight coefficient β_x for every unique entry. Continuous variables such as speed and position are discretized by binning and treated as categorical variables. After training the model with 90% of the data the fit is tested with the remaining 10% of the data and the variance explained by the testing data is used for all further analysis.

To test the influence of single behavioral variables multiple linear models were created. First, we created single variable models to see how much variance each variable explained on its own and a full model using all the variables together (Figure 16B-E, first column). Second, we identified the unique contribution of each variable. For this we calculated the difference of the explained variance for the full model from that of the reduced model, where one variable is shifted for every variable (Figure 16B-E, middle column). Last, we identified the cells that significantly coded for a specific variable by testing if the real behavioral vector removed from the full model led to a larger drop in explained variance than in 95% of the cases after removing a shuffled behavioral vector for that variable 1000 times (Figure 16B-E, right column). Two regressors were used across all tasks, position and speed. A third regressor, head direction, was used for all tasks except for the T-maze WM task.

Position modulates mPFC activity strongest across all behaviors

The average amount of variance explained by the full model varied between 4% and 14% across all tasks (Figure 16B-E, left). Most of the variance could be explained in the T-maze

task (14.2 ± 0.3%) and the smallest amount during FC (4.0 ± 0.2% FC, 10.9 ± 0.3% EPM, 5.2 ± 0.2% NO, 4.7 ± 0.1% SI). Across all tasks, position alone explained the highest amount of variance across all tested regressors. Explained variance was highest during the EPM (9.5 ± 0.3% and lowest during FC with only 1.8 ± 0.1% (Figure 16 B-E, left; 7.7 ± 0.2% T-maze WM, 4.1 ± 0.1% NO, 3.0 ± 0.1% SI). Position also had the highest unique contribution and the largest number of significantly modulated cells across all tasks except FC, where no unique contribution reached 1% (Figure 16 B-E, center). The unique contribution ranged from 0.7 ± 0.1% during FC to 5.9 ± 0.3% during EPM exploration. Nearly two-thirds of all cells were modulated by position in the T-maze WM task (63.4%) and less than 20% during FC (Figure 16B-E, right, 19.5% FC, 35.5% EPM, 23.3% NO, 25.2% SI). During FC the CS+ had a slightly higher unique contribution (0.8 ± 0.1% CS+, 0.7 ± 0.1% position) and more cells were modulated by speed (19.5%) or head direction (17.3%) than position (15.6%). Speed had a substantially lower unique contribution of about 0.3% across all behaviors (0.33 ± 0.01% T-maze WM, 0.35 ± 0.04% EPM, 0.32 ± 0.03% NO, 0.28 ± 0.02 SI, 0.39 ± 0.03 FC). The contribution of the head direction was slightly higher, with about 0.5% during NO, SI and FC and 0.9% in the EPM (not measured for T-maze WM). The position of the animal in an environment seems to influence mPFC activity strongly, also when spatial information is not required for task execution. Other general behavioral variables like the head direction or the movement speed of the animal were less well represented.

The other used variables showed substantially lower contributions, only reward in the T-maze WM task had a unique contribution above 1% all other variables explained less (Figure 16B-E, center). Interestingly, many cells still were significantly modulated by those task variables with many cells being modulated by multiple variables (Figure 16B-E, right). The events reward, opening of the start door and arm entry still modulated between 40 - 54% of the cells during T-maze WM per variable while about 20% were modulated by either phase, running direction, or speed. Goal representation was quite limited with only 8% while nearly no cell was modulated directly by trial correctness (1.8%).

During EPM exploration 16.9% of cells were modulated by head direction and 13.0% by speed (Figure 16C), similar to the values for NO (19.7% head direction and 17.4% speed, Figure 16D), SI (17.9% and 19.0%, Figure 16E) or FC (17.3% and 19.5%, Figure 16F). The object identity nearly did not play any role (0.4% modulated cells) during NO. During SI 5-7% of the cells were modulated by the zone entry and interaction type across the whole session. The CS+ modulated about 13.9% of the cells during FC while the CS– (2.6%) and freezing did not influence many cells (2.5%). This shows that, apart from the CS+ representation during FC extinction learning, the task-specific variables were not as strongly encoded by the whole population of mPFC neurons.

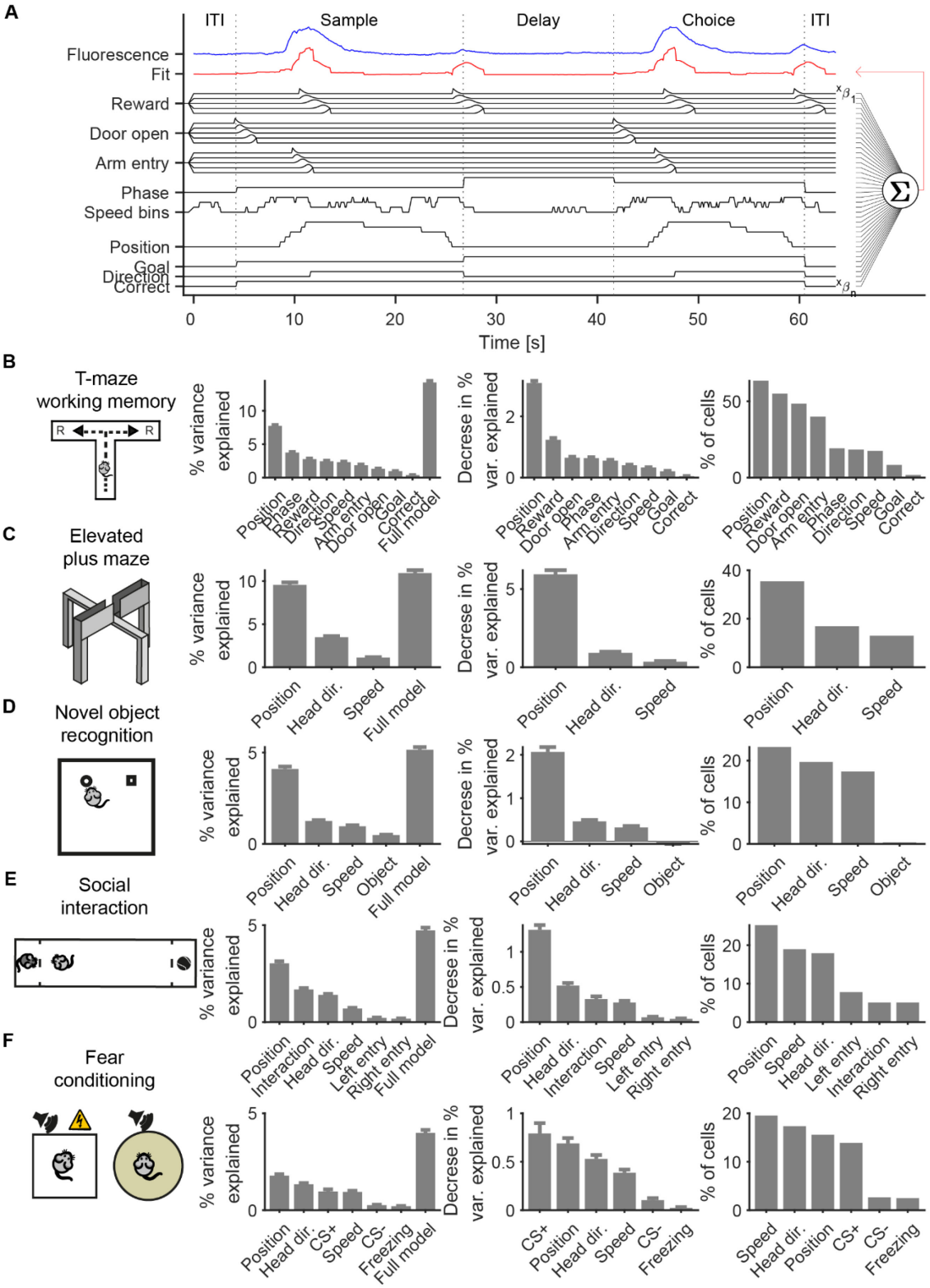

Figure 16: Linear modeling of task variables to identify task features that influence cell activity. **A**: GLM for the T-maze working memory task. We try to model the fluorescence trace of a single cell (blue) by calculating the weighted sum of different task variables at these time points. Events (Reward, door open and arm entry) are convolved with splines to get a better temporal representation of these events. Continuous variables (position, speed) are binned and treated as categorical variables. For every time bin the fit (red) is created by summing up the beta coefficients $\beta_{1 \rightarrow n}$ multiplied with the state of the associated variable. **B-F**: Left: Variable explained by single variable models and full model. Middle:

Decrease in variance explained when each variable was removed from the full model. Right: Number of cells significantly modulated by each variable. **B**: Modeling results for the T-maze working memory task. **C**: Modeling results for the EPM task. **D**: Modeling results from the novel object recognition task including the OF phase. **E**: Modeling results from the social interaction task **F**: Modeling results from Fear conditioning (only extinction sessions). Bars represent mean ± s.e.m over neurons (left, middle) or proportion (right).

It is apparent that many cells encode multiple behavioral variables. During the T-maze WM task, approximately 10% of neurons respond to no variable, while 16% respond to only one variable (data not shown). However, during other tasks, roughly 50% do not code for any variable and about 30% code for just one variable. This results in approximately 20% of neurons coding for multiple variables during those tasks and 74% for the WM task. During WM about 16% code for five or more behavioral variables. While some of the cells are not engaged in the task, overall most of the cells show task engagement.

Stability in coding across sessions of the same and different tasks

Finding many mPFC neurons coding for different task variables raises the question whether these codes are stably encoded across multiple sessions of the same task. General behavioral variables (position, speed, head direction) could also be encoded by the same neurons across multiple tasks. Additionally, ensembles of neurons could code for task-specific variables across different tasks, even if they are not related. So as a next step we compared the activity of neurons recorded across sessions within the same and across different behaviors. First we compared spatial activity of single neurons across sessions within the same task and as a second step we correlated the unique contribution of all behavioral variables across all different task combinations.

Stable coding for positions across multiple sessions of the same task

Generalized linear modeling revealed spatial coding to be one of the prevalent features across all tested behaviors. To identify whether the same cells showed similar spatial coding patterns in two sessions of the same task we started by correlating spatial activity across two sessions of the same task. Indeed, across all five tasks we found cells with similar firing patterns across two sessions (Figure 17A-E, left column). Across all cells that were imaged in pairs of sessions of the same task the spatial correlation was higher than expected by chance (Figure 17A-E, middle column, $p<0.001$, Wilcoxon rank sum test, SWM: n=2194, EPM: n=192, NO: n=163, SI: n=221, FC: n=164). Additionally, the reduction in explained variance after removing position from each GLM was correlated across sessions of the same task (Figure 17A-E, right column). For this we correlated vectors of all cells imaged in two different sessions together for all animals and compared it with vectors for shuffled cell pairs. This is a more general measurement if a cell codes for positions than the direct spatial correlation, as a cell would not necessarily need to be active at the same location to get correlated values here. Hereby the

correlation was highest in the T-maze WM task with an r value of 0.57 followed by SI with 0.37 and the EPM with 0.31. The correlation between two sessions of the NO task (r=0.25) and FC (r=0.24) were much lower than in the other tasks but still highly significant. These results show that cells with spatial representations of the environment on average keep their representation across multiple days and also with the exposure to different environments in between. Additionally, finding this stability indicates that the cell alignment process worked reliably.

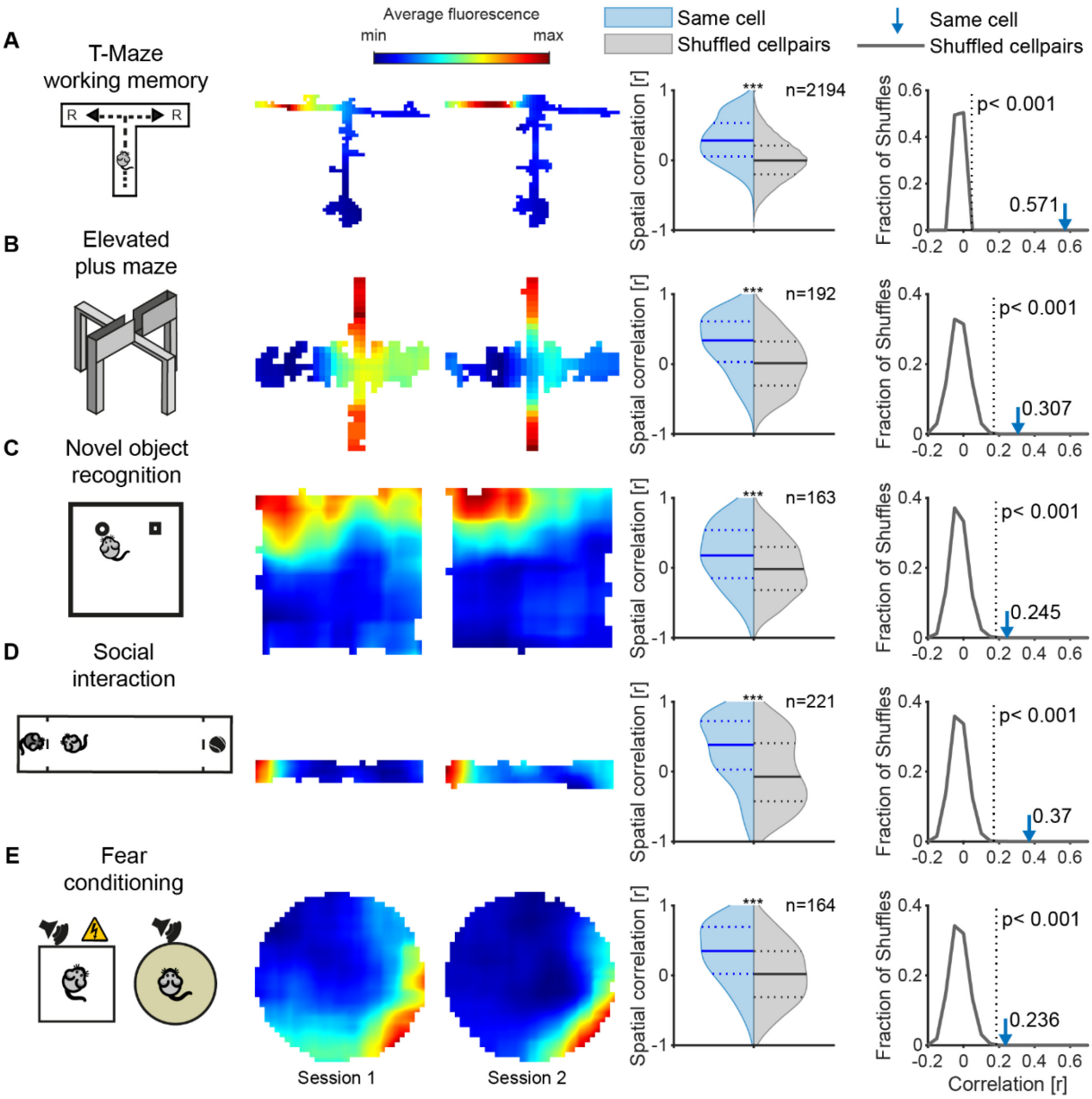

Figure 17: Stable spatial coding across multiple sessions within different behaviors. **A**: left column: Example heatmap of a cell showing similar spatial firing patterns across two sessions of the WM task. Middle column: Comparing distributions of spatial correlations across cell pairs (blue) and shuffled cell pairs (gray). Same cells across two sessions of the T-maze WM task show a higher average spatial correlation than expected by chance. The solid line indicates the median, dotted lines indicate the 25 and 75 percentiles. Right column: Correlation of reduction in explained variance for the regressor

"Position" in the T-maze WM task for the same cell is higher than for random cell pairs. The arrow indicates the correlation between two sessions of the same cells, the gray line is the distribution of correlations of shuffled cell pairs, the dotted line indicates the p value below 0.001. **B-E:** same as A but for the EPM (**B**), the NO recognition task (**C**), the SI task (**D**) and FC (**E**). ***p<0.001 Wilcoxon rank sum test.

Cells that code for position in one task tend to also code for position in other tasks

This second measurement of correlating the unique contribution for variables across sessions enabled us to compare position coding across tasks, as the differently shaped task environments cannot be correlated directly. So, we used the unique contribution of the position regressor in our linear model and correlated it across different tasks for all cells that were found in sessions of each task. This was compared again to a distribution of random cell pairs by shuffling the cell pairs for each task combination 1000 times. We first compared all sessions of the T-maze WM task with sessions of all other tasks and found that cells coding for *position* in the T-maze also coded for *position* in the other tasks as indicated by a higher than chance correlation (Figure 18A; SWM-EPM: r=0.18, p<0.001; SWM-NO: r=0.06 , p=0.011; SWM-SI: r=0.10, p<0.001; SWM-FC: r=0.13 , p<0.001; Compared to shuffle).

Afterwards we compared the correlation of the unique contribution for position in actual cell pairs to random cell pairs across the other possible task combinations not containing the T-maze but found significant differences only for the SI and NO task combination (Figure 18B, r=0.16, p<0.001, Wilcoxon rank sum test) but not between the other tasks. Herby it is worth noting, that the statistical power of the T-maze WM task paired with itself or other tasks is much higher, due to the higher number of sessions in the T-maze WM task leading to a higher number of cell pairs (SWM-SWM: n=4388, SWM-EPM: n=1718, SWM-NO: n=1906, SWM-SI: n=1871, SWM-FC: n=1574, EPM-EPM: n=334, EPM-NO: n=755, EPM-SI: n=698, EPM-FC: n=538, NO-NO: n=424, NO-SI: n=837, NO-FC: n=719, SI-SI: n=414, SI-FC: n=652, FC-FC: n=358, half of that for the same regressor in the same task, see methods). After subsampling the number of cell pairs to the minimum number of cell pairs across all combinations (n=334) only the SWM-EPM combination was significant (p=0.03 corrected for multiple comparisons, data not shown) while other significant differences were not detected (data not shown; SWM-NO: p=1; SWM-SI: p=1; SWM-FC: p=0.333; corrected for multiple comparisons, compared to distribution of shuffled cell pairs). The r values were nearly unaffected by the subsampling procedure. These results suggest that cells that code for position in one task also code for position in the other tasks, although a higher number of cells might be required to identify these differences.

Similar to the position predictor we also tested for stability of speed coding across all task combinations (Figure 18C). The correlation between the reduction in explained variance was higher than chance for all task combinations but for the EPM with itself (p=0.66 corrected for

multiple comparisons) and the EPM with FC (p=0.06 corrected for multiple comparisons). All other task combinations were significant, ranging between r=0.09 for the SWM-EPM correlation and r=0.57 for the FC-FC correlation (p<0.001 for all except SWM-EPM p=0.015 corrected for multiple comparisons). Similar to position coding, many cells also coded for speed across multiple sessions of the same task and also other tasks. The level of stability was even higher than for position coding.

Correlated coding for other task variables

We then tested all possible task and predictor combinations for correlated representations across sessions (Figure 18D). The strongest correlations, both within and across tasks, were found for position and speed. Moreover, 10 (3 within the same task) out of 15 task combinations showed significant correlations for the speed predictor and 8 (4 within the same task) out of 15 for position (after correction for multiple comparisons). It should be noted that within task correlations for the same predictors have lower statistical power due to a lower cell number. Also, checking across different predictors, cells that coded for speed often also coded for position. Hereby 5 out of 20 position-speed combinations across the same or different tasks were significantly correlated across sessions.

Another trend that can be seen is that most significant correlations include the T-maze WM task. Again, this can be attributed to higher statistical power of the combinations including the WM task in comparison to other tasks combinations. After subsampling the number of cell pairs, again most of the significant correlations could not be detected, across different tasks only speed is correlated in the EPM-SI combination ($p=2.6*10^{-5}$) and within each task only same predictors are correlated (data not shown, SWM: Reward, Door open, Arm entry, Phase, Speed, Position; EPM: Position; SI: Position, Speed; FC: Speed, Head direction, $p<1.23*10^{-4}$ for all).

Coding for the same variable is more stable within the same than across tasks

Next, we wanted to see whether the degree of stability in encoding task variables depended on whether the same or different tasks were compared. A trend to lower correlation of reduction in explained variance for the same variable across different tasks in comparison for the same task was found (Figure 18B-D). To test this further, we compared this for the three variables that are available in multiple tasks, position, speed, and head direction. Indeed, for position (Figure 19A; p<0.001) and head direction (p=0.0095, Wilcoxon rank sum test) the correlation was lower across different tasks than in the same task. For speed a trend in the same direction was visible (p=0.075). This shows that across session coding for the same variable was higher within the same task than between different tasks.

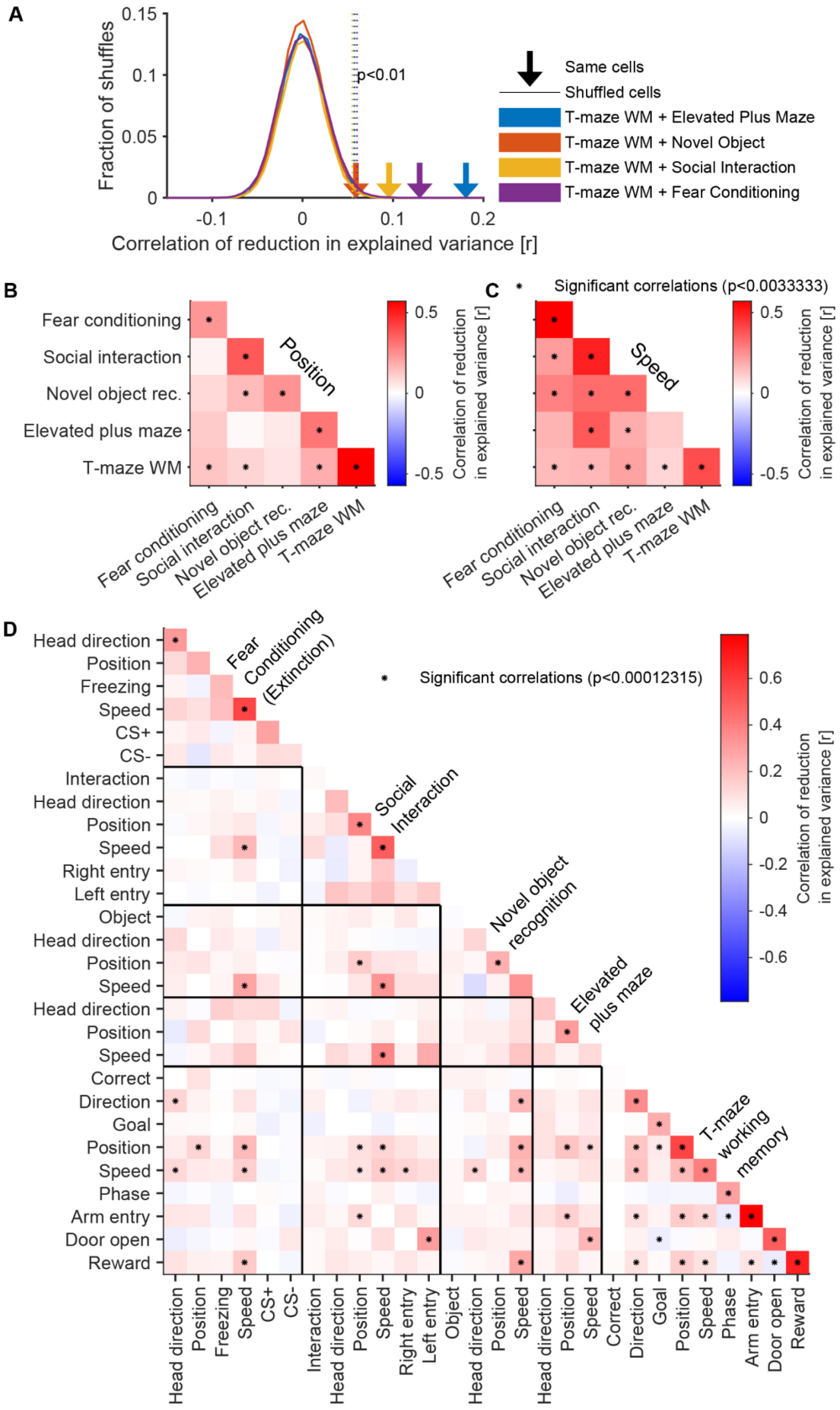
A
Fraction of shuffles
0.15
0.1
0.05
0
p<0.01
-0.1
0
0.1
0.2
Correlation of reduction in explained variance [r]
Same cells
Shuffled cells
T-maze WM + Elevated Plus Maze
T-maze WM + Novel Object
T-maze WM + Social Interaction
T-maze WM + Fear Conditioning
B
Fear conditioning
Social interaction
Novel object rec.
Elevated plus maze
T-maze WM
Position
0.5
0
-0.5
Correlation of reduction in explained variance [r]
C
Significant correlations (p<0.0033333)
Speed
D
Head direction
Position
Freezing
Speed
CS+
CS-
Interaction
Right entry
Left entry
Object
Correct
Direction
Goal
Phase
Arm entry
Door open
Reward
Fear Conditioning (Extinction)
Social Interaction
Novel object recognition
Elevated plus maze
T-maze working memory
Significant correlations (p<0.00012315)
0.6
0.4
0.2
-0.2
-0.4
-0.6

Figure 18: Stability in coding for speed and positions within and across tasks. **A**: Correlation of reduction of explained variance for position regressor between the T-maze WM task and the other tasks. Arrows indicate the correlation between the same cell, solid line in same color is the distribution of shuffled cell pairs, the dashed line indicates the p value below 0.01. **B**: Correlation matrix of reduction in explained variance for "position" regressor between all task combinations. * indicate significant combinations, p<0.0003, correction for multiple comparisons. **C**: Like B but for "speed" regressor. **D**: like B but for all regressors across all tasks. *$p<1.2*10^{-4}$. (SWM-SWM: n=4388, SWM-EPM: n=1718, SWM-NO: n=1906, SWM-SI: n=1871, SWM-FC: n=1574, EPM-EPM: n=334, EPM-NO: n=755, EPM-SI: n=698, EPM-FC: n=538, NO-NO: n=424, NO-SI: n=837, NO-FC: n=719, SI-SI: n=414, SI-FC: n=652, FC-FC: n=358; n=n/2 for same-task-same-variable correlations, see methods). Significance level adjusted for multiple comparisons

The differences in correlation within compared to across tasks could reflect differences in the different time span between the sessions. To address this we performed an analysis of covariance (ANCOVA). We used the number of sessions in between two sessions (time) as a factor (continuous variable) and grouped them for either the same or different tasks (categorical independent variable). The ANCOVA was only performed for the position and the speed predictor, as the head direction was not evaluated during the T-maze and all spontaneous task sessions had always the same number of sessions in between them. We only found an influence of the group (Figure 19B, C, p<0.001 for position and speed) but no influence of the time between the sessions (position: p=0.997, speed: p=0.265), and also no interaction effect (position: p=0.601, speed: p=0.723) indicating a parallel slope for both variables. The slope itself is nearly 0 with the standard error similar to or even larger than the slope (position: 0.001 ± 0.004; speed: -0.006 ±0.005), indicating no change in correlation over time.

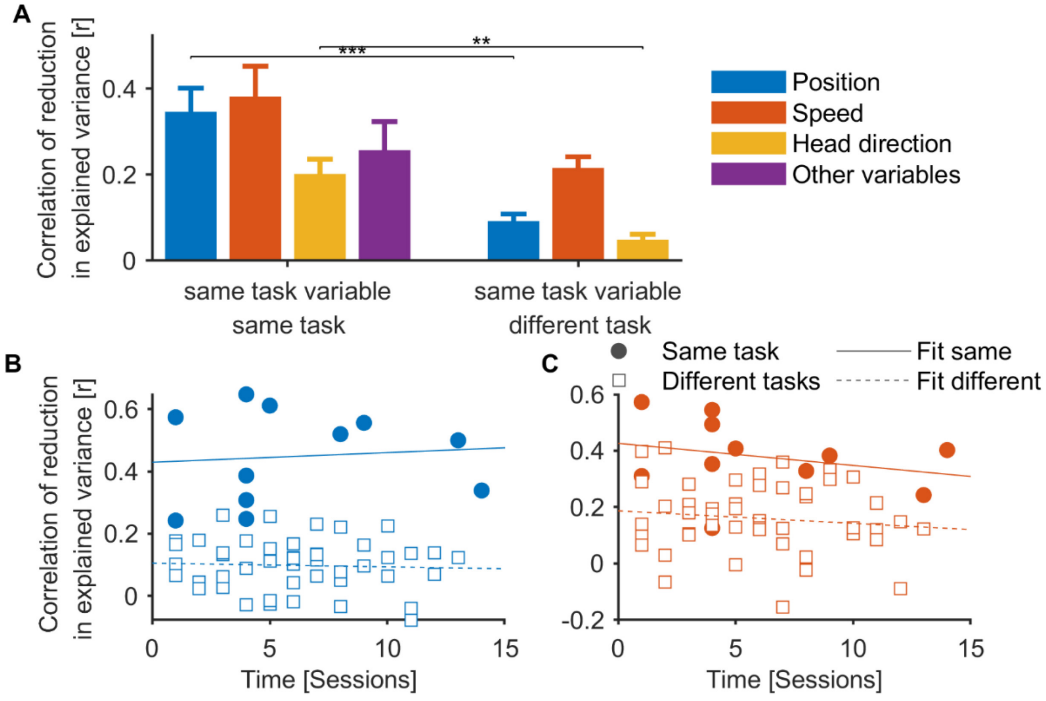

Figure 19: Within task coding is more stable than across task coding and independent of time between sessions. **A**: Task variables were more stably encoded within a task than across multiple tasks. position:

p<0.001, speed: p=0.075, head direction: p=0.0095; n=5 task combinations for position & speed same task, 10 different tasks; n=4 task combinations for head direction same task, 6 different tasks, Wilcoxon rank sum test. **B**: Correlation for position across sessions was dependent on task identity and independent of the time between the sessions. Every point is a possible session separation within each task combination. ANCOVA: Main effect of task identity (same or other p<0.001), no effect of session difference (p=0.99), no interaction effect of task identity x session difference (p=0.60). Linear fit: same task: y=0.0031x+0.4294, different tasks: y=-0.0011+0.0987. **C**: As B but for speed. Main effect of task identity (same or other p<0.001), no effect of session difference (p=0.99), no interaction effect of task identity x session difference (p=0.60) ANCOVA with session difference as factor and same or different task as groups. Linear fit: same tasks: y=-0.0078x+0.4264, different tasks: y=-0.0042+0.1870.

Cells code for similar task-relevant features across the same and different tasks

After finding that the same cells encoded general behavioral variables across sessions and tasks we wanted to test if the cells also coded for the same specific task-relevant features within and across tasks. First, we wanted to see if specific features are stably encoded within multiple sessions of the same task. After seeing clear responses to the CS+ during both extinction sessions (Figure 15H-J) we wanted to see whether the same cells respond to the tones across sessions. We found that most cells that responded to the CS+ during extinction II also responded in a similar way to the CS+ during extinction I (Figure 20A). The average response to the CS+ was highly correlated between both extinction sessions (Figure 20B, $p=3.2*10^{-8}$) but not between extinction II and habituation (p=0.79) or extinction II and conditioning (p=0.58, Compared to zero, Wilcoxon signed-rank test). The correlation between extinction II and I was also stronger than that between extinction II and habituation ($p=1.34*10^{-6}$) and between extinction II and conditioning ($p=2.20*10^{-6}$) while there was no difference between the correlations of habituation and extinction II and the correlations of conditioning and extinction II (p=0.57, Wilcoxon rank sum test). This indicates a change in CS responsiveness after the conditioning session.

We also found cells that were similarly active in related situations across different tasks. In both the OF and EPM tasks we found cells that coded for anxiogenic features of the environments, a possible signature for safe, enclosed areas or exposed, open areas on the other hand (for details see Figure 11, Figure 12). These anxiogenic features seem to be encoded by the same neurons across both of those tasks with examples showing excitation for either the safe or the exposed regions (Figure 20C, D) across both tasks. To compare this for all cells systematically we correlated the difference scores “open vs closed” of the EPM (Figure 11I) to the difference scores “center vs corner” in the OF (Figure 12I) and found a higher than chance correlation (Figure 20E; n=893, r=0.19, $p<5*10^{-5}$, compared to distribution

from random cell pairs). This indicates that indeed the same neurons encode the anxiety state or exposure of the animal across both environments.

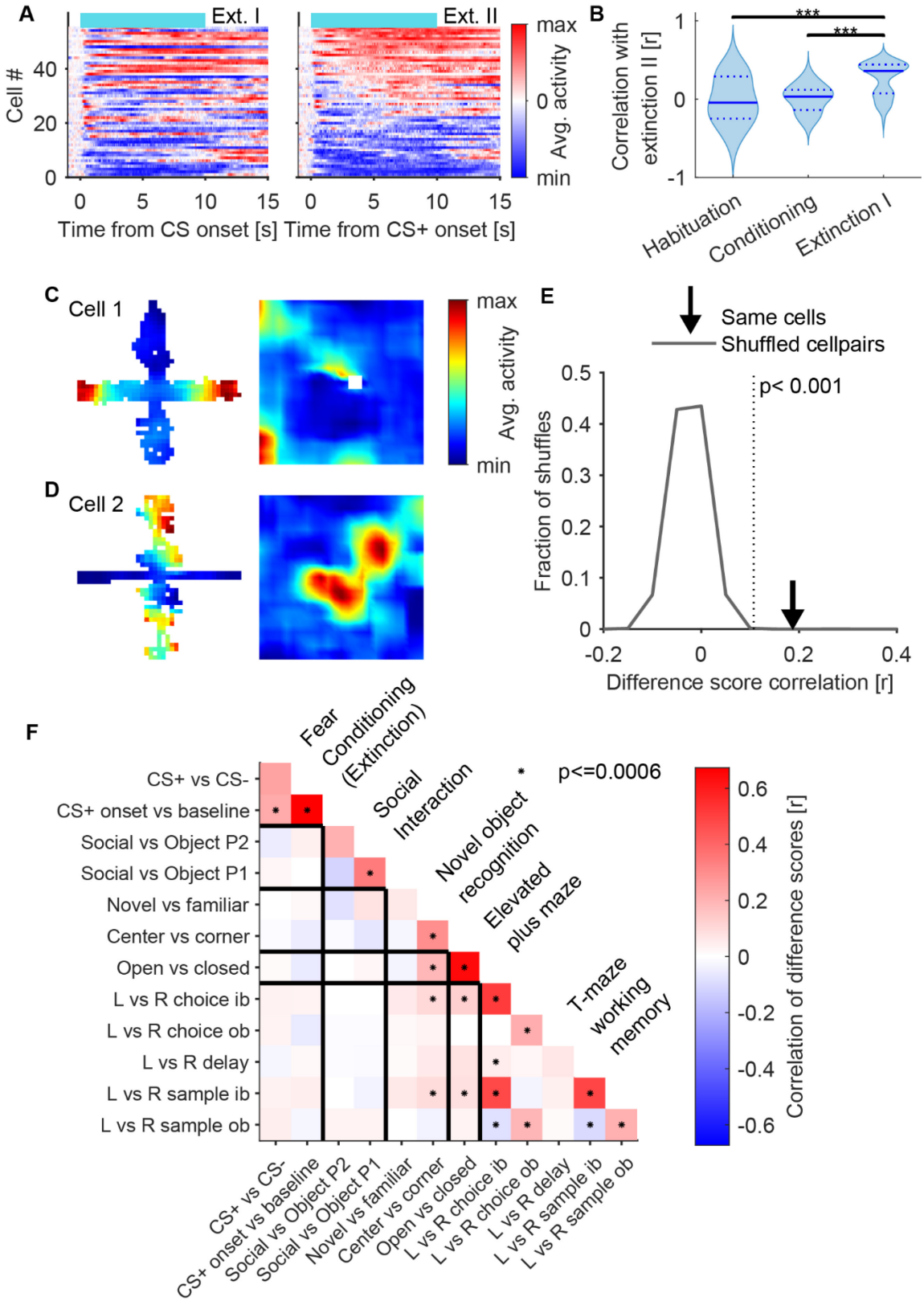

Figure 20: Cells code for task-specific features across sessions and for common features across tasks. **A**: Cells respond in a similar way to the CS+ between both extinction sessions. Sorted by the response

to the CS+ during extinction II, only cells with significant CS+ onset responses are shown. Normalized to baseline response before CS onset., Blue lines indicate the CS+ duration. **B**: The correlated CS+ response between cells is higher between the two extinction sessions in comparison to the correlation of extinction II with habituation or conditioning. ***p<0.001, Wilcoxon rank sum test. **C**: Cell example showing activity in safe areas during two different tasks. Cell shows increased activity in the closed arms of the EPM and in the corners during OF exploration. **D**: Like C but increased activity in the open arms and in the center of the OF, the exposed areas. **E**: Correlation of the difference score between the open and the closed arm in the EPM and the center and the corner in the OF reveal that cells code for the same anxiolytic features across the EPM and OF. The arrow marks the real data while the solid line indicates the shuffled distribution of random cell pairs, dotted line indicates the significance threshold of p<0.001. **F**: Correlation matrix of difference scores across sessions and tasks. * indicates significant combinations, p<0.0006, corrected for multiple comparisons. SWM-SWM: n=4388, SWM-EPM: n=2027, SWM-NO: n=1906, SWM-SI: n=1871, SWM-FC: n=1574, EPM-EPM: n=484, EPM-NO: n=893, EPM-SI: n=738, EPM-FC: n=538, NO-NO: n=424, NO-SI: n=837, NO-FC: n=719, SI-SI: n=414, SI-FC: n=652, FC-FC: n=358,half of that for same task and same difference score (see methods).

We now used the same approach to compare the difference scores of different task features across all behavioral tasks. Nearly all task-specific features were significantly correlated with themselves across sessions of the same task (Figure 20F). Exceptions, after correcting for multiple comparisons with a p-threshold of 0.0006, were the “left vs right” differences in the delay phase of the SWM task (n=2194, r=0.066, $p=1.8*10^{-3}$, comparison to shuffle), “novel vs familiar” score in the NO task (n=162, r=0.059, p=0.31), the “social vs object” differences in the second phase of the SI task (n=207, r=0.21, $p=3.6*10^{-3}$) and the “CS+ CS-“ differences during FC (n=179, r=0.24, $p=1.3*10^{-3}$). Again, the statistical effect could be underestimated by the lower number of cell pairs in same-task-same-difference score correlations (see methods). This also might lead to more significant correlations within the SWM task, as again most cells were recorded in that task. Across phases the left-right differences between both outbound runs (r=0.19) and inbound (r=0.48, $p<5*10^{-5}$) runs were correlated positively, while the sample outbound run was negatively correlated with both sample (r=-0.10) and choice inbound (r=-0.8, $p<5*10^{-5}$). During FC the onset response of the CS+ was correlated positively with the CS+ CS- difference (r=0.22, $p<5*10^{-5}$). There were only a few features that were significantly correlated across the tasks. Apart from the already mentioned correlation of anxiolytic features in the EPM and OF both inbound runs in the T-maze were correlated with the “open vs closed” (sample inbound: r=0.081, $p=5*10^{-5}$, choice inbound: r=0.125, $p<5*10^{-5}$) and “center vs corner” (sample inbound: r=0.094, $p<1*10^{-4}$, choice inbound: r=0.103, $p<5*10^{-5}$) scores. Surprisingly also the left vs right difference during delay in the SWM was correlated with the open vs closed difference in the EPM (r=0.076, $p=4*10^{-4}$).

Discussion

Miniscope imaging in the mPFC of mice

The PFC is the subject of many animal studies using different investigation methods to better understand cognition. In this study we added to this field by investigating activity in the mPFC of mice in relation to different behavioral states, tasks, and events. By using 1-photon miniature microscope imaging of virus-mediated GCaMP6 activation in pyramidal neurons we were able to follow the same cells over multiple weeks and investigated long-term changes in activation patterns across time and tasks. While most previous studies focused on a single behavioral task, we recorded the activity of many neurons throughout five different behaviors and compared activity across sessions of the same or other tasks. To our knowledge this is the first study systematically exploring neural activity in the mPFC over multiple tasks and sessions.

We chose miniscope imaging to be able to follow the same cells over a long time, fully aware of its limitations in temporal and spatial resolution. While direct electrophysiological recordings yield better temporal resolution and modern probes have at least comparable simultaneously recorded cell numbers, it is difficult to follow the same neurons over time. This problem can be solved using imaging approaches, where one can identify the location of neurons, at least in relation to each other, but voltage imaging approaches with action potential resolution are not yet available in freely moving animals (Knöpfel & Song, 2019). Voltage sensors that work on spike time resolution are not bright enough for miniaturized CMOS imaging chips, additionally most chips lack the necessary frame rate. Calcium indicators on the other hand are readily available, can be genetically encoded to target specific cell populations, have a good dynamic range and sensitivity but measure only calcium influx linked to action potentials with much slower kinetics and a non-linear response for high frequency firing (Masatoshi, 2020). Another issue with 1-photon calcium imaging is the low spatial resolution on the z-axis leading to more noisy signals by out of focus fluorescence by neurons below the imaging plane. To limit the influence of this we used CNMF-E to extract the cells from our video signal which separates the background from the signal (Zhou et al., 2016). One very recent development to tackle this problem would be miniaturized 2-photon imaging, which yields lower cell numbers than 1-photon miniscope imaging but with higher resolution, a higher weight and higher costs but with high resolution on the z-axis (Zong et al., 2021).

Our virus-mediated approach of GCaMP expression worked well showing an even distribution in the target area (see Figure 7A). The nuclei were not stained in most cells indicating no GCaMP in that part of the cell. Filled nuclei are known as a sign for indicator overexpression

with a reduced signal intensity and dynamic range (Tian et al., 2009). We used relatively small 0.5 mm wide GRIN lenses to avoid damaging too much brain tissue in comparison to wider lenses that are also used for miniscope imaging. The small field of view of about 0.75 mm x 0.48 mm in the miniscope v3_2 also made using larger lenses unnecessary. With the larger field of view of the miniscope v4, more neurons could have been recorded simultaneously. But larger lenses would have caused more damage to the brain and the surgical procedures would have had to be adapted to reduce intracranial pressure.

Performance during the spatial working memory task is dependent on delay duration

We could not find influences on behavioral performance caused by the weight of the miniscope, the implanted lens that destroys some tissue and fibers of passage or the light used for calcium sensor excitation. T-maze performance was similar in comparison to another study from our lab in the exact same T-maze WM task (Vogel, **Hahn** et al., 2022). Increasing the delay duration to 60 s increased WM load and reduced the performance slightly, similar to what was reported in other studies (I. Lee & Kesner, 2003; Tamura et al., 2017). The animals were not getting faster in later re-testing sessions of the task, but we found that they were slightly faster in the sample phase in comparison to the choice phase. This might be explained as they do not need to choose between the two arm options during the sample phase but can just run in the direction of the open door. Interestingly, the animals were faster during the long delay trials, indicating that they may have become more impulsive. This reduced trial duration in long delay sessions could be attributed to the missing time of reward consumption in the (increased number of) incorrect trials. This can be excluded, as there is no difference in time between the always rewarded sample phase and the choice phase during long delay trials.

Neurons in the mPFC encode spatial location dependent on current task phase

As expected, we found similar firing patterns along different task phases and spatial locations in our larger set of animals in comparison to our previous publication (Vogel, **Hahn** et al., 2022). Again, the correlated activity between the sample outbound runs and the choice outbound runs but not the inbound runs can clearly be observed in many cells. Also, the different activity patterns between left and right trials could still be observed, again in all phases but during the delay (Bolkan et al., 2017; Spellman et al., 2015; Vogel, **Hahn** et al., 2022). Interestingly, the number of neurons discriminating between left and right was above chance already during the start of the choice phase, which could be a representation of action planning. The fraction of neurons discriminating between left and right in the goal arm during the outbound runs was increased from about 20% in our previous study to nearly 30%. This increase may be due to a

higher signal-to-noise ratio in the additional animals because they were imaged with the Miniscope v4 using a more sensitive chip.

Similarly, the population decoding accuracy was increased in comparison to our previous study to nearly 100% for the whole sample inbound run and at 100% during both outbound runs in the goal arm, which could be due to the higher cell number (and also the higher number of neurons encoding left-right differences). Again, no decoding was possible during the delay phase, which has already been reported in many studies (Bohm & Lee, 2020; Bolkan et al., 2017; Ito et al., 2015b; Jung et al., 1998; Spellman et al., 2015; Vogel, **Hahn** et al., 2022). Surprisingly, we found below chance decoding during the sample outbound run before the animal makes a choice. This can be explained if the animals did also remember the previous choice goal and plan to go to the opposite goal in the next trial in combination with the pseudo-random trial structure that allowed only two consecutive trials going to the same goal.

Anxiety levels during EPM exploration are stable across sessions

Arm exploration times in the EPM of about 25% are slightly higher than the about 20% that are typically reported in the literature (Adhikari et al., 2011; Tucker & McCabe, 2017), some studies report even less (Stern et al., 2010; Walf & Frye, 2007). It is widely accepted that the open arms exploration time is a measurement of anxiety, so it seems the animals in our study were less anxious. This lower anxiety level may be due to the very low light conditions in comparison to other studies (Adhikari et al., 2011; Stern et al., 2010; Tucker & McCabe, 2017), so the animals felt less exposed in the open arms. Another reason could be that in the current study the animals were food restricted and therefore were more motivated to explore for food. They were also already trained in another maze-based task, in which they receive food rewards. It can also be noted that often just five minutes of exploration time are used (Tucker & McCabe, 2017; Walf & Frye, 2007). We saw more similar but still higher exploration times for each arm type when looking at the first five minutes only. We increased the exploration time to ten minutes (like in Adhikari et al., 2011) to increase imaging duration for better cell extraction and higher statistical power. This increase in time spent in the maze seems to increase how safe an animal feels and increase open arm exploration as we saw when we compared the first five minutes to the whole ten minutes of exploration. In that sense it is a bit surprising that exploration times did not change between the first and the second EPM session. Others reported a decrease in open arm exploration for daily or weekly EPM exposure (Tucker & McCabe, 2017), indicating that they did not get less but more anxious, or maybe the value for exploration just decreased. Again, this was not done in food restricted animals.

Prefrontal neurons discriminate between exposed and safe areas

Similar to what has been described using electrophysiological recordings (Adhikari et al., 2011) our calcium imaging measurements showed that many prefrontal neurons code for the anxiogenic features of the EPM. Although the animals spent more time in the closed arms, the number of neurons that were more active in any arm type was similar between open and closed arms. The distribution of EPM scores looks very similar and also the number of modulated cells does not deviate much from the aforementioned study. This also explains the diverse and partly contradictory results finding increases or decreases in open arm exploration after lesioning or silencing the mPFC (Jinks & McGregor, 1997; Shah & Treit, 2003; Stern et al., 2010; Sullivan & Gratton, 2002). Depending on which subpopulation of neurons is affected strongest, anxiolytic or anxiogenic effects may be created.

Similar cells that discriminate between threat and safety can be seen in the OF between the anxiogenic center and the safer corners. Again, the animals spend more time in the safe areas, but the number of neurons coding for safe or anxiogenic areas is similar. Additionally, the first PC of the spatial activity of all neurons shows a similar pattern discriminating between the center and the corners indicating a very relevant feature for cellular activity. Similar cell responses have also been reported in other studies (Weible et al., 2009), also in other brain areas like the amygdala (Gründemann et al., 2019).

Correlates for familiar and novel objects in the mPFC

The animals explored both identical objects equally during the first phase of the NO task as indicated by the time spent exploring them and the number of visits to either object. During the second phase the animals showed a clear preference for the novel object in session 1 of the NO task but this effect was gone during session 2, although two completely new objects were used during that test. A similar drop in preference for novel objects is described in another study (Weible et al., 2009), but in their case for a novel object test after a novel location test.

As expected, we found some neurons responding to the objects in both phases of the object recognition task. While there was no discrimination between the same objects in phase I (nearly 20% responding to either object), during phase II 20% responded to the novel object and only 10% to the familiar one. This stands in contrast to the results from another study that found about 20% responding to either object (20% familiar, 19% novel, Wang et al., 2021). One main difference in their study was that they recorded not only pyramidal neurons but also recorded interneurons, and the interneurons predominantly changed their activity in correspondence to the objects. Looking at pyramidal neurons alone, they found 1.5 times more cells responding to the novel object than to the familiar one. In addition, they saw that many

cells were inhibited, and although it is possible to detect inhibition using single-photon calcium imaging, increases in activity are better detected because of baseline fluorescence levels.

Novelty during social interactions seems to be more relevant for mPFC activity than the interaction itself

During the SI task, all animals preferred the social target over the object at the beginning of the first session, but this effect faded quickly. Already after the first 5 minutes of the first phase no difference could be seen. In the second phase neither the number of visits nor the time spent in the two zones was different, similar to what has been reported in the literature, with comparable numbers for exploration times (E. Lee et al., 2016). Other studies reported already much less interaction time for the first phase, just 20% with the social target and 10% with the object (Xu et al., 2022). There was only a slight trend for increased time spent with the social target compared to the object during the second SI session in our study, and no difference was found in the number of visits to either target. This might be because the food restricted animals might lose interest in social interactions after the novelty effect is gone.

Similar to what others have reported, many cells in the mPFC change their activity in the vicinity of the social target (Lee et al., 2016; Xu et al., 2022). As it has been reported in some of these publications using electrophysiology and calcium imaging, we also saw mainly excited cells. Likewise, the increased c-Fos expression after social interaction hints in a similar direction (Avale et al., 2011; Kim et al., 2015). Only few cells decreased their activity, which conflicts with the findings of Liang and colleagues reporting that, next to an ensemble with increased activity also a large ensemble of neurons that decreases its activity (Liang et al., 2018).

Interestingly, we saw many cells increasing their activity during social interactions only at the beginning of the first phase, which might be an indication of novelty processing instead of pure sociability. Still, during the second phase, without a behavioral preference, we still see many cells discriminating between the object and the social target, but the difference in activity is lower. Still, as many cells are modulated during phase II as during phase I.

Clear CS representations in the mPFC after fear learning

All mice learned the association between the CS+ and the US. While the tones themselves did not elicit fear in a neutral context, pairing them with a noxious foot shock led to increased freezing thereafter. Although the animals showed some generalization and fear responses were higher during the CS- presentation after conditioning compared to habituation, freezing during the CS+ was substantially higher. We also saw successful extinction learning, but not

within the first extinction session, differently from what is often reported in other studies (Garcia et al., 2006; Milad & Quirk, 2002; Salinas-Hernández et al., 2018; Sierra-Mercado et al., 2011; Vidal-Gonzalez et al., 2006). While these other studies often report freezing levels that are in the range of 60-80% during the first CS presentations, in our study the animals froze much less with only about 30% throughout the first extinction session. Most of these studies were also conducted in rats which may have different freezing levels than mice, but also studies in mice typically have higher freezing rates (Salinas-Hernández et al., 2018). As the foot shock intensity was similar to what is used in other studies, one possible explanation for this is that the animals in this study were food restricted and therefore more active searching for food. Additionally, the fear conditioning sessions were conducted towards the end of the behavioral training and the extensive handling and exposure to different environments might influence their overall fear level. A similar study also conducted two other tasks before FC also found lower freezing levels although shock intensity and duration were substantially higher (Gründemann et al., 2019). This is supported by the findings in the EPM that the mice explored the open arms more than what other studies have reported.

Only very few neurons responded to both CS during the habituation sessions which may be expected since there was no behavioral relevance and no changes in behavior were observed. After forming the association during the conditioning session, quite many cells can be seen that either increase or decrease their activity to the CS+ but not the CS-. Hereby different activity profiles can be seen with cells showing often strong onset responses or sustained, sometimes down ramping activity. The number of responsive cells decreases in the second extinction session, again correlated with a decrease in behavioral response, like what has been reported before (Baeg et al., 2001; Burgos-Robles et al., 2009; Chang et al., 2010).

While strong electrical artifacts hinder electrophysiological recordings during foot shocks, they do not influence calcium imaging, so a clear response to the shock can be seen. Here it comes apparent that quite many cells respond to the shock with either inhibition or excitation seemingly independent from their response during the tone. Although there are already some cells that seem to be tone responsive, this US response is much stronger. One possible reason for seeing so few CS+ responsive cells is that only 5 CS+ US pairings are presented, with the first CS+ still meaningless because the US is presented after it.

Using linear modeling to find behavioral correlates in the mPFC

Linear modeling has been proven to be a valuable tool to identify task variables relevant for neural coding (Engelhard et al., 2019; Pinto & Dan, 2015; Vogel, **Hahn** et al., 2022). We chose to utilize GLMs to identify which task features have the strongest influence on mPFC activity. One issue with GLMs is that a linear relationship between task variables and spiking activity

cannot be assumed. To overcome this, we categorized the variables by binning them and used the bins as individual variables. Another issue is that events which are happening at a discrete time point can elicit activity in the brain over a longer period, especially with calcium imaging data where transients are slow. Therefore, we convolved event time points with splines to spread their influence over a longer period (Engelhard et al., 2019).

Our models explained most of the variance for the T-maze task followed by the EPM. In both these tasks the behavioral demand is stable across the whole session, in the other three tasks there are changes within each session. In the NO task first the OF is empty, afterwards the objects are introduced, one of which changes in the last phase, as in the SI task. Additionally, during SI we see a drop in interest for the social target correlated with a direct decrease in the amplitude of activity changes and the number of cells responding. During FC, at least in the second session, we see a clear extinction effect with a lower response towards the end. The number of predictors does not seem to play a role for the amount of variance explained. The highest explained variance in the SWM task comes together with the highest number of variables but the lowest number of variables in the EPM has the second highest amount of variance explained.

To compare single behavioral variables and events we calculated single variable models for each variable independently. We tried to avoid correlations between behavioral variables as much as possible but cannot exclude a remaining effect. To control for the effect of correlations between predictor variables, (for example at a position x the animal always has the same speed y), we not only calculated the explained variance of a single variable model but also the decrease in explained variance after removing one of the variables from the full model. This gives us the unique contribution of every variable that is not explained by any other variable in our model.

Position is one of the strongest influencers of prefrontal activity across a wide range of behaviors

We found that across all behaviors, position by itself was the strongest predictor of mPFC activity. This was already known for the T-maze SWM task for a subset of the current dataset (Vogel, **Hahn** et al., 2022) and other studies also report strong position encoding in different spatial tasks (M. W. Jones & Wilson, 2005; Jung et al., 1998; Ma et al., 2022; Powell & David Redish, 2014), but is a bit surprising for FC as there is no clear spatial component during that task. This indicates that the current position of the animal is encoded in the mPFC activity independent of an active task engagement (Ma et al., 2022) or exploration movements. In all other tasks the different positions have different task-relevant meanings, in the EPM and OF they have different anxiogenic features, during NO there are different object locations and

during SI the social target and the object is also bound to specific (but changing) positions. Next to the highest variance explained by position for the single variable models, removing position from the full model also shows the strongest decrease in variance explained for all tasks except for FC. For FC the highest decrease is seen after removing the CS+, to which we saw a strong response already with the previous analysis. The amount of variance explained for position cannot be solely attributed to the size of the environment or the number of spatial bins. Although the number of spatial bins is lowest in the FC task together with the lowest decrease in explained variance, the number of bins is highest in the NO task with only the third highest decrease in explained variance. However, we cannot exclude an effect of the complexity of the environment. In the more complex mazes, a higher amount of variance is explained by position. With different arms and wall heights, locations might be more different than in the rectangular or circular arenas of the other tasks. Throughout the mPFC seems to show strong position coding in all tasks, especially when the current behavior is dependent on spatial information.

Again, the highest number of neurons that significantly coded for a variable was observed for position in all tasks, except FC. In FC, the number was the third highest but with only a 4% difference compared to the strongest predictor, speed. Interestingly, many neurons coded for more than one variable within each task, which might be an indicator for mixed selectivity in the mPFC instead of sparse coding, consistent with our findings for the SWM task-specifically (Vogel, **Hahn** et al., 2022). This would allow for a high flexibility with fewer cells in comparison to the sparse coding approach, where every cell is activated specifically to a particular task aspect. Most cells were observed coding for variables in the T-maze task in comparison to the other tasks where the cell numbers were substantially lower, potentially due to the highest behavioral demand and distinct task phases. However, we also tested the largest number of variables for the WM task. No effect of the number of tested variables could be found for the other tasks, thus it is improbable that this is the exclusive cause for a higher number of significant cells.

Coding for other behavioral variables in the mPFC

Apart from position most variables had an average unique contribution of less than 1%. Only the reward time point in the SWM task had an average contribution of 1.2% with more than 50% of the cells being responsive to the reward time point. This is consistent with the literature that quite many mPFC cells respond to reward delivery (Fuster, 2015; Le Merre et al., 2017; Pinto & Dan, 2015; Vogel, **Hahn** et al., 2022). Although the contribution was much smaller for the other variables, there were still quite a few cells that were significantly coding for task-specific variables. Not a single neuron had an above-chance unique contribution for the object

locations during the NO task. This is surprising, especially after seeing many neurons coding for the objects during the NO task using our task-specific analysis. This may be due to a change in meaning of these locations across phases that the GLM does not account for. Changes may happen even within each phase as the novel object becomes more familiar over time. Another reason could be that the variance may already be similarly well explained by position. That would also explain why the number of neurons coding for left or right entries and interaction types in the SI task are rather low, although we found many neurons discriminating between the social target and the object.

The level of representation for the CS- or freezing in the mPFC was also low. While a clear representation of the CS- is not anticipated, representations of freezing state have been shown in the mPFC (Bagur et al., 2021) and other brain areas (Gründemann et al., 2019). We additionally found the representation of other behavioral states such as the head direction and movement speed in the mPFC. The lack of identification of a clear freezing correlate in our GLM cannot be due to correlations with speed, as even in the single variable model, not influenced by other behavioral variables, only 0.2% of the variance is explained by freezing.

The number of neurons that coded for head direction or speed was quite stable across the behavioral tasks with about 13 to 20% of the cells. This shows that there is a clear representation of behavioral variables in the mPFC that is not relevant for task performance. Again, here the low number of cells with 13% detected during the EPM could be attributed to the lower statistical power caused by the shorter session length of the EPM in comparison with the other tasks.

Stable position coding in the mPFC within each behavior

With many cells recorded across multiple sessions we wanted to identify whether they are coding stably for similar task features or change their activity flexibly. Seeing the strong representation of spatial positions in the mPFC we decided to start with position coding. As mentioned above we found many cells being consistently activated throughout a session at the same locations within each behavioral task. Next, we compared if those cells are activated at the same location in the other sessions of the same task.

Indeed, we found many cells that showed similar spatial firing patterns across multiple sessions of the same task. Across all tasks the spatial correlation across one cell recorded in two sessions of the same task was higher than that of random cell pairs. While the effect could originate in the stable encoding of task dependent position features like the left-right preferences in the SWM task or anxiety features in the EPM this cannot be the case for the NO and SI task, as locations are pseudo-randomly counterbalanced there. If the cells would just code for the novel object or social target, we would expect a negative spatial correlation

when the positions are switched. Lastly, during fear conditioning the different positions have no meaning for the task. Together this indicates that most cells indeed code stably for different positions, similar to what has been described before (Powell & David Redish, 2014).

This can also be used as a quality control for our cell alignment algorithm (Sheintuch et al., 2017). If the assignment of cells would not work, we would expect spatial correlations at chance level (similar to random cell pairings). One could argue that cells that are aligned across two sessions have a higher signal-to-noise ratio and might therefore show a better correlation for position coding than cells that are not aligned. To avoid possible influences of those cells, we used only the cells identified across the multiple sessions as random cell pairs for our shuffled distribution.

As another way to compare spatial coding across sessions, we correlated the unique contribution of the position predictor from our linear modeling approach across all cells recorded in two sessions. This measure ignores the actual spatial location that a cell encodes but asks more generally whether a cell that encodes position in one session also encodes position in the other session. Using this measure, we found that cells also encode positions across sessions, so a cell that codes for position in one session is more likely to also encode position in another session.

Encoding of position and speed across different behaviors

Correlating the unique contribution of the position predictor across different sessions enabled us to compare position coding across the different tasks, where a direct correlation was not possible due to the differently shaped environments. Again, we found that the same cells encoded positions across the different environments for some task combinations but not all. One reason could be the lower statistical power as the result of lower cell numbers for specific task combinations. Other possibilities are that the cells encode positions only in some environments or in combination with specific task demands. Another reason could be that cells that seem to code for positions in the maze actually code for other task features like anxiogenic features in the EPM or social locations during SI.

Using the same measure of correlating the unique contribution from our linear models also made it possible to compare the other task variables within and even across tasks in all possible combinations. The unique contribution of the speed predictor was highly correlated within and across tasks. All task combinations were significantly correlated, except the combinations of the EPM-EPM and EPM-FC. Here we may be underestimating the stability, as the same cells showed stability in speed encoding in all other task combinations also including the EPM and FC. The reason for the lack of significance may be that the EPM-EPM and EPM-FC has the lowest number of cells, as the correlation R-values are similar to other

combinations and the p-values are below 0.05 (but above the multiple-comparison-corrected p-value of 0.003).

Even ignoring this we see a much stronger stability in speed coding across all tasks compared to positions. One reason for this could be that movement speed is an intrinsic behavioral variable; no matter what environment the animal is in and what task it performs, speed is independent of it. Position coding may be highly dependent on the different environments, and additional task-related features in combination with specific positions might play a bigger role, which cannot be translated to other tasks.

Within-task stability for task-specific variables

Many of the other task-specific variables were correlated across sessions. While in the T-maze all variables but the correctness of a trial showed significant correlations across two sessions, only speed, position or head direction were significantly correlated in the other tasks. While we would not expect stability for the variables that are not well represented in mPFC coding like the correctness in the T-maze, the object identity during NO or the CS- during FC it was surprising not to see correlations across other variables like the CS+. Checking the correlation values reveals that they are quite similar to the values with significant correlations in the T-maze and again the low statistical power, especially in the same-task, same-variable combinations might be at fault here. This is likely also the reason for no within-task but across-variables correlations apart from the T-maze.

Correlated coding for similar variables across tasks

Across different tasks we mostly see correlations between the general behavioral variables position, speed and, with a smaller effect size, head direction, not only paired with themselves but also with each other. This might indicate that these are represented by a common ensemble across the different tasks. Interestingly no negative correlations can be seen within each task or across different tasks, indicating that if a neuron codes for variable A it is not less likely that it also codes for variable B in another task. This indicates that cells are quite flexibly activated and differently engaged across different tasks. Stability in coding was mostly stronger within a task than across different tasks.

Long term stability in coding for position or speed

To exclude, that this effect of higher within task stability originates in different time spans between the sessions of same or other tasks we tested the influence of time between two sessions on stability. Surprisingly we did not observe any change in stability over time, indicating that the lower stability across tasks is not caused by different times between the sessions. Hereby the time difference ranges from 1 to 15 sessions (0 - 20 days) without a clear

trend over time for both the position and speed variable either within or across tasks. It also means that coding stability is not influenced by the performance of other tasks in between but returns to the original code thereafter, similar to what Sauer and colleagues showed for switches between environments within a day (Sauer et al., 2022).

Nevertheless, we can also observe a change in representations over time, known as "representational drift," which has been reported in other brain regions (Rule et al., 2019). It should be noted that not all cells encode for the same variables on a day-to-day basis, and the possibility cannot be excluded that additional cells would alter their activity patterns over extended time periods exceeding those examined, up to 20 days. For the other tasks besides the SWM task, we only have two sessions to compare. In these cases, there is always a difference of three sessions for the spontaneous tasks and just one session for fear conditioning. Thus, we cannot make any statements regarding different time differences in these cases.

Stability in representations of task-relevant variables

After observing stability in the general representation of positions and speed in each task, we sought to determine if this is also true for more specific task-related coding. In order to accomplish this, we analyzed activity differences between pairs of task-specific situations and correlated them across all paired cells.

For the SWM task, we calculated the difference between left and right trials specifically during the outbound and inbound runs for the sample and choice phases as well as the delay phase. Consistency was observed in all phases except for the delay phase, where no significant difference in activity was detected. Additionally, a negative correlation was observed between the outbound and inbound runs during the sample phase across sessions. This is not surprising as we already discovered opposing representations in the data collected from individual cells within each session (Vogel, **Hahn** et al., 2022).

During our study of the EPM, we analyzed the activity differences between the open and closed arms. We discovered some level of stability in these differences across sessions. In regards to the NO task, we compared the activity in the center and corner during the OF phase and found this activity to be correlated across sessions. However, we could not identify stability in the representations for object identity during the novel object phase. The reason for this may be that fewer cells showed a clear representation for object identity to begin with and additionally the behavior was not stable across both sessions. For the SI task we correlated the difference between the activity at the social target and the object during both social phases independently and found some stability in the representation during the first phase but not the second phase. This might be explained by a different behavior (less preference for the social

target) during the second phase. Additionally, the behavior was again different across the sessions. Interestingly, there was a trend to a negative correlation across the phases. This might be due to the representation of spatial- instead of just social features, as the sides of the boxes are switched between the phases. For Fear conditioning we compared the CS+ onset activity to a pre-CS period, where we found some stability, and the CS+ and the CS- representations, where only a slight trend for stability has been found.

Stable representation of anxiogenic features across tasks

Only a few task-relevant variables demonstrated correlated representations across the different tasks. One prominent exception was the representation of the open-closed differences in the EPM and the center-corner differences in the OF phase. In both environments the cells coded in the same way for the safe or anxiogenic areas of the environment. This might be an indication of cells representing either safe or fear eliciting regions. This stands in contrast to results in the amygdala, where ensembles of cells have been described that code for the preferred closed arm and the center in a similar way (Gründemann et al., 2019). The authors report that the same cells are also activated when the animal begins to freeze during FC. Here we don't see any correlations to the CS+ coding during FC (where the animal tends to freeze in comparison to the CS-). The CS+ could also be seen as a form of anxiogenic signal, so it seems it is not the anxiety level per se that is activating these cells. It may also be that fear, as a response to a stimulus that causes freezing, and anxiety, as a preference for safer areas, are represented differently.

Very surprisingly we found that the left-right differences in the inbound runs also were correlated with the open-closed differences in the EPM and the center-corner differences in the OF. The correlation was very small but higher than expected by chance suggesting a role of anxiogenic features also in the T-maze. While it cannot be ruled out completely that one of the arms in the T-maze induces greater anxiety than the other, we do not anticipate this to be the case due to the absence of a clear T-maze arm-preference in the animals. It is noteworthy that these correlations occur with the inbound run differences, in which the animal moves towards the start box (in the same direction and, to some extent, at the same location in the stem). There might be another feature that these cells represent that we have overlooked so far.

Limitations of the study

Seeing a diverse range of responses within the different behavioral tasks raises the question where these differences originate. Although we already limited the population of neurons to pyramidal cells by using a CamKII promoter, we still image a wide variety of neurons receiving input from different brain areas and projecting to different targets. Understanding how these

projections influence a cell's activity or form sub populations could help understanding why cells are differently activated across multiple tasks.

Although we used a wide range of behavioral tasks, we are still limited in the range of tested behaviors. Observing an overlap in anxiogenic coding between different tasks suggests a group of neurons coding for anxiety levels, but apart from this we have very little overlap across the tasks. Another WM task or another conditioning task might be beneficial to see other ensembles emerging that code for memory content or rewards across different environments. We are also limited in the duration of imaging, three weeks is a very short period in the lifetime of a neuron, so we cannot make any claim on long term stability.

Apart from the limitations of one-photon calcium imaging mentioned above we use mostly models to analyze relevant behavioral variables but are limited in the variables that we can put in and, in the accuracy, with that they are measured. We also assume linearity using our linear models which might overlook nonlinear interrelationships between task variables and neural codes. We did not examine potential interaction effects among behavioral variables in our GLM, which could enhance the explained variance but also complicate the interpretation of the results. With pairwise interactions, we already observed a nearly two-fold increase (Vogel, **Hahn** et al., 2022) in explained variance.

Although we are confident in the method, we cannot rule out the possibility that cells recorded in different sessions and aligned as a single cell are actually two different cells. We do not expect this to be the case for all cells and the above chance correlation of basic spatial coding is a clear indication that this is not the case. If anything, we just underestimate the level of stability the cells have, when we group cells together, that are not actually the same cell (false positives). This would add random cell pairings to our tests and dilute the results. On the other hand, we could overestimate stability, if cells are not at all active in another task or session and therefore are not detected, as only active cells get extracted by CNMF-E. These cells that are not active in a session-pair are currently not included in the way we test for stability. If a cell is active in one session but not the other, there is no stability, but we cannot exclude technical limitations as the reason for cells not being detected or identified across sessions, so it is also difficult to treat these cells as "unstable".

References

Adhikari, A., Topiwala, M. A., & Gordon, J. A. (2011). Single units in the medial prefrontal cortex with anxiety-related firing patterns are preferentially influenced by ventral hippocampal activity. *Neuron*, *71*(5), 898–910. https://doi.org/10.1016/j.neuron.2011.07.027

Aggleton, J. P., Neave, N., Nagle, S., & Sahgal, A. (1995). A comparison of the effects of medial prefrontal, cingulate cortex, and cingulum bundle lesions on tests of spatial memory: Evidence of a double dissociation between frontal and cingulum bundle contributions. *Journal of Neuroscience*, *15*(11), 7270–7281. https://doi.org/10.1523/jneurosci.15-11-07270.1995

Akirav, I., & Maroun, M. (2006). Ventromedial prefrontal cortex is obligatory for consolidation and reconsolidation of object recognition memory. *Cerebral Cortex*, *16*(12), 1759–1765. https://doi.org/10.1093/cercor/bhj114

Akirav, I., Raizel, H., & Maroun, M. (2006). Enhancement of conditioned fear extinction by infusion of the GABA A agonist muscimol into the rat prefrontal cortex and amygdala. *European Journal of Neuroscience*, *23*(3), 758–764. https://doi.org/10.1111/j.1460-9568.2006.04603.x

Asaad, W. F., Rainer, G., & Miller, E. K. (1998). Neural Activity in the Primate Prefrontal Cortex during Associative Learning). Medial temporal structures critical for long-term memories are also important: dam-age to the hippocampus and/or subjacent cortex (Mur. *Neuron*, *21*, 1399–1407.

Asaad, W. F., Rainer, G., & Miller, E. K. (2000). Task-specific neural activity in the primate prefrontal cortex. *Journal of Neurophysiology*, *84*(1), 451–459. https://doi.org/10.1152/jn.2000.84.1.451

Asif-Malik, A., Dautan, D., Young, A. M. J., & Gerdjikov, T. V. (2017). Altered cortico-striatal crosstalk underlies object recognition memory deficits in the sub-chronic phencyclidine model of schizophrenia. *Brain Structure and Function*, *222*(7), 3179–3190. https://doi.org/10.1007/s00429-017-1393-3

Aultman, J. M., & Moghaddam, B. (2001). Distinct contributions of glutamate and dopamine receptors to temporal aspects of rodent working memory using a clinically relevant task. *Psychopharmacology*, *153*(3), 353–364. https://doi.org/10.1007/s002130000590

Avale, M. E., Chabout, J., Pons, S., Serreau, P., De Chaumont, F., Olivo-Marin, J.-C., Bourgeois, J.-P., Maskos, U., Changeux, J.-P., & Granon, S. (2011). Prefrontal nicotinic receptors control novel social interaction between mice. *The FASEB Journal*, *25*(7), 2145–2155. https://doi.org/10.1096/fj.10-178558

Baeg, E. H., Kim, Y. B., Huh, K., Mook-Jung, I., Kim, H. T., & Jung, M. W. (2003). Dynamics of population code for working memory in the prefrontal cortex. *Neuron*, *40*(1), 177–188. https://doi.org/10.1016/S0896-6273(03)00597-X

Baeg, E. H., Kim, Y. B., Jang, J., Kim, H. T., Mook-Jung, I., & Jung, M. W. (2001). Fast spiking and regular spiking neural correlates of fear conditioning in the medial prefrontal cortex of the rat. *Cerebral Cortex (New York, N.Y. : 1991)*, *11*(5), 441–451. https://doi.org/10.1093/cercor/11.5.441

Bagur, S., Lefort, J. M., Lacroix, M. M., de Lavilléon, G., Herry, C., Chouvaeff, M., Billand, C., Geoffroy, H., & Benchenane, K. (2021). Breathing-driven prefrontal oscillations regulate maintenance of conditioned-fear evoked freezing independently of initiation. *Nature Communications*, *12*(1). https://doi.org/10.1038/s41467-021-22798-6

Baran, S. E., Armstrong, C. E., Niren, D. C., & Conrad, C. D. (2010). Prefrontal cortex lesions and sex differences in fear extinction and perseveration. *Learning & Memory*, *17*(5), 267–278. https://doi.org/10.1101/lm.1778010

Barker, G. R. I., Bird, F., Alexander, V., & Warburton, E. C. (2007). Recognition memory for objects, place, and temporal order: A disconnection analysis of the role of the medial prefrontal cortex and perirhinal cortex. *Journal of Neuroscience*, *27*(11), 2948–2957. https://doi.org/10.1523/JNEUROSCI.5289-06.2007

Blum, S., Runyan, J. D., & Dash, P. K. (2006). Inhibition of prefrontal protein synthesis following recall does not disrupt memory for trace fear conditioning. *BMC Neuroscience*, *7*, 1–10. https://doi.org/10.1186/1471-2202-7-67

Bohm, C., & Lee, A. K. (2020). Canonical goal-selective representations are absent from prefrontal cortex in a spatial working memory task requiring behavioral flexibility. *ELife*, *9*, 1–20. https://doi.org/10.7554/eLife.63035

Bolkan, S. S., Stujenske, J. M., Parnaudeau, S., Spellman, T. J., Rauffenbart, C., Abbas, A. I., Harris, A. Z., Gordon, J. A., & Kellendonk, C. (2017). Thalamic projections sustain prefrontal activity during working memory maintenance. *Nature Neuroscience*, *20*(7), 987–996. https://doi.org/10.1038/nn.4568

Bonelli, R. M., & Cummings, J. L. (2007). Frontal-subcortical circuitry and behavior. *Dialogues in Clinical Neuroscience*, *9*(2), 141–151. https://doi.org/10.31887/dcns.2007.9.2/rbonelli

Bouton, M. E. (1994). Conditioning, Remembering, and Forgetting. *Journal of Experimental Psychology: Animal Behavior Processes*, *20*(3), 219–231. https://doi.org/10.1037/0097-7403.20.3.219

Brabander, J. M. de, Bruin, J. P. C. de, & Eden, C. G. van. (1991). Comparison of the effects of neonatal and adult medial prefrontal cortex lesions on food hoarding and spatial delayed alternation. *Behavioural Brain Research*, *42*(1), 67–75. https://doi.org/10.1016/S0166-4328(05)80041-5

Brito, G. N. O., & Brito, L. S. O. (1990). Septohippocampal system and the prelimbic sector of frontal cortex: A neuropsychological battery analysis in the rat. *Behavioural Brain Research*, *36*(1–2), 127–146. https://doi.org/10.1016/0166-4328(90)90167-D

Brodmann, K. (1909). *Vergleichende Lokalisationslehre der Großhirnrinde in ihren Prinzipien dargestellt auf Grund des Zellenbaues*. *44*(0).

Broersen, L. M., Heinsbroek, R. P. W., de Bruin, J. P. C., Joosten, R. N. J. M. A., van Hest, A., & Olivier, B. (1994). Effects of local application of dopaminergic drugs into the dorsal part of the medial prefrontal cortex of rats in a delayed matching to position task: comparison with local cholinergic blockade. *Brain Research*, *645*(1–2), 113–122. https://doi.org/10.1016/0006-8993(94)91644-6

Broersen, L. M., Heinsbroek, R. P. W., de Bruin, J. P. C., Uylings, H. B. M., & Olivier, B. (1995). The role of the medial prefrontal cortex of rats in short-term memory functioning: further support for involvement of cholinergic, rather than dopaminergic mechanisms. *Brain Research*, *674*(2), 221–229. https://doi.org/10.1016/0006-8993(95)00025-L

Brown, V. J., & Bowman, E. M. (2002). Rodent models of prefrontal cortical function. *Trends in Neurosciences*, *25*(7), 340–343. https://doi.org/10.1016/S0166-2236(02)02164-1

Brozoski, T. J., Brown, R. M., Rosvold, H. E., & Goldman, P. S. (1979). Cognitive Deficit Caused by Regional Depletion of Dopamine in Prefrontal Cortex of Rhesus Monkey. *Science*, *205*(4409), 929–932. https://doi.org/10.1126/science.112679

Bryda, E. C. (2013). The Mighty Mouse: The Impact of Rodents on Advances in Biomedical Research. *Missouri Medicine*, *June*, 207–211.

Bubser, M., & Schmidt, W. J. (1990). 6-Hydroxydopamine lesion of the rat prefrontal cortex increases locomotor activity, impairs acquisition of delayed alternation tasks, but does not affect uninterrupted tasks in the radial maze. *Behavioural Brain Research*, *37*(2), 157–168. https://doi.org/10.1016/0166-4328(90)90091-R

Burgos-Robles, A., Vidal-Gonzalez, I., & Quirk, G. J. (2009). Sustained conditioned responses in prelimbic prefrontal neurons are correlated with fear expression and extinction failure. *Journal of Neuroscience*, *29*(26), 8474–8482. https://doi.org/10.1523/JNEUROSCI.0378-09.2009

Butter, C. M., Snyder, D. R., & McDonald, J. A. (1970). Effects of orbital frontal lesions on aversive and aggressive behaviors in rhesus monkeys. *Journal of Comparative and Physiological Psychology*, *72*(1), 132–144. https://doi.org/10.1037/h0029303

Camp, M., Norcross, M., Whittle, N., Feyder, M., D'Hanis, W., Yilmazer-Hanke, D., Singewald, N., & Holmes, A. (2009). Impaired Pavlovian fear extinction is a common phenotype across genetic lineages of the 129 inbred mouse strain. *Genes, Brain and Behavior*, *8*(8), 744–752. https://doi.org/10.1111/j.1601-183X.2009.00519.x

Carlén, M. (2017). What constitutes the prefrontal cortex? *Science*, *358*(6362), 478–482. https://doi.org/10.1126/science.aan8868

Chang, C. hui, Berke, J. D., & Maren, S. (2010). Single-unit activity in the medial prefrontal cortex during immediate and delayed extinction of fear in rats. *PLoS ONE*, *5*(8). https://doi.org/10.1371/journal.pone.0011971

Chao, O. Y., de Souza Silva, M. A., Yang, Y.-M., & Huston, J. P. (2020). The medial prefrontal cortex - hippocampus circuit that integrates information of object, place and time to construct episodic memory in rodents: Behavioral, anatomical and neurochemical properties. *Neuroscience & Biobehavioral Reviews*, *113*(1), 373–407. https://doi.org/10.1016/j.neubiorev.2020.04.007

Clausen, B., Schachtman, T. R., Mark, L. T., Reinholdt, M., & Christoffersen, G. R. J. (2011). Impairments of exploration and memory after systemic or prelimbic D1-receptor antagonism in rats. *Behavioural Brain Research*, *223*(2), 241–254. https://doi.org/10.1016/j.bbr.2011.03.069

Condé, F., Audinat, E., Maire-Lepoivre, E., & Crépel, F. (1990). Afferent connections of the medial frontal cortex of the rat. A study using retrograde transport of fluorescent dyes. I. Thalamic afferents. *Brain Research Bulletin*, *24*(3), 341–354. https://doi.org/10.1016/0361-9230(90)90088-H

Constantinidis, C., Franowicz, M. N., & Goldman-Rakic, P. S. (2001). The sensory nature of mnemonic representation in the primate prefrontal cortex. *Nature Neuroscience*, *4*(3), 311–316. https://doi.org/10.1038/85179

de Visser, L., Baars, A. M., Van't Klooster, J., & van den Bos, R. (2011). Transient inactivation of the medial prefrontal cortex affect both anxiety and decision-making in male Wistar rats. *Frontiers in Neuroscience*, *5*(SEP), 1–8. https://doi.org/10.3389/fnins.2011.00102

Delatour, B., & Gisquet-Verrier, P. (1996). Prelimbic cortex specific lesions disrupt delayed-variable response tasks in the rat. *Behavioral Neuroscience*, *110*(6), 1282–1298. https://doi.org/10.1037/0735-7044.110.6.1282

Delatour, B., & Gisquet-Verrier, P. (1999). Lesions of the prelimbic-infralimbic cortices in rats do not disrupt response selection processes but induce delay-dependent deficits: Evidence for a role in working memory? *Behavioral Neuroscience*, *113*(5), 941–955. https://doi.org/10.1037/0735-7044.113.5.941

Dudchenko, P. A. (2004). An overview of the tasks used to test working memory in rodents. *Neuroscience and Biobehavioral Reviews*, *28*(7), 699–709. https://doi.org/10.1016/j.neubiorev.2004.09.002

Dunnett, S. B., Nathwani, F., & Brasted, P. J. (1999). Medial prefrontal and neostriatal lesions disrupt performance in an operant delayed alternation task in rats. *Behavioural Brain Research*, *106*(1–2), 13–28. https://doi.org/10.1016/S0166-4328(99)00076-5

Engelhard, B., Finkelstein, J., Cox, J., Fleming, W., Jang, H. J., Ornelas, S., Koay, S. A., Thiberge, S. Y., Daw, N. D., Tank, D. W., & Witten, I. B. (2019). Specialized coding of sensory, motor and cognitive variables in VTA dopamine neurons. *Nature*, *570*(7762), 509–513. https://doi.org/10.1038/s41586-019-1261-9

Ennaceur, A., & Delacour, J. (1988). A new one-trial test for neurobiological studies of memory in rats. 1: Behavioral data. *Behavioural Brain Research*, *31*(1), 47–59. https://doi.org/10.1016/0166-4328(88)90157-X

Ennaceur, A., Neave, N., & Aggleton, J. P. (1997). Spontaneous object recognition and object location memory in rats: The effects of lesions in the cingulate cortices, the medial prefrontal cortex, the cingulum bundle and the fornix. *Experimental Brain Research*, *113*(3), 509–519. https://doi.org/10.1007/PL00005603

Euston, D. R., Gruber, A. J., & McNaughton, B. L. (2012). The Role of Medial Prefrontal Cortex in Memory and Decision Making. *Neuron*, *76*(6), 1057–1070. https://doi.org/10.1016/j.neuron.2012.12.002

Ferenczi, E. A., Zalocusky, K. A., Liston, C., Grosenick, L., Warden, M. R., Amatya, D., Katovich, K., Mehta, H., Patenaude, B., Ramakrishnan, C., Kalanithi, P., Etkin, A., Knutson, B., Glover, G. H., & Deisseroth, K. (2016). Prefrontal cortical regulation of brainwide circuit dynamics and reward-related behavior. *Science*, *351*(6268). https://doi.org/10.1126/science.aac9698

Fitzgerald, P. J., Whittle, N., Flynn, S. M., Graybeal, C., Pinard, C. R., Gunduz-Cinar, O., Kravitz, A. v., Singewald, N., & Holmes, A. (2014). Prefrontal single-unit firing associated with deficient extinction in mice. *Neurobiology of Learning and Memory*, *113*, 69–81. https://doi.org/10.1016/j.nlm.2013.11.002

Fujisawa, S., Amarasingham, A., Harrison, M. T., & Buzsáki, G. (2008). Behavior-dependent short-term assembly dynamics in the medial prefrontal cortex. *Nature Neuroscience*, *11*(7), 823–833. https://doi.org/10.1038/nn.2134

Funahashi, S., Bruce, C. J., & Goldman-Rakic, P. S. (1989). Mnemonic coding of visual space in the monkey's dorsolateral prefrontal cortex. *Journal of Neurophysiology*, *61*(2), 331–349. https://doi.org/10.1152/jn.1989.61.2.331

Funahashi, S., Chafee, M. v., & Goldman-Rakic, P. S. (1993). Prefrontal neuronal activity in rhesus monkeys performing a delayed anti-saccade task. *Nature*, *365*(6448), 753–756. https://doi.org/10.1038/365753a0

Funahashi, S., Inoue, M., & Kubota, K. (1997). Delay-period activity in the primate prefrontal cortex encoding multiple spatial positions and their order of presentation. *Behavioural Brain Research*, *84*(1–2), 203–223. https://doi.org/10.1016/S0166-4328(96)00151-9

Fuster, J. M. (1973). Unit activity in prefrontal cortex during delayed-response performance: neuronal correlates of transient memory. *Journal of Neurophysiology*, *36*(1), 61–78. https://doi.org/10.1152/jn.1973.36.1.61

Fuster, J. M. (2015). The prefrontal cortex. In *The Prefrontal Cortex*. https://doi.org/10.1097/00005053-199002000-00012

Fuster, J. M., & Alexander, G. E. (1971). Neuron Activity Related to Short-Term Memory. *Science*, *173*(3997), 652–654. https://doi.org/10.1126/science.173.3997.652

Fuster, J. M., & Bauer, R. H. (1974). Visual short-term memory deficit from hypothermia of frontal cortex. *Brain Research*, *81*(3), 393–400. https://doi.org/10.1016/0006-8993(74)90838-5

Fuster, J. M., Bodner, M., & Kroger, J. K. (2000). Cross-modal and cross-temporal association in neurons of frontal cortex. *Nature*, *405*(6784), 347–351. https://doi.org/10.1038/35012613

Gabbott, P. L. A., Warner, T. A., Jays, P. R. L., Salway, P., & Busby, S. J. (2005). Prefrontal cortex in the rat: Projections to subcortical autonomic, motor, and limbic centers. *Journal of Comparative Neurology*, *492*(2), 145–177. https://doi.org/10.1002/cne.20738

Gao, L., Liu, S., Gou, L., Hu, Y., Liu, Y., Deng, L., Ma, D., Wang, H., Yang, Q., Chen, Z., Liu, D., Qiu, S., Wang, X., Wang, D., Wang, X., Ren, B., Liu, Q., Chen, T., Shi, X., … Yan, J. (2022). Single-neuron projectome of mouse prefrontal cortex. *Nature Neuroscience*, *25*(4), 515–529. https://doi.org/10.1038/s41593-022-01041-5

Garcia, R., Chang, C. H., & Maren, S. (2006). Electrolytic lesions of the medial prefrontal cortex do not interfere with long-term memory of extinction of conditioned fear. *Learning and Memory*, *13*(1), 14–17. https://doi.org/10.1109/TLA.2006.1642444

Garcia-Font, N., Mitchell-Heggs, R., Saxena, K., Gabbert, C., Taylor, G., Mastroberadino, G., Spooner, P. A., Gobbo, F., Dabrowska, J. K., Chattarji, S., Kind, P. C., Schultz, S. R., & Morris, R. G. M. (2022). Ca2+ imaging of self and other in medial prefrontal cortex during social dominance interactions in a tube test. *Proceedings of the National Academy of Sciences of the United States of America*, *119*(31), 1–12. https://doi.org/10.1073/pnas.2107942119

Giustino, T. F., & Maren, S. (2015). The role of the medial prefrontal cortex in the conditioning and extinction of fear. *Frontiers in Behavioral Neuroscience*, *9*(NOVEMBER), 1–20. https://doi.org/10.3389/fnbeh.2015.00298

Granon, S., Vidal, C., Thinus-Blanc, C., Changeux, J. P., & Poucet, B. (1994). Working memory, response selection, and effortful processing in rats with medial prefrontal lesions. *Behavioral Neuroscience*, *108*(5), 883–891. https://doi.org/10.1037/0735-7044.108.5.883

Greenberg, P. A., & Wilson, F. A. W. (2004). Functional stability of dorsolateral prefrontal neurons. *Journal of Neurophysiology*, *92*(2), 1042–1055. https://doi.org/10.1152/jn.00062.2004

Groenewegen, H. J. (1988). Organization of the afferent connections of the mediodorsal thalamic nucleus in the rat, related to the mediodorsal-prefrontal topography. *Neuroscience*, *24*(2), 379–431. https://doi.org/10.1016/0306-4522(88)90339-9

Gründemann, J., Bitterman, Y., Lu, T., Krabbe, S., Grewe, B. F., Schnitzer, M. J., & Lüthi, A. (2019). Amygdala ensembles encode behavioral states. *Science*, *364*(6437). https://doi.org/10.1126/science.aav8736

Gutzeit, V. A., Ahuna, K., Santos, T. L., Cunningham, A. M., Sadsad Rooney, M., Muñoz Zamora, A., Denny, C. A., & Donaldson, Z. R. (2020). Optogenetic reactivation of prefrontal social neural ensembles mimics social buffering of fear. *Neuropsychopharmacology*, *45*(6), 1068–1077. https://doi.org/10.1038/s41386-020-0631-1

Hainmueller, T., & Bartos, M. (2018). Parallel emergence of stable and dynamic memory engrams in the hippocampus. *Nature*, *558*(7709), 292–296. https://doi.org/10.1038/s41586-018-0191-2

Handley, S. L., & Mithani, S. (1984). Effects of alpha-adrenoceptor agonists and antagonists in a maze-exploration model of 'fear'-motivated behaviour. *Naunyn-Schmiedeberg's Archives of Pharmacology*, *327*(1), 1–5. https://doi.org/10.1007/BF00504983

Hannesson, D. K., Howland, J. G., & Phillips, A. G. (2004). Interaction between perirhinal and medial prefrontal cortex is required for temporal order but not recognition memory for objects in rats. *Journal of Neuroscience*, *24*(19), 4596–4604. https://doi.org/10.1523/JNEUROSCI.5517-03.2004

Heidbreder, C. A., & Groenewegen, H. J. (2003). The medial prefrontal cortex in the rat: Evidence for a dorso-ventral distinction based upon functional and anatomical characteristics. *Neuroscience and Biobehavioral Reviews*, *27*(6), 555–579. https://doi.org/10.1016/j.neubiorev.2003.09.003

Heilbronner, S. R., Rodriguez-Romaguera, J., Quirk, G. J., Groenewegen, H. J., & Haber, S. N. (2016). Circuit-Based Corticostriatal Homologies Between Rat and Primate. *Biological Psychiatry*, *80*(7), 509–521. https://doi.org/10.1016/j.biopsych.2016.05.012

Hogg, S. (1996). A review of the validity and variability of the elevated plus-maze as an animal model of anxiety. *Pharmacology Biochemistry and Behavior*, *54*(1), 21–30. https://doi.org/10.1016/0091-3057(95)02126-4

Hoover, W. B., & Vertes, R. P. (2007). Anatomical analysis of afferent projections to the medial prefrontal cortex in the rat. *Brain Structure and Function*, *212*(2), 149–179. https://doi.org/10.1007/s00429-007-0150-4

Hoshi, E., Shima, K., & Tanji, J. (2000). Neuronal activity in the primate prefrontal cortex in the process of motor selection based on two behavioral rules. *Journal of Neurophysiology*, *83*(4), 2355–2373. https://doi.org/10.1152/jn.2000.83.4.2355

Huang, W. C., Zucca, A., Levy, J., & Page, D. T. (2020). Social Behavior Is Modulated by Valence-Encoding mPFC-Amygdala Sub-circuitry. *Cell Reports*, *32*(2), 107899. https://doi.org/10.1016/j.celrep.2020.107899

Ito, H. T., Zhang, S. J., Witter, M. P., Moser, E. I., & Moser, M. B. (2015a). A prefrontal-thalamo-hippocampal circuit for goal-directed spatial navigation. *Nature*, *522*(7554), 50–55. https://doi.org/10.1038/nature14396

Ito, H. T., Zhang, S., Witter, M. P., Moser, E. I., & Moser, M. (2015b). A prefrontal–thalamo–hippocampal circuit for goal-directed spatial navigation. *Nature*, *522*(7554), 50–55. https://doi.org/10.1038/nature14396

Iversen, S. D., & Mishkin, M. (1970). Perseverative interference in monkeys following selective lesions of the inferior prefrontal convexity. *Experimental Brain Research*, *11*(4), 376–386. https://doi.org/10.1007/BF00237911

Jacobsen, C. F. (1935). FUNCTIONS OF FRONTAL ASSOCIATION AREA IN PRIMATES. *Archives of Neurology And Psychiatry*, *33*(3), 558. https://doi.org/10.1001/archneurpsyc.1935.02250150108009

Jentsch, J. D., Tran, A., Le, D., Youngren, K. D., & Roth, R. H. (1997). Subchronic phencyclidine administration reduces mesoprefrontal dopaminev utilization and impairs prefrontal cortical-dependent cognition in the rat. *Neuropsychopharmacology*, *17*(2), 92–99. https://doi.org/10.1016/S0893-133X(97)00034-1

Jinks, A. L., & McGregor, I. S. (1997). Modulation of anxiety-related behaviours following lesions of the prelimbic or infralimbic cortex in the rat. *Brain Research*, *772*(1–2), 181–190. https://doi.org/10.1016/S0006-8993(97)00810-X

Jodo, E., Katayama, T., Okamoto, M., Suzuki, Y., Hoshino, K., & Kayama, Y. (2010). Differences in responsiveness of mediodorsal thalamic and medial prefrontal cortical neurons to social interaction and systemically administered phencyclidine in rats. *Neuroscience*, *170*(4), 1153–1164. https://doi.org/10.1016/j.neuroscience.2010.08.017

Jones, M. (2002). A Comparative Review of Rodent Prefrontal Cortex and Working Memory. *Current Molecular Medicine*, *2*(7), 639–647. https://doi.org/10.2174/1566524023361989

Jones, M. W., & Wilson, M. A. (2005). Theta Rhythms Coordinate Hippocampal–Prefrontal Interactions in a Spatial Memory Task. *PLoS Biology*, *3*(12), e402. https://doi.org/10.1371/journal.pbio.0030402

Jung, M. W., Qin, Y., McNaughton, B. L., & Barnes, C. a. (1998). Firing characteristics of deep layer neurons in prefrontal cortex in rats performing spatial working memory tasks. *Cerebral Cortex*, *8*(5), 437–450. https://doi.org/10.1093/cercor/8.5.437

Kentros, C. G., Agnihotri, N. T., Streater, S., Hawkins, R. D., & Kandel, E. R. (2004). Increased attention to spatial context increases both place field stability and spatial memory. *Neuron*, *42*(2), 283–295. https://doi.org/10.1016/S0896-6273(04)00192-8

Kesner, R. P. (2000). Subregional analysis of mnemonic functions of the prefrontal cortex in the rat. *Psychobiology*, *28*(2), 219–228. https://doi.org/10.3758/bf03331980

Kim, H., Sofie, A., Wang, X., Deisseroth, K., Carle, M., Wang, X., Deisseroth, K., Carle, M., Kim, H., & Sofie, A. (2016). Prefrontal Parvalbumin Neurons in Control of Article Prefrontal Parvalbumin Neurons in Control of Attention. *Cell*, *164*, 208–218. https://doi.org/10.1016/j.cell.2015.11.038

Kim, Y., Venkataraju, K. U., Pradhan, K., Mende, C., Taranda, J., Turaga, S. C., Arganda-Carreras, I., Ng, L., Hawrylycz, M. J., Rockland, K. S., Seung, H. S., & Osten, P. (2015). Mapping social behavior-induced brain activation at cellular resolution in the mouse. *Cell Reports*, *10*(2), 292–305. https://doi.org/10.1016/j.celrep.2014.12.014

Kingsbury, L., Huang, S., Wang, J., Gu, K., Golshani, P., Wu, Y. E., & Hong, W. (2019). Correlated Neural Activity and Encoding of Behavior across Brains of Socially Interacting Animals. *Cell*, *178*(2), 429-446.e16. https://doi.org/10.1016/j.cell.2019.05.022

Knöpfel, T., & Song, C. (2019). Optical voltage imaging in neurons: moving from technology development to practical tool. *Nature Reviews Neuroscience*, *20*(12), 719–727. https://doi.org/10.1038/s41583-019-0231-4

Kojima, S., & Goldman-Rakic, P. S. (1982). Delay-related activity of prefrontal neurons in rhesus monkeys performing delayed response. *Brain Research*, *248*(1), 43–50. https://doi.org/10.1016/0006-8993(82)91145-3

Kojima, S., & Goldman-Rakic, P. S. (1984). Functional analysis of spatially discriminative neurons in prefrontal cortex of rhesus monkey. *Brain Research*, *291*(2), 229–240. https://doi.org/10.1016/0006-8993(84)91255-1

Kolb, B. (1974). Social behavior of rats with chronic prefrontal lesions. *Journal of Comparative and Physiological Psychology*, *87*(3), 466–474. https://doi.org/10.1037/h0036969

Krettek, J. E., & Price, J. L. (1977). The cortical projections of the mediodorsal nucleus and adjacent thalamic nuclei in the rat. *Journal of Comparative Neurology*, *171*(2), 157–191. https://doi.org/10.1002/cne.901710204

Kubota, K., & Niki, H. (1971). Prefrontal cortical unit activity and delayed alternation performance in monkeys. *Journal of Neurophysiology*, *34*(3), 337–347. https://doi.org/10.1152/jn.1971.34.3.337

Larsen, J. K., & Divac, I. (1978). Selective ablations within the prefrontal cortex of the rat and performance of delayed alternation. *Physiological Psychology*, *6*(1), 15–17. https://doi.org/10.3758/BF03326684

Laubach, M., Amarante, L. M., Swanson, K., & White, S. R. (2018). What, If Anything, Is Rodent Prefrontal Cortex? *Eneuro*, *5*(5), ENEURO.0315-18.2018. https://doi.org/10.1523/ENEURO.0315-18.2018

le Merre, P., Ährlund-Richter, S., & Carlén, M. (2021). The mouse prefrontal cortex: Unity in diversity. *Neuron*, *109*(12), 1925–1944. https://doi.org/10.1016/j.neuron.2021.03.035

Le Merre, P., Esmaeili, V., Charrière, E., Galan, K., Salin, P.-A., Petersen, C. C. H., & Crochet, S. (2017). Reward-Based Learning Drives Rapid Sensory Signals in Medial Prefrontal Cortex and Dorsal Hippocampus Necessary for Goal-Directed Behavior. *Neuron*, 83–91. https://doi.org/10.1016/j.neuron.2017.11.031

LeDoux, J. E. (2000). Emotion circuits in the brain. *Annual Review of Neuroscience*, *23*, 155–184. https://doi.org/10.1146/annurev.neuro.23.1.155

Lee, E., Rhim, I., Lee, J. W., Ghim, J.-W., Lee, S., Kim, E., & Jung, M. W. (2016). Enhanced Neuronal Activity in the Medial Prefrontal Cortex during Social Approach Behavior. *The Journal of Neuroscience*, *36*(26), 6926–6936. https://doi.org/10.1523/jneurosci.0307-16.2016

Lee, I., & Kesner, R. P. (2003). Time-dependent relationship between the dorsal hippocampus and the prefrontal cortex in spatial memory. *Journal of Neuroscience*, *23*(4), 1517–1523. https://doi.org/10.1523/jneurosci.23-04-01517.2003

Lein, E. S., Hawrylycz, M. J., Ao, N., Ayres, M., Bensinger, A., Bernard, A., Boe, A. F., Boguski, M. S., Brockway, K. S., Byrnes, E. J., Chen, L., Chen, L., Chen, T. M., Chin, M. C., Chong, J., Crook, B. E., Czaplinska, A., Dang, C. N., Datta, S., … Jones, A. R. (2007). Genome-wide atlas of gene expression in the adult mouse brain. *Nature*, *445*(7124), 168–176. https://doi.org/10.1038/nature05453

Leonard, C. M. (1969). The prefrontal cortex of the rat. I. cortical projection of the mediodorsal nucleus. II. efferent connections. *Brain Research*, *12*(2), 321–343. https://doi.org/10.1016/0006-8993(69)90003-1

Liang, B., Zhang, L., Barbera, G., Chen, R., Li, Y., & Lin, D.-T. (2018). Distinct and Dynamic ON and OFF Neural Ensembles in the Prefrontal Cortex Code Social Exploration. *Neuron*, 1–15. https://doi.org/10.1016/j.neuron.2018.08.043

Liu, D., Gu, X., Zhu, J., Zhang, X., Han, Z., Yan, W., Cheng, Q., Hao, J., Fan, H., Hou, R., Chen, Z., Chen, Y., & Li, C. T. (2014). Medial prefrontal activity during delay period contributes to learning of a working memory task. *Science*, *346*(6208), 458–463. https://doi.org/10.1126/science.1256573

Ma, X., Zheng, C., Chen, Y., Pereira, F., & Li, Z. (2022). Working memory and reward increase the accuracy of animal location encoding in the medial prefrontal cortex. *Cerebral Cortex*, 1–15. https://doi.org/10.1093/cercor/bhac205

Maharjan, D. M., Dai, Y. Y., Glantz, E. H., & Jadhav, S. P. (2018). Disruption of dorsal hippocampal – prefrontal interactions using chemogenetic inactivation impairs spatial learning. *Neurobiology of Learning and Memory*, *155*, 351–360. https://doi.org/10.1016/j.nlm.2018.08.023

Mankin, E. A., Sparks, F. T., Slayyeh, B., Sutherland, R. J., Leutgeb, S., & Leutgeb, J. K. (2012). Neuronal code for extended time in the hippocampus. *Proceedings of the National Academy of Sciences of the United States of America*, *109*(47), 19462–19467. https://doi.org/10.1073/pnas.1214107109

Masatoshi, I. (2020). Genetically Encoded Calcium Indicators to Probe Complex Brain Circuit Dynamics in vivo. *Neuroscience Research*. https://doi.org/10.1016/j.neures.2020.05.013

Mathis, A., Mamidanna, P., Cury, K. M., Abe, T., Murthy, V. N., Mathis, M. W., & Bethge, M. (2018). DeepLabCut: markerless pose estimation of user-defined body parts with deep learning. *Nature Neuroscience*, *21*(9), 1281–1289. https://doi.org/10.1038/s41593-018-0209-y

McClelland, W. J., & Colman, F. D. (1967). Activity and different types of electric shock stimuli. *Psychonomic Science*, *7*(11), 391–392. https://doi.org/10.3758/BF03331139

Meyers, E. M., Freedman, D. J., Kreiman, G., Miller, E. K., & Poggio, T. (2008). Dynamic population coding of category information in inferior temporal and prefrontal cortex. *Journal of Neurophysiology*, *100*(3), 1407–1419. https://doi.org/10.1152/jn.90248.2008

Milad, M. R., & Quirk, G. J. (2002). Neurons in medial prefrontal cortex signal memory for fear extinction. *Nature*, *420*(6911), 70–74. https://doi.org/10.1038/nature01138

Miller, E. K., Erickson, C. A., & Desimone, R. (1996). Neural mechanisms of visual working memory in prefrontal cortex of the macaque. *Journal of Neuroscience*, *16*(16), 5154–5167. https://doi.org/10.1523/jneurosci.16-16-05154.1996

Miller, E. K., Freedman, D. J., & Wallis, J. D. (2002). The prefrontal cortex: Categories, concepts and cognition. *Philosophical Transactions of the Royal Society B: Biological Sciences*, *357*(1424), 1123–1136. https://doi.org/10.1098/rstb.2002.1099

Morgan, M. A., & LeDoux, J. E. (1995). Differential Contribution of Dorsal and Ventral Medial Prefrontal Cortex to the Acquisition and Extinction of Conditioned Fear in Rats. *Behavioral Neuroscience*, *109*(4), 681–688. https://doi.org/10.1037/0735-7044.109.4.681

Morgan, M. A., Romanski, L. M., & LeDoux, J. E. (1993). Extinction of emotional learning: Contribution of medial prefrontal cortex. *Neuroscience Letters*, *163*(1), 109–113. https://doi.org/10.1016/0304-3940(93)90241-C

Murray, A. J., Woloszynowska-Fraser, M. U., Ansel-Bollepalli, L., Cole, K. L. H., Foggetti, A., Crouch, B., Riedel, G., & Wulff, P. (2015). Parvalbumin-positive interneurons of the prefrontal cortex support working memory and cognitive flexibility. *Scientific Reports*, *5*(June), 1–14. https://doi.org/10.1038/srep16778

Murugan, M., Jang, H. J., Park, M., Miller, E. M., Cox, J., Taliaferro, J. P., Parker, N. F., Bhave, V., Hur, H., Liang, Y., Nectow, A. R., Pillow, J. W., & Witten, I. B. (2017). Combined Social and Spatial Coding in a Descending Projection from the Prefrontal Cortex. *Cell*, *171*(7), 1663-1677.e16. https://doi.org/10.1016/j.cell.2017.11.002

Nagai, T., Takuma, K., Kamei, H., Ito, Y., Nakamichi, N., Ibi, D., Nakanishi, Y., Murai, M., Mizoguchi, H., Nabeshima, T., & Yamada, K. (2007). Dopamine D1 receptors regulate protein synthesis-dependent long-term recognition

memory via extracellular signal-regulated kinase 1/2 in the prefrontal cortex. *Learning and Memory*, *14*(3), 117–125. https://doi.org/10.1101/lm.461407

Niki, H. (1974a). Differential activity of prefrontal units during right and left delayed response trials. *Brain Research*, *70*(2), 346–349. https://doi.org/10.1016/0006-8993(74)90324-2

Niki, H. (1974b). Prefrontal unit activity during delayed alternation in the monkey. I. Relation to direction of response. *Brain Research*, *68*(2), 185–196. https://doi.org/10.1016/0006-8993(74)90388-6

Nonneman, A. J., & Kolb, B. (1979). Functional recovery after serial ablation of prefrontal cortex in the rat. *Physiology and Behavior*, *22*(5), 895–901. https://doi.org/10.1016/0031-9384(79)90334-2

Park, J. C., Bae, J. W., Kim, J., & Jung, M. W. (2019). Dynamically changing neuronal activity supporting working memory for predictable and unpredictable durations. *Scientific Reports*, *9*(1), 1–10. https://doi.org/10.1038/s41598-019-52017-8

Pezze, M. A., Marshall, H. J., Fone, K. C. F., & Cassaday, H. J. (2015). Dopamine D1 receptor stimulation modulates the formation and retrieval of novel object recognition memory: Role of the prelimbic cortex. *European Neuropsychopharmacology*, *25*(11), 2145–2156. https://doi.org/10.1016/j.euroneuro.2015.07.018

Pezze, M. A., Marshall, H. J., Fone, K. C. F., & Cassaday, H. J. (2017). Role of the anterior cingulate cortex in the retrieval of novel object recognition memory after a long delay. *Learning and Memory*, *24*(7), 310–317. https://doi.org/10.1101/lm.044784.116

Pinto, L., & Dan, Y. (2015). Cell-Type-Specific Activity in Prefrontal Cortex during Goal-Directed Behavior. *Neuron*, *87*(2), 437–450. https://doi.org/10.1016/j.neuron.2015.06.021

Pnevmatikakis, E. A., & Giovannucci, A. (2017). NoRMCorre: An online algorithm for piecewise rigid motion correction of calcium imaging data. *Journal of Neuroscience Methods*, *291*, 83–94. https://doi.org/10.1016/j.jneumeth.2017.07.031

Powell, N. J., & David Redish, A. (2014). Complex neural codes in rat prelimbic cortex are stable across days on a spatial decision task. *Frontiers in Behavioral Neuroscience*, *8*(APR), 1–16. https://doi.org/10.3389/fnbeh.2014.00120

Preuss, T. M. (1995). Do rats have prefrontal cortex? The Rose-Woolsey-Akert program reconsidered. *Journal of Cognitive Neuroscience*, *7*(1), 1–24. https://doi.org/10.1162/jocn.1995.7.1.1

Preuss, T. M., & Wise, S. P. (2022). Evolution of prefrontal cortex. *Neuropsychopharmacology*, *47*(1), 3–19. https://doi.org/10.1038/s41386-021-01076-5

Quiroga, R. Q., Reddy, L., Kreiman, G., Koch, C., & Fried, I. (2005). Invariant visual representation by single neurons in the human brain. *Nature*, *435*(7045), 1102–1107. https://doi.org/10.1038/nature03687

Ragozzino, M. E., Adams, S., & Kesner, R. P. (1998). Differential involvement of the dorsal anterior cingulate and prelimbic- infralimbic areas of the rodent prefrontal cortex in spatial working memory. *Behavioral Neuroscience*, *112*(2), 293–303. https://doi.org/10.1037/0735-7044.112.2.293

Rainer, G., Asaad, W. F., & Miller, E. K. (1998). Memory fields of neurons in the primate prefrontal cortex. *Proceedings of the National Academy of Sciences of the United States of America*, *95*(25), 15008–15013. https://doi.org/10.1073/pnas.95.25.15008

Reed, P., Mitchell, C., & Nokes, T. (1996). Intrinsic reinforcing properties of putatively neutral stimuli in an instrumental two-lever discrimination task. *Animal Learning and Behavior*, *24*(1), 38–45. https://doi.org/10.3758/BF03198952

Reep, R. L., & Corwin, J. v. (1999). Topographic organization of the striatal and thalamic connections of rat medial agranular cortex. *Brain Research*, *841*(1–2), 43–52. https://doi.org/10.1016/S0006-8993(99)01779-5

Riga, D., Matos, M. R., Glas, A., Smit, A. B., Spijker, S., & van den Oever, M. C. (2014). Optogenetic dissection of medial prefrontal cortex circuitry. *Frontiers in Systems Neuroscience*, *8*(DEC), 1–19. https://doi.org/10.3389/fnsys.2014.00230

Rigotti, M., Barak, O., Warden, M. R., Wang, X. J., Daw, N. D., Miller, E. K., & Fusi, S. (2013). The importance of mixed selectivity in complex cognitive tasks. *Nature*, *497*(7451), 585–590. https://doi.org/10.1038/nature12160

Rubin, A., Geva, N., Sheintuch, L., & Ziv, Y. (2015). Hippocampal ensemble dynamics timestamp events in long-term memory. *ELife*, *4*(DECEMBER2015), 1–16. https://doi.org/10.7554/eLife.12247

Rule, M. E., O'Leary, T., & Harvey, C. D. (2019). Causes and consequences of representational drift. *Current Opinion in Neurobiology*, *58*, 141–147. https://doi.org/10.1016/j.conb.2019.08.005

Salinas-Hernández, X. I., Vogel, P., Betz, S., Kalisch, R., Sigurdsson, T., & Duvarci, S. (2018). Dopamine neurons drive fear extinction learning by signaling the omission of expected aversive outcomes. *ELife*, *7*, 1–25. https://doi.org/10.7554/eLife.38818

Sauer, J. F., Folschweiller, S., & Bartos, M. (2022). Topographically organized representation of space and context in the medial prefrontal cortex. *Proceedings of the National Academy of Sciences of the United States of America*, *119*(6), 4–11. https://doi.org/10.1073/pnas.2117300119

Sawaguchi, T., & Goldman-Rakic, P. S. (1991). D1 Dopamine Receptors in Prefrontal Cortex: Involvement in Working Memory. *Science*, *251*(4996), 947–950. https://doi.org/10.1126/science.1825731

Seamans, J. K., Floresco, S. B., & Phillips, A. G. (1995). Functional Differences Between the Prelimbic and Anterior Cingulate Regions of the Rat Prefrontal Cortex. *Behavioral Neuroscience*, *109*(6), 1063–1073. https://doi.org/10.1037/0735-7044.109.6.1063

Seamans, J. K., Lapish, C. C., & Durstewitz, D. (2008). Comparing the prefrontal cortex of rats and primates: Insights from electrophysiology. *Neurotoxicity Research*, *14*(2–3), 249–262. https://doi.org/10.1007/BF03033814

Sesack, S. R., Deutch, A. Y., Roth, R. H., & Bunney, B. S. (1989). Topographical organization of the efferent projections of the medial prefrontal cortex in the rat: An anterograde tract-tracing study with Phaseolus vulgaris leucoagglutinin. *Journal of Comparative Neurology*, *290*(2), 213–242. https://doi.org/10.1002/cne.902900205

Shah, A. A., & Treit, D. (2003). Excitotoxic lesions of the medial prefrontal cortex attenuate fear responses in the elevated-plus maze, social interaction and shock probe burying tests. *Brain Research*, *969*(1–2), 183–194. https://doi.org/10.1016/S0006-8993(03)02299-6

Sheintuch, L., Rubin, A., Brande-eilat, N., Geva, N., Sheintuch, L., Rubin, A., Brande-eilat, N., Geva, N., Sadeh, N., Pinchasof, O., & Ziv, Y. (2017). Tracking the Same Neurons across Multiple Days in Resource Tracking the

Same Neurons across Multiple Days in Ca 2 + Imaging Data. *CellReports*, *21*(4), 1102–1115. https://doi.org/10.1016/j.celrep.2017.10.013

Sierra-Mercado, D., Padilla-Coreano, N., & Quirk, G. J. (2011). Dissociable roles of prelimbic and infralimbic cortices, ventral hippocampus, and basolateral amygdala in the expression and extinction of conditioned fear. *Neuropsychopharmacology*, *36*(2), 529–538. https://doi.org/10.1038/npp.2010.184

Sobotka, S., Diltz, M. D., & Ringo, J. L. (2005). Can delay-period activity explain working memory? *Journal of Neurophysiology*, *93*(1), 128–136. https://doi.org/10.1152/jn.01002.2003

Spellman, T., Rigotti, M., Ahmari, S. E., Fusi, S., Gogos, J. A., & Gordon, J. A. (2015). Hippocampal-prefrontal input supports spatial encoding in working memory. *Nature*, *522*(7556), 309–314. https://doi.org/10.1038/nature14445

Stern, C. A. J., Do Monte, F. H. M., Gazarini, L., Carobrez, A. P., & Bertoglio, L. J. (2010). Activity in prelimbic cortex is required for adjusting the anxiety response level during the elevated plus-maze retest. *Neuroscience*, *170*(1), 214–222. https://doi.org/10.1016/j.neuroscience.2010.06.080

Sullivan, R. M., & Gratton, A. (2002). Behavioral effects of excitotoxic lesions of ventral medial prefrontal cortex in the rat are hemisphere-dependent. *Brain Research*, *927*(1), 69–79. https://doi.org/10.1016/S0006-8993(01)03328-5

Takahashi, A., Nagayasu, K., Nishitani, N., Kaneko, S., & Koide, T. (2014). Control of Intermale Aggression by Medial Prefrontal Cortex Activation in the Mouse. *PLoS ONE*, *9*(4), e94657. https://doi.org/10.1371/journal.pone.0094657

Tamura, M., Spellman, T. J., Rosen, A. M., Gogos, J. A., & Gordon, J. A. (2017). Hippocampal-prefrontal theta-gamma coupling during performance of a spatial working memory task. *Nature Communications*, *8*(1), 2182. https://doi.org/10.1038/s41467-017-02108-9

Tanimizu, T., Kono, K., & Kida, S. (2018). Brain networks activated to form object recognition memory. *Brain Research Bulletin*, *141*, 27–34. https://doi.org/10.1016/j.brainresbull.2017.05.017

Thompson, L. T., & Best, P. J. (1990). Long-term stability of the place-field activity of single units recorded from the dorsal hippocampus of freely behaving rats. *Brain Research*, *509*(2), 299–308. https://doi.org/10.1016/0006-8993(90)90555-P

Tian, L., Hires, S. A., Mao, T., Huber, D., Chiappe, M. E., Chalasani, S. H., Petreanu, L., Akerboom, J., McKinney, S. A., Schreiter, E. R., Bargmann, C. I., Jayaraman, V., Svoboda, K., & Looger, L. L. (2009). Imaging neural activity in worms, flies and mice with improved GCaMP calcium indicators. *Nature Methods*, *6*(12), 875–881. https://doi.org/10.1038/nmeth.1398

Tucker, L. B., & McCabe, J. T. (2017). Behavior of male and female C57Bl/6J mice is more consistent with repeated trials in the elevated zero maze than in the elevated plus maze. *Frontiers in Behavioral Neuroscience*, *11*(January), 1–8. https://doi.org/10.3389/fnbeh.2017.00013

Tuscher, J. J., Taxier, L. R., Fortress, A. M., & Frick, K. M. (2018). Chemogenetic inactivation of the dorsal hippocampus and medial prefrontal cortex, individually and concurrently, impairs object recognition and spatial memory consolidation in female mice. *Neurobiology of Learning and Memory*, *156*(September), 103–116. https://doi.org/10.1016/j.nlm.2018.11.002

Uylings, H. B. M., Groenewegen, H. J., & Kolb, B. (2003). Do rats have a prefrontal cortex? *Behavioural Brain Research*, *146*(1–2), 3–17. https://doi.org/10.1016/j.bbr.2003.09.028

van Eden, C. G., & Uylings, H. B. M. (1985). Cytoarchitectonic development of the prefrontal cortex in the rat. *Journal of Comparative Neurology*, *241*(3), 253–267. https://doi.org/10.1002/cne.902410302

van Haaren, F., van Zijderveld, G., van Hest, A., de Bruin, J. P. C., van Eden, C. G., & van de Poll, N. E. (1988). Acquisition of Conditional Associations and Operant Delayed Spatial Response Alternation: Effects of Lesions in the Medial Prefrontal Cortex. *Behavioral Neuroscience*, *102*(4), 481–488. https://doi.org/10.1037/0735-7044.102.4.481

Vertes, R. P. (2002). Analysis of projections from the medial prefrontal cortex to the thalamus in the rat, with emphasis on nucleus reuniens. *The Journal of Comparative Neurology*, *442*(2), 163–187. https://doi.org/10.1002/cne.10083

Vidal-Gonzalez, I., Vidal-Gonzalez, B., Rauch, S. L., & Quirk, G. J. (2006). Microstimulation reveals opposing influences of prelimbic and infralimbic cortex on the expression of conditioned fear. *Learning and Memory*, *13*(6), 728–733. https://doi.org/10.1101/lm.306106

Vogel, P., **Hahn, J.**, Duvarci, S., & Sigurdsson, T. (2022). Prefrontal pyramidal neurons are critical for all phases of working memory. *Cell Reports*, *39*(2), 110659. https://doi.org/10.1016/j.celrep.2022.110659

Vogt, B. A., Hof, P. R., Zilles, K., Vogt, L. J., Herold, C., & Palomero-Gallagher, N. (2013). Cingulate area 32 homologies in mouse, rat, macaque and human: Cytoarchitecture and receptor architecture. *Journal of Comparative Neurology*, *521*(18), 4189–4204. https://doi.org/10.1002/cne.23409

Walf, A. A., & Frye, C. A. (2007). The use of the elevated plus maze as an assay of anxiety-related behavior in rodents. *Nature Protocols*, *2*(2), 322–328. https://doi.org/10.1038/nprot.2007.44

Wang, C., Furlong, T. M., Stratton, P. G., Lee, C. C. Y., Xu, L., Merlin, S., Nolan, C., Arabzadeh, E., Marek, R., & Sah, P. (2021). Hippocampus–prefrontal coupling regulates recognition memory for novelty discrimination. *Journal of Neuroscience*, *34*(3), 9617–9632. https://doi.org/10.1523/JNEUROSCI.1202-21.2021

Wang, F., Zhu, J., Zhu, H., Zhang, Q., Lin, Z., & Hu, H. (2011). Bidirectional control of social hierarchy by synaptic efficacy in medial prefrontal cortex. *Science*, *334*(6056), 693–697. https://doi.org/10.1126/science.1209951

Wang, Q., Ding, S. L., Li, Y., Royall, J., Feng, D., Lesnar, P., Graddis, N., Naeemi, M., Facer, B., Ho, A., Dolbeare, T., Blanchard, B., Dee, N., Wakeman, W., Hirokawa, K. E., Szafer, A., Sunkin, S. M., Oh, S. W., Bernard, A., … Ng, L. (2020). The Allen Mouse Brain Common Coordinate Framework: A 3D Reference Atlas. *Cell*, *181*(4), 936-953.e20. https://doi.org/10.1016/j.cell.2020.04.007

Weible, A. P., Rowland, D. C., Pang, R., & Kentros, C. (2009a). Neural correlates of novel object and novel location recognition behavior in the mouse anterior cingulate cortex. *Journal of Neurophysiology*, *102*(4), 2055–2068. https://doi.org/10.1152/jn.00214.2009

Weible, A. P., Rowland, D. C., Pang, R., & Kentros, C. (2009b). Neural correlates of novel object and novel location recognition behavior in the mouse anterior cingulate cortex. *Journal of Neurophysiology*, *102*(4), 2055–2068. https://doi.org/10.1152/jn.00214.2009

Xu, P., Chen, A., Li, Y., Xing, X., & Lu, H. (2019). Medial prefrontal cortex in neurological diseases. *Physiological Genomics*, *51*(9), 432–442. https://doi.org/10.1152/physiolgenomics.00006.2019

Xu, P., Yue, Y., Su, J., Sun, X., Du, H., Liu, Z., Simha, R., Zhou, J., Zeng, C., & Lu, H. (2022). Pattern decorrelation in the mouse medial prefrontal cortex enables social preference and requires MeCP2. *Nature Communications*, *13*(1), 1–14. https://doi.org/10.1038/s41467-022-31578-9

Yang, S.-T., Shi, Y., Wang, Q., & Li, B.-M. (2015). Neuronal representation of audio-place associations in the medial prefrontal cortex of rats. *Molecular Brain*, *8*(1), 56. https://doi.org/10.1186/s13041-015-0147-5

Yang, Y., & Mailman, R. B. (2018). Strategic neuronal encoding in medial prefrontal cortex of spatial working memory in the T-maze. *Behavioural Brain Research*, *343*(October 2017), 50–60. https://doi.org/10.1016/j.bbr.2018.01.020

Yizhar, O., Fenno, L. E., Prigge, M., Schneider, F., Davidson, T. J., Ogshea, D. J., Sohal, V. S., Goshen, I., Finkelstein, J., Paz, J. T., Stehfest, K., Fudim, R., Ramakrishnan, C., Huguenard, J. R., Hegemann, P., & Deisseroth, K. (2011). Neocortical excitation/inhibition balance in information processing and social dysfunction. *Nature*, *477*(7363), 171–178. https://doi.org/10.1038/nature10360

Yoon, T., Okada, J., Jung, M., & Kim, J. (2008). Prefrontal cortex and hippocampus subserve different components of working memory in rats. *Learning & Memory*, *15*, 97–105. https://doi.org/10.1101/lm.850808.to-sample

Zhou, P., Resendez, S. L., Rodriguez-Romaguera, J., Jimenez, J. C., Neufeld, S. Q., Giovannucci, A., Friedrich, J., Pnevmatikakis, E. A., Stuber, G. D., Hen, R., Kheirbek, M. A., Sabatini, B. L., Kass, R. E., & Paninski, L. (2018). Efficient and accurate extraction of in vivo calcium signals from microendoscopic video data. *ELife*, *7*, 1–37. https://doi.org/10.7554/eLife.28728

Zhou, P., Resendez, S. L., Stuber, G. D., Kass, R. E., & Paninski, L. (2016). *Efficient and accurate extraction of in vivo calcium signals from microendoscopic video data*. 1–14. http://arxiv.org/abs/1605.07266

Zhu, X. O., Brown, M. W., McCabe, B. J., & Aggleton, J. P. (1995). Effects of the novelty or familiarity of visual stimuli on the expression of the immediate early gene c-fos in rat brain. *Neuroscience*, *69*(3), 821–829. https://doi.org/10.1016/0306-4522(95)00320-I

Zong, W., Wu, R., Chen, S., Wu, J., Wang, H., Zhao, Z., Chen, G., Tu, R., Wu, D., Hu, Y., Xu, Y., Wang, Y., Duan, Z., Wu, H., Zhang, Y., Zhang, J., Wang, A., Chen, L., & Cheng, H. (2021). Miniature two-photon microscopy for enlarged field-of-view, multi-plane and long-term brain imaging. *Nature Methods*, *18*(1), 46–49. https://doi.org/10.1038/s41592-020-01024-z